Shear effects on the properties and separation characteristics of whey protein precipitates

Edmond Philip Byrne BE MSc MIEI AMIChemE

A thesis presented to the National University of Ireland

in fulfilment of the requirements for the degree of

Doctor of Philosophy (PhD)

Under the supervision and direction of

Dr. John J. Fitzpatrick

April 2001

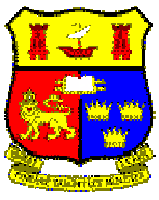

Department of Process Engineering
Faculty of Engineering
University College, Cork

1.1 Contents

1.2 Acknowledgements

It is with great pleasure, dispensed with a reasonable dose of relief that I write these, the final words, chronologically at least, of my PhD dissertation. First of all I'd like to thank Dr. John Fitzpatrick for supervising this work. Over the past four and a half years he has generously provided me with his time, advice, insights and support for which I'll be forever grateful. I'd like to thank Professor E. Chris Synnott, retired head of the department for allowing me the opportunity to come to UCC to undertake this project and Professor Fernanda A.R. Oliveira, current head for her full support and for being so generous in facilitating my finishing of it. I'd also like to thank Mr. Diarmuid A. MacCarthy, former acting head, who has always been extremely supportive of me throughout my career, from the time I called into his office as a third year UCD undergraduate chemical engineer and asked him about opportunities for food process engineers. I'd also like to thank Dr. Kevin Cronin for his generous support and advice throughout my time at UCC. Thanks also to Dr. Barry O'Connor and all in the Faculty of Engineering, the Faculty of Food Science and Technology and throughout UCC who've assisted me.

The support staff in the department are second to none. I'd like to offer sincerest thanks to Ms. Rita Kelleher for her endless support and advice as department senior executive officer. I also wish to thank the technical staff who've provided me with immeasurable assistance; Mr Denis Ring for his assistance and expertise in the lab and Mr. John Barrett for providing similar assistance and support on computer related matters as well as workshop technicians, Mr. Adrian O'Connor and latterly, Mr. Paul Conway. I'd like to thank Mr. Tim Twomey for putting up with sharing an office with me and to all the above for providing added daily stimulation through some lively tea-room discourse on the topics of the day. Great stuff!

I'd like to thank Dr. Nigel J. Titchener-Hooker at the department of Biochemical Engineering, University College London, for facilitating my pilot scale work at the Advanced Centre for Biochemical Engineering, UCL, for reviewing my work there and for agreeing to act as extern examiner. I'd also like to thank Mr. Lars Pampel for his help and advice and to all the people I came into contact with during my period there including Mr. Billy Doyle and his fellow technicians.

I'd also like to thank Professor Ronnie Magee of the Department of Chemical Engineering at the Queen's University of Belfast for agreeing to act as extern examiner.

I wish to thank Professor Brian McKenna, head of the dept. of Food Science at UCD, who supervised my masters degree there and provided me with active support and encouragement to go on and undertake a PhD. I'd also like to thank all the staff of the dept. of Chemical Engineering at UCD for providing me with a very good undergraduate education and the necessary basis upon which to attempt this project and to my teachers at St. Kieran's College, Kilkenny. I'd like to thank Mr. John O'Shea, head of the dept. of Chemical and Process Engineering, Cork Institute of Technology, for providing me with the opportunity to develop my career in parallel with my PhD work through two years of teaching at CIT and to all the students at both UCC and CIT that I've had the pleasure of helping on their way to becoming engineers; particularly those I supervised in the lab on various summer vacation or final year projects; Erin Powell (Univ. of Saskatchewan, Canada; visiting), Camilla Hegarty, Paul Finn, David Deasy, Cormac Murphy, Catherine Horgan, Séamus Buckley, Michael Murphy, Gerald Purtill, Taidgh Horgan and Michael O'Neill.

Financially, I'd like to thank the Department of Agriculture, Food and Rural Development, Kildare Street, Dublin 2, who funded this work under the national Non-Commissioned Food Research Programme (NCFRP) and Professor Charles Daly, Dean of the Faculty of Food Science and Technology and his fellow members of the Faculty Staff Mobility

Programme Committee for funding my time at UCL. I'd also like to thank Dairygold for supplying whey protein concentrate.

On a personal level, I'd like to thank Dr. Darren O'Beirne and Dr. Markus Gaiser, who each provided me with the inspiration and motivation to get my PhD finished, but who are primarily just very good friends in life.

I'd like to thank my younger sister and brothers; Maria, Pat and Robert who I'm very proud to name as fellow siblings and to my aunt Brigid who has always been interested in our education and career.

I'd like to thank my girlfriend Clare, a wonderful woman who I met two years ago, and who has always given me her full support as I've completed this dissertation. We should be able to spend some more time together now Clare!

Finally, I wish to thank the two people that have had most influence on my life and without whose incredible support I could never have got this far. I am immensely proud of my parents Patrick and Bridget, who despite having had few educational opportunities or qualifications themselves, have always realised the value of education and through their immense wisdom, encouragement and self sacrifice made sure that we were never short of anything either educationally or in any other respect. Testament to this is the possibility that by the end of this year they'll be able to count among their children an engineer, a dentist, a financial trader and a teacher, who together may have earned as many as seven university degrees.

To you mum and dad, I dedicate this.

1.3 Presentations

The following is a list of presentations made in relation to this work:

Conference presentations:

Byrne, E.P., Fitzpatrick, J.J., (2000), Separation characteristics of precipitated whey proteins subjected to shear during and subsequent to precipitate formation, ICEF8, International Conference on Engineering and Food, 9-13 April 2000, Puebla, Mexico.

Byrne, E.P., Fitzpatrick, J.J., (2000), Effect of shear and ageing time on the particle size distribution of precipitates formed during whey protein fractionation. Research 2000: Stretching the Boundaries of Chemical Engineering, IChemE Conference, 6-7 January 2000, Bath, England.*

Byrne, E.P., Fitzpatrick, J.J., (2000), A study on how shear affects the fractal geometry of whey protein precipitates with implications for centrifugal separation. 30th University College Cork Annual Food Science and Technology Research Conference, 19-20 September 2000, Cork, Ireland.

Byrne, E.P., Fitzpatrick, J.J., (1999), An investigation into the effects of shear on the separation properties of whey protein precipitates. 29th University College Cork Annual Food Science and Technology Research Conference, 16-17 September 1999, Cork, Ireland.

* poster presentation

1.4 Abstract

Selective isoelectric whey protein precipitation and aggregation is carried out at laboratory scale in a standard configuration batch agitation vessel. Geometric scale-up of this operation is implemented on the basis of constant impeller power input per unit volume and subsequent clarification is achieved by high speed disc-stack centrifugation. Particle size and fractal geometry are important in achieving efficient separation while aggregates need to be strong enough to resist the more extreme levels of shear that are encountered during processing, for example through pumps, valves and at the centrifuge inlet zone.

This study investigates how impeller agitation intensity and ageing time affect aggregate size, strength, fractal dimension and hindered settling rate at laboratory scale in order to determine conditions conducive for improved separation. Particle strength is measured by observing the effects of subjecting aggregates to moderate and high levels of process shear in a capillary rig and through a partially open ball-valve respectively. The protein precipitate yield is also investigated with respect to ageing time and impeller agitation intensity. A pilot scale study is undertaken to investigate scale-up and how agitation vessel shear affects centrifugal separation efficiency.

Laboratory scale studies show that precipitates subject to higher impeller shear-rates during the addition of the precipitation agent are smaller but more compact than those subject to lower impeller agitation and are better able to resist turbulent breakage. They are thus more likely to provide a better feed for more efficient centrifugal separation. Protein precipitation yield improves significantly with ageing, and 50 minutes of ageing is required to obtain a 70 - 80% yield of α-lactalbumin.

Geometric scale-up of the agitation vessel at constant power per unit volume results in aggregates of broadly similar size exhibiting similar trends but with some differences due to the absence of dynamic similarity due to longer circulation time and higher tip speed

in the larger vessel. Disc stack centrifuge clarification efficiency curves show aggregates formed at higher shear-rates separate more efficiently, in accordance with laboratory scale projections. Exposure of aggregates to highly turbulent conditions, even for short exposure times, can lead to a large reduction in particle size. Thus, improving separation efficiencies can be achieved by the identification of high shear zones in a centrifugal process and the subsequent elimination or amelioration of such.

1.5 Nomenclature

A	capillary tube cross sectional area, m^2
b_c	caulk width on discs in disc stack centrifuge, m
C	concentration (volume fraction)
d	particle diameter or capillary tube diameter (depending on context), m
D	agitator impeller diameter, m
d_{10}	particle diameter below which 10% of particles exist by volume, m
d_{50}	median particle diameter, m
d_{90}	particle diameter below which 90% of particles exist by volume, m
D_f	fractal dimension
d_p	Stokes falling particle diameter, m
E	Euclidean dimension of space
f	Fanning friction factor (equals 16/Re for laminar flow)
F	force acting on a particle, N
F_1	Σ correction factor for spacers between discs in disc stack centrifuge
F_g	gravity force on a particle, N
g	acceleration due to gravity, ms^{-2}
$\dot{G}$	average spatial shear-rate within a standard configuration stirred-tank due to impeller agitation, s^{-1}
i,j,k	subscripts which define particle sizes where, for collision purposes $d_k^3 = d_i^3 + d_j^3$ (chapter 3)
I	scattered light intensity
k	proportionality constant
K	proportionality constant
K_B	Boltzmann constant (1.38×10^{-23} JK^{-1})
M	aggregate particle mass, kg
m_o	mass of a primary particle, kg
n	solvent refractive index or hindered settling index, depending on context

N	number concentration of particles (chapter 3) or agitator impeller speed, rev/s
N_c	centrifuge speed, rev/min
N_o	number of primary particles
N_p	agitator power number, taken as equal to 5 for a 6 bladed Rushton impeller in a standard configuration agitation vessel at an impeller Re greater than 10^4.
N_q	dimensionless impeller pumping capacity
OD_{feed}	optical density of a feed sample taken from disc stack centrifuge during operation
OD_{ref}	optical density of a clarified control precipitate solution sample
$OD_{supernatant}$	optical density of a supernatant sample taken from disc stack centrifuge during operation
P	impeller power input, W
q	scattering wave vector, nm^{-1}
Q	volumetric flowrate, m^3s^{-1}
r	radial distance form centre of an aggregate particle or from axial centre of capillary tube (depending on context) or aggregate particle radius, m
r_c	centrifuge rotor radius, m
RCF	relative centrifugal force
Re	Reynolds' number
r_i	centrifuge inner disc radius, m
r_{min}	radius of the smallest aggregate, m
r_o	centrifuge outer disc radius or primary particle radius, m
$r_{o\ min}$	radius of a small single primary particle, m
R_t	capillary tube radius, m
t	time, s
T	absolute temperature, K
t_c	mean particle vessel circulation time, s
u_x	velocity of fluid in direction of capillary tube, ms^{-1}

V	effective agitation vessel volume, m^3
$V(C)$	hindered settling velocity (concentration dependent), ms^{-1}
V_o	primary particle volume, m^3
V_p	aggregate particle volume, m^3
V_t	Stokes terminal velocity for a single spherical particle falling under gravity in an expanse of fluid, ms^{-1}
Z_C	number of caulks per disc in disc stack centrifuge
Z_S	number of discs in disc stack centrifuge

Greek Symbols:

α	effectiveness factor for collisions in forming aggregates
Δ	particle diffusivity = $K_B T/6\pi r\mu$, m^2/s
ΔP	pressure drop across length of capillary tube, Nm^{-2}
ε	average turbulent energy dissipation rate per unit mass, W/kg
γ	shear-rate, s^{-1}
$\bar{\gamma}_m$	mass average shear-rate in capillary tube, s^{-1}
γ_w	shear-rate at capillary tube wall, s^{-1}
η	turbulent microscale dimension, m
μ	dynamic viscosity of fluid, Nsm^{-2}
π	pi (≈ 3.141593)
ν	kinematic viscosity of suspending fluid ($= \mu/\rho$), m^2/s
ρ	fluid density, kg/m^3
ρ_{Df}	density of a fractal aggregate, kg/m^3
ρ_o	density of a primary particle, kg/m^3
ρ_p	particle bulk density, kg/m^3
ρ_s	density of solid protein phase, kg/m^3
Σ	centrifugal sigma value, m^2
λ	laser light wavelength in a vacuum, nm (632.8nm for He-Ne laser)

θ	laser light scattering angle or half the disc stack centrifuge conical disc angle (depending on context), degrees
ω	centrifugal angular velocity, radians/s

Chapter 2 Introduction and background

Milk is the perfect food for the neonate of mammalian species and provides the young with the ideal type and mix of carbohydrates, proteins and fats to ensure rapid growth in addition to helping impart immunity via antibody proteins known as immunoglobulins. Bovine milk provides the general human population with a source of food which is rich in proteins with high nutritional value. Dairy proteins also have a number of useful functional properties and can be used, if isolated from milk or from other dairy proteins, as food ingredients with a wide range of potential applications. Dairy proteins can be divided into two distinct groups; caseins are the homogeneous group of proteins which precipitate at pH 4.6 and are present in cheese and are used as a food ingredient while the remaining non-homogeneous group of proteins are known as whey proteins and have a wide range of nutritional and functional properties.

Whey is a by-product of cheese or casein production and traditionally it has been seen as a waste product or fed to animals, particularly pigs. However, in more recent times, as the potential benefits of whey proteins have been recognized, there has been an accompanying increase in the production of products such as whey protein concentrate (WPC) and whey protein isolate (WPI). These products incorporate all the individual whey proteins present in milk in much the same proportions and thus have nutritional and functional properties reflecting the relative preponderance of each. They are used mainly as food ingredients for the purpose of imparting relevant properties on the product being produced.

α-lactalbumin (α-la) and β-lactoglobulin (β-lg) are the two principal whey proteins present in milk and together they comprise about two thirds (about one-sixth and one-half respectively) of total whey proteins present in bovine milk. Thus between them they are the proteins most responsible for the excellent nutritional and functional (gelation, emulsification, foaming, etc.) properties of WPC and WPI. However each has its own set of distinct properties. α-lactalbumin, for example has excellent emulsification properties while β-lactoglobulin is an excellent gelling agent. Moreover α-lactalbumin comprises a

liberal dose of essential amino acids and is the most abundant whey protein in human milk, in contrast to β-lactoglobulin which is largely absent from human milk. This makes it an ideal ingredient for infant formulae and for high performance protein products such as those taken by athletes. β-lactoglobulin on the other hand has been blamed in some instances for the allergenic reaction that some infants suffer towards cows' milk.

Thus with such widely diverging nutritional and functional properties it would appear that separation of the whey proteins into their individual component species ought to be a useful and economically rewarding exercise. However, in practice this is not yet carried out on any appreciable scale. Separation of the individual whey proteins has do date been confined to laboratory and pilot scale projects. Given that many of the potential uses to which either a pure α-lactalbumin or β-lactoglobulin product could be put are already adequately covered by either WPC or WPI, any proposed industrial separation process would need to be both simple and cost efficient. In addition, a suitable market sufficiently different from that currently occupied by WPC/WPI (i.e. as a food ingredient conferring general functional or nutritional properties) and which would command a reasonable price for the product would need to be identified. Such a market potentially lies in the differentiating nutritional and functional properties of the respective proteins.

A simple and often used method of separating proteins is by selective isoelectric precipitation of one (or more) species with a suitable precipitation agent often accompanied by a temperature adjustment while the other species remain(s) in solution. Agitation of the solution is often employed in order to effect effective distribution of the precipitation agent throughout the protein solution and precipitates are usually aged to allow for optimum mass transfer of the precipitating protein(s) from solution. Physical separation of the proteins can then be effected by centrifugal separation or by some other means such as ultrafiltration. Precipitate proteins can then be re-dissolved as necessary by readjusting pH and temperature to suitable values. This process can be designed so that relatively little or no protein denaturation is incurred in instances where denaturation may be undesirable.

In this study an α-lactalbumin precipitate phase is separated from a soluble phase rich in β-lactoglobulin from a feed consisting of aqueous whey protein concentrate solution by isoelectric precipitation. This is carried out at both laboratory and pilot scales.

The speed of the agitator impeller is directly related to the applied shear-rate for a given agitation vessel and solution. Applied shear-rate during the period of addition of the precipitation agent (when most precipitation and aggregate formation occurs) and during a subsequent ageing period is likely to be an important parameter in determining the eventual size, compactness and strength of the aggregates, as is ageing time itself.

Particle size is evidently important in any subsequent centrifugal or filtration based separation process at any scale (from laboratory to industrial). Moreover, particle compactness can be expressed in its simplest form as density and this too is an important parameter in determining ease of centrifugal separation as defined by Stokes. However, protein precipitate aggregates do not exhibit consistent spatial density and are typically fractal in form, their density decreasing with radial distance, and so their level of compactness is more accurately described by their fractal dimension. Thirdly, particle strength is an important parameter on pilot or industrial scale separation processes as particles are likely to experience shear-rates far in excess of those experienced in the agitation vessel as they are transferred from between the vessel and the separating equipment (travelling through pumps, valves, pipes, etc.) and also within the separation equipment itself particularly if a centrifuge is employed (e.g. extremely high shear-rates are typical of conditions at the feed zone of disc stack centrifuges).

In this work, precipitate particles are taken from the agitation vessel at laboratory scale and exposed to process shear-rates (through valves and pipes) which are similar to those which might prevail during pilot or industrial scale processing in order to determine in a controlled way the effects of agitation vessel shear-rate on particle properties and thus enable one to make recommendations on agitation vessel shear conditions which

ought achieve subsequent optimum centrifugal separation. These recommendations are tested at pilot scale by comparing with clarification efficiency characteristic curves provided by a disc stack centrifuge for precipitates formed at various pilot scale agitation vessel shear-rates.

Thus this work investigates two overlapping interests:
On a more general level it aims to understand the effects of applying various impeller shear-rates in an agitation vessel on the structural properties of precipitate particles, thereby seeking to discover how aggregates react to increased shear exposure during subsequent processing and how efficient centrifugal separation can be achieved.

On a level specifically related to the proteins involved, the work examines the effects of agitation vessel shear-rate and ageing time on whey protein precipitates with a view towards determining agitation vessel conditions that are most conducive to the efficient isoelectric precipitation and fractionation of the individual whey proteins.

If a better understanding of the nature of protein aggregates formed and aged by isoelectric precipitation in an agitation vessel is achieved, particularly in relation to how such aggregates react when subsequently subjected to far greater shear-rates during processing, then this can aid design of pilot and industrial scale protein fractionation processes. Moreover, in the specific case of whey proteins, a better understanding of the shear-rate and ageing conditions for efficient whey protein fractionation can help enhance the viability of this suggested fractionation process on a large scale.

Chapter 3 Objectives of this work

There exist a number of objectives contained within the overall aims of this work as presented in chapter 1. These objectives are outlined below.

The first set of objectives, involving laboratory scale whey protein precipitation in an agitation vessel, are as follows;

- Investigate how impeller agitation during the addition of a precipitation agent and during ageing affect precipitate particle size distribution (PSD) and strength.

- Investigate how ageing time and impeller agitation during the addition of a precipitation agent and ageing affect the concentration of β-lactoglobulin in the supernatant and α-lactalbumin in precipitate phase.

- Investigate how impeller agitation during the addition of a precipitation agent and during ageing affect the fractal geometry and hindered settling characteristics of precipitates.

The second set of objectives, involving pilot scale whey protein precipitation in an agitation vessel followed by centrifugal separation, are as follows;

- Investigate how vessel geometric scale-up at constant power per unit volume affects precipitate particle size distribution (PSD) and strength.

- Investigate how impeller agitation during the addition of a precipitation agent and during ageing affect centrifugal clarification efficiency.

The final objective is to;

- Make process recommendations for improving the fractionation of whey proteins by isoelectric precipitation and centrifugation at pilot and industrial scale.

Chapter 4 Literature Review

4.1.1 Milk and whey proteins

4.1.1.1Dairy proteins

Milk provides the neonate of mammalian species with their complete nutritional requirements and provides many additional physiological functions. All of the major proteins present in milk, with the exception of serum albumin and the immunoglobulins, are synthesized by epithelial cells in the mammary gland from amino acids extracted from the blood. Whey is liquid in form at ambient temperature and pressure, being comprised mainly of water and contains a rich matrix of carbohydrate, fat, proteins, and minerals and vitamins (Table 3.1).

Table 3.1 Typical composition of bovine milk (Walstra et al, 1999).

Component	*Range (% w/w)*
Water	85.3-88.7
Lactose	3.8-5.3
Fat	2.5-5.5
Protein (total; casein + whey)	2.3-4.4
Casein	1.7-3.5
Minerals	0.57-0.83
Organic acids	0.12-0.21

Dairy proteins are a heterogeneous group of proteins containing about 95% the total nitrogen in milk. They are endowed with a rich mix of nutritional, physiological and functional properties which render them suitable for a range of uses and applications. Table 3.2 outlines the various proteins present in bovine milk, their size and frequency. A comprehensive list of dairy proteins and their properties is provided in the report of the 'Committee on the Nomenclature and Methodology of Milk Proteins', part of the American Dairy Science Association (Eigel et al, 1984). This report provides the fifth and

still most recent comprehensive revision on the nomenclature of dairy proteins (Mather, 2000).

Table 3.2 Typical size and abundance of proteins in milk (Walstra et al, 1999).

Protein	*Molecular weight (Da)*	*g /kg milk (% of total proteins)*
Casein		26 (78.5)
α_{s1}-Casein	~23,600	10.0 (31)
α_{s2}-Casein	~25,200	2.6 (8)
β-Casein	~23,983	9.3 (28)
κ-Casein	~19,550	3.3 (10)
γ-Casein	~20,500	0.8 (2.4)
Whey proteins		6.3 (19)
β-lactoglobulin (β-lg)	18,283	3.2 (9.8)
α-lactalbumin (α-la)	14,176	1.2 (3.7)
Bovine serum albumin (BSA)	66,267	0.4 (1.2)
Casein derived peptides	4,000-40,000	0.8 (2.4)
Immunoglobulins		0.8 (2.4)
IgG1, IgG2	~150,000	0.65 (1.8)
IgA	~385,000	0.14 (0.4)
IgM	~900,000	0.05 (0.2)
Miscellaneous		
Lactoferrin	86,000	0.8 (2.5)
Transferrin	76,000	0.1
Membrane proteins		0.1
Enzymes		0.6 (2)

Dairy proteins can be broken down into two broad groups; caseins and whey proteins. Isoelectric precipitation of casein at pH 4.6 is employed during the production of cheese though a number of other methods are also used for the production of casein and caseinates (Mulvihill, 1989). Whey proteins are defined as the heterogeneous group of soluble proteins that remain in solution during casein precipitation either by acid addition (at pH ~4.6) to produce acid whey or by rennet addition (at pH ~6.7) to produce rennet or sweet whey. They constitute about 17-20% of total protein present in bovine milk and provide an extremely rich, if traditionally under utilised, source of nutrients and functional properties. Raw whey is liquid in form and has a relatively low protein content (Table 3.3) but it is usually concentrated to form a creamy coloured powder known as whey protein concentrate (WPC) or whey protein isolate (WPI) (see section 3.1.3). β-lactoglobulin (β-lg) and α-lactalbumin (α-la) are the principal whey proteins in bovine milk and together they constitute about 70% of total whey proteins in rennet produced whey protein concentrate (WPC) and higher proportions in acid produced WPC (Gésan-Guiziou et al, 1999).

Table 3.3 Percentage composition of rennet and acid whey (Morr, 1989).

Component	*Rennet whey (dry)*	*Acid whey (dry)*
Water	93.4	93.6
Lactose	4.9 (74)	4.4 (69)
Fat	0.2 (3)	0.04 (0.6)
Protein	0.8 (12)	0.7 (11)
Minerals	0.5 (8)	0.8 (12)
Lactic acid	0.2 (3)	0.5 (8)

4.1.1.2Milk and whey protein concentrate production

Geographical spread

Worldwide whey production is confined almost exclusively to the European Union, North America, Australia and New Zealand. Although less than 45% of the total $4.8*10^8$ tonnes of fresh milk worldwide is produced in these countries (Table 3.5), they produce all but 2% of the worlds dried whey (Table 3.7).

Table 3.4 Worldwide annual whole fresh cows milk production, 1992-1999.

'000 tonnes	**1992**	**1993**	**1994**	**1995**	**1996**	**1997**	**1998**	**1999**
Africa	**15,406**	**15,354**	**16,023**	**16,982**	**17,498**	**17,981**	**18,522**	**18,824**
Asia	**73,627**	**75,606**	**77,484**	**79,443**	**80,801**	**81,367**	**88,892**	**90,503**
Europe	**235,714**	**230,133**	**224,622**	**221,850**	**216,590**	**212,052**	**212,008**	**209,353**
EU15	122,093	120,630	120,580	122,467	122,289	121,253	121,317	121,078
N.&C. Amer.	**86,453**	**86,662**	**88,323**	**89,420**	**89,169**	**90,707**	**91,964**	**94,612**
Oceania	**15,064**	**16,631**	**18,215**	**17,821**	**19,067**	**20,429**	**20,880**	**21,259**
S. America	**34,523**	**35,363**	**36,538**	**38,759**	**41,732**	**43,891**	**45,815**	**46,108**
World	**460,786**	**459,749**	**461,204**	**464,275**	**464,858**	**466,427**	**478,081**	**480,659**

The main whey producing countries are France, the USA, the Netherlands and Germany who between produce some 1,509 million tonnes of the total world production of 1,852 million tonnes in 1999 (Table 3.7). However, the Netherlands and France are easily the highest per litre converters of fresh milk to whey. Both countries convert on average over 2% of their fresh milk to dry whey on a weight per weight basis, well ahead of all other countries, which invariably convert less than 1%. These statistics, along with more detailed milk and whey production figures are presented in Tables 3.4 to 3.7.

Table 3.5 Percentage of worldwide whole fresh milk production in selected countries, 1992-1999.

	1992	1993	1994	1995	1996	1997	1998	1999
Austria	0.7	0.7	0.7	0.7	0.7	0.7	0.7	0.7
Belgium-Lux.	0.8	0.8	0.8	0.8	0.8	0.7	0.8	0.7
Denmark	1.0	1.0	1.0	1.0	1.0	1.0	1.0	0.9
Finland	0.5	0.5	0.5	0.5	0.5	0.5	0.5	0.5
France	5.6	5.5	5.5	5.5	5.4	5.3	5.2	5.1
Germany	6.1	6.1	6.0	6.2	6.2	6.2	5.9	5.9
Greece	0.1	0.2	0.2	0.2	0.2	0.2	0.2	0.2
Ireland, Rep.	1.2	1.1	1.2	1.2	1.1	1.1	1.1	1.1
Italy	2.4	2.3	2.3	2.4	2.5	2.4	2.4	2.3
Netherlands	2.6	2.4	2.4	2.4	2.4	2.3	2.3	2.3
Portugal	0.3	0.3	0.3	0.4	0.4	0.4	0.4	0.4
Spain	1.3	1.3	1.3	1.3	1.3	1.3	1.3	1.3
Sweden	0.7	0.7	0.7	0.7	0.7	0.7	0.7	0.7
UK	3.2	3.2	3.3	3.2	3.2	3.2	3.1	3.1
EU15	**26.5**	**26.2**	**26.1**	**26.4**	**26.3**	**26.0**	**25.4**	**25.2**
Canada	**1.7**	**1.6**	**1.7**	**1.7**	**1.7**	**1.7**	**1.7**	**1.7**
USA	**14.8**	**14.9**	**15.1**	**15.2**	**15.0**	**15.2**	**14.9**	**15.3**
Australia	**1.5**	**1.6**	**1.8**	**1.8**	**1.9**	**2.0**	**2.0**	**2.0**
New Zealand	**1.7**	**2.0**	**2.1**	**2.0**	**2.2**	**2.4**	**2.3**	**2.4**
% of world prod.	**44.5**	**44.4**	**44.7**	**45.1**	**45.0**	**44.9**	**44.1**	**44.3**

Table 3.6 Worldwide annual dry whey production, 1992-1999.

'000 tonnes	1992	1993	1994	1995	1996	1997	1998	1999
Africa	1.06	1.22	1.25	1.23	1.29	1.17	1.18	1.18
Europe	1,044	1,040	1,039	1,137	1,170	1,141	1,179	1,150
North America	631	613	622	607	585	587	595	603
Oceania	44.5	51.1	55.8	65.9	72.5	91.1	105.0	97.7
World	**1,721**	**1,705**	**1,719**	**1,810**	**1,828**	**1,820**	**1,881**	**1,852**

Table 3.7 Percentage of worldwide dry whey production in selected countries, 1992-1999.

	1992	1993	1994	1995	1996	1997	1998	1999
Austria	-	-	-	0.2	0.3	0.4	0.5	0.5
Belgium-Lux.	0.18	0.21	0.20	0.19	0.19	0.19	0.19	0.19
Denmark	1.5	1.4	1.5	1.8	1.9	1.9	1.8	1.8
Finland	0.8	0.8	0.9	0.6	0.2	0.2	0.3	0.3
France	27.6	28.1	28.9	29.8	28.3	27.7	29.8	28.6
Germany	9.1	8.6	9.2	8.5	10.1	10.9	10.5	10.7
Ireland, Rep.	1.9	1.7	1.4	2.1	1.9	1.7	1.8	1.8
Italy	0.2	0.2	0.3	0.3	0.3	0.3	0.3	0.3
Netherlands	16.1	16.9	14.6	15.4	16.8	15.4	13.1	13.3
Portugal	-	-	-	0.09	0.02	0.02	0.03	0.03
Sweden	0.16	0.16	0.16	0.08	0.04	0.04	0.04	0.04
UK	1.9	2.0	2.2	2.8	3.0	2.5	2.7	2.7
EU15	59.6	60.0	59.4	61.9	63.0	61.2	60.9	60.2
Canada	4.1	4.2	4.2	4.1	4.3	3.9	3.2	3.7
USA	32.6	31.8	32.0	29.4	27.7	28.3	28.5	28.9
Australia	1.8	2.2	2.2	2.6	2.7	2.6	3.0	3.0
New Zealand	0.8	0.8	1.1	1.0	1.2	2.4	2.6	2.3
% of world prod.	**98.8**	**99.0**	**98.9**	**99.0**	**98.9**	**98.4**	**98.1**	**98.0**

Production patterns

"I do not agree with them on this account, but also because the remedies they use are few in number; for, with the exception of acute diseases, the only medicines which they give are drastic purgatives, with whey, and milk at certain times."

So ventured Hippocrates, c.460–c.370 B.C., Greek physician, father of medicine, while ridiculing the contemporary Cnidian school of medical opinion. Whey indeed has a long history but despite its excellent functional and nutritional value it has traditionally been seen as an unwelcome by-product of cheese or casein production, and was used mainly for animal feed. Indeed, more than two-thirds of whey produced was disposed of as

waste as recently as the mid to late 1970's (Maubois and Ollivier, 1997). However as the range of uses and applications for whey has increased so has its level of production and utilization. This is evidenced by Fig. 3.1, which shows a healthy rate of growth of whey production compared with slower growth in milk production on a global and European basis between 1961 and 1999. Indeed this contrast is most apparent in the European Union. In the 15 years to 1999 since the imposition of the Common Agricultural Policy driven milk super levy in 1984 within European Union states, fresh milk production has actually decreased by 10% while dry whey production has increased by some 43% (Fig. 3.1).

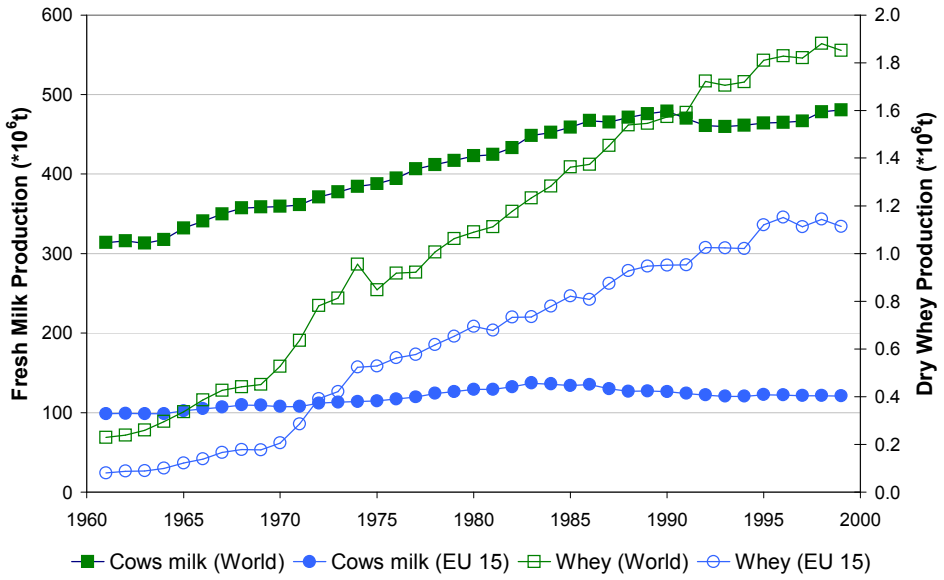

Figure 3.1 World and European fresh milk and dry whey production, 1961-1999.

One might argue that the increased production of whey might be attributed more to increased levels of cheese production from cows milk rather than being driven by any increased demand for dairy proteins (casein and whey) during this period. However Fig. 3.2 shows this not to be the case as the increased rate of dry whey production also

surpasses the rate of increase of cheese production (the plot includes only cheese from whole or skim cows milk and whey cheeses or non-cows milk cheeses are not included) over the period studied.

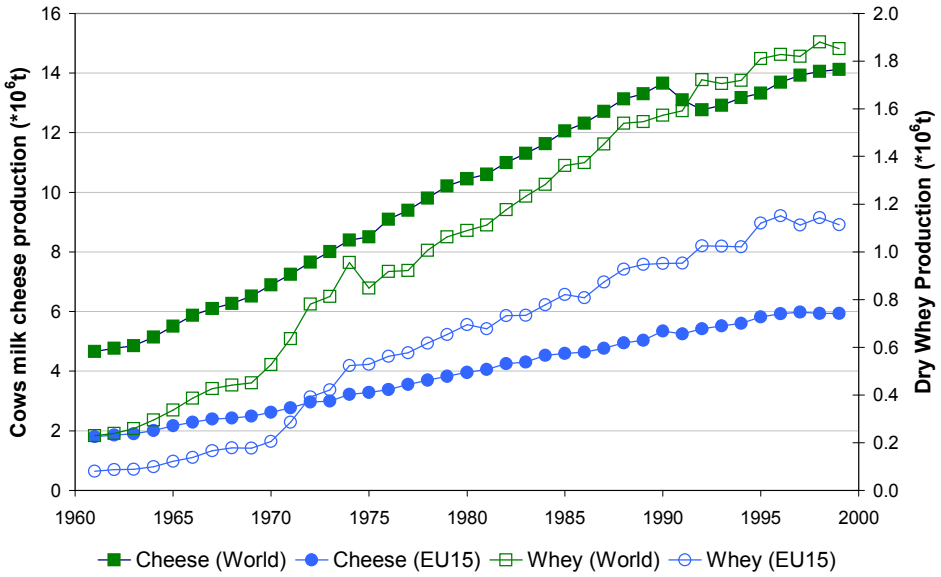

Figure 3.2 World and European cows milk cheese and dry whey production, 1961-1999.

Thus there has been a steady increase in dairy protein production over the past number of decades fuelled by a growing demand for whey proteins in particular as their functional and nutritional benefits have assumed increased significance. All data presented in section 3.1.2 are sourced from the statistical databases compiled and supplied by the Food and Agriculture Organisation (FAO) of the United Nations (2000).

4.1.1.3Whey protein concentrate manufacture

Production of whey

Whey is usually produced from whole or skim milk either by isoelectric precipitation of casein through acid addition or by rennet addition. Hydrochloric acid is the most commonly used acid and results in casein coagulation at pH 4.6 though sulphuric acid and lactic acid have also been used (Pearce, 1992). Rennet addition results in the hydrolysis of κ-casein which causes casein to coagulate. A range of other less commonly used methods of preparing casein and whey proteins exist though different methods produce whey of slightly different composition. These include centrifugation of casein micelles, calcium ($CaCl_2$) addition, salting out methods involving, for example, $(NH_4)_2SO_4$ or $MgSO_4$, ultrafiltration, chromatography (gel permeation or ion exchange), ethanol precipitation and cryoprecipitation (Fox and McSweeney, 1998).

Production of whey protein concentrate

The most common method for producing whey protein concentrate from acid or rennet whey is a process involving ultrafiltration and/or diafiltration. The process is described in detail by Morr (1989) and in the Ultrafiltration and Microfiltration Handbook (Cheryan, 1998) but a brief description is provided here. Reverse osmosis is sometimes employed initially to boost solids concentration before the whey is subjected to a pre-treatment process that may involve gentle heat treatment (to minimise protein denaturation during the subsequent process), pH adjustment, addition of calcium or calcium complexing agents (to prevent the formation of insoluble and colloidal calcium phosphate complexes), and gentle centrifugation or quiescent standing to remove larger solid materials such as insoluble cheese curd, milk fat, etc. Pre-treatment improves the efficiency of subsequent separation techniques and helps preserve the proteins excellent nutritional and functional properties (Rinn et al, 1990). Much of the lactose, salts and minerals are then removed either by ultrafiltration (a membrane filtration process) or diafiltration (an ultrafiltration process where water is added during the process to further remove lactose and salts), followed by vacuum evaporation and either freeze-drying or spray drying. Ultrafiltration is employed for the manufacture of whey protein concentrate containing 35% to 55% whey protein while diafiltration, which

produces a purer protein concentrate, is used to produce 65% to 85% WPC. Other methods of WPC production include demineralisation by electrodialysis and/or ion exchange, thermal evaporation of water and crystallisation of lactose (Fox and McSweeney, 1998). Whey protein isolate (WPI) is a product with even higher concentration of protein (> 90%) and is produced using ion exchange chromatography followed by washing (to rid of lactose and salts), pH adjustment and spray drying. An alternative method employed to produce WPI pioneered in the USA by Glanbia (2000) involves cross-flow microfiltration which results in a WPI which has more calcium and less sodium than a production process involving ion exchange though protein concentration is lower (Jost et al, 1999).

4.1.1.4Functionality and uses of whey proteins

Functional properties

The functional properties of WPC are heavily influenced by the functionalities of its two main proteins, α-lactalbumin and β-lactoglobulin, and by their relative abundance. Table 3.8 demonstrates the typical amounts of proteins present in bovine milk. The functional properties of these two proteins are quite dissimilar and will be discussed separately in detail in sections 3.1.5 and 3.1.6.

Whey protein concentrates find many functional uses as a food ingredient as they are used to convey such properties as solubility, gelation, water holding capacity (swelling), viscosity, emulsification, and foaming (Walstra et al, 1999). Thus whey protein concentrates find uses as ingredients in a wide range of foods including bakery products (Cocup and Sanderson, 1987), infant formulae (Jost et al, 1999) and nutritional speciality products (McDermott, 1987), chocolate and confectionary (Campbell and Pavlasek, 1987), meat products (van den Hoven, 1987), beverages, deserts and textured food products (de Wit, 1989b).

Table 3.8 Typical protein composition in rennet whey protein concentrate (Sources; Morr (1989), Pearce (1989), Huffman (1997), Gésan-Guiziou et al (1999)).

Whey Protein	*% of total whey protein (w/w)*
β-lactoglobulin (β-lg)	45-55
α-lactalbumin (α-la)	14-18
Immunoglobulins (Ig)	5-11
Bovine serum albumin (BSA)	2-6
Casein derived peptides (proteose peptides)	20-26
Enzymes	< 2

The functional properties of different whey protein concentrates may vary quite substantially depending upon the production process used and the relative amounts of, for example, fat and minerals present. For example, protein levels in WPC can have an effect on the rheological properties of resulting gels (Mleko et al, 1994) as well as gelation time (Steventon et al, 1991). Protein solubility, which is important for beverages, ranges from 85% to over 90% among 34% whey protein concentrates (Harper and Man Lee, 1997). The degree of solubility can be negatively affected, for instance by pasteurisation of the ultrafiltration retentate during WPC production though not by pasteurisation of the raw milk (Morr, 1987). Likewise, the presence of lipids (consisting mainly phospholipids and milk fat globule membrane material (Morr, 1989)), which tend to decrease with increased WPC protein content, leads to a marked decrease in foam forming properties and stability (Richert et al, 1974). Mineral content in WPC can also have an effect on functionality and levels of calcium and other minerals can vary quite considerably depending on manufacturing process (Morr, 1989). Generally lactose is considered a filler and has little effect on protein functionality.

Uses

Whey proteins find a wide range of applications as food ingredients as a result of their numerous functional properties (Morr, 1992). In addition, whey proteins provide the

highest nutritional value for human beings, far ahead of any other source of protein (Hambraeus, 1992). Table 3.9, adapted from de Wit (1989b) and Fox and McSweeney (1998) outlines a number of these applications which stem from their physiological or pharmaceutical properties in addition to their functional or nutritional properties. Further applications of whey proteins may stem from their potential antioxidant (Decker et al, 1997), anti-cancer (McIntosh et al, 1995; Smithers et al, 1997, Parodi, 1998) and anti-tumour effects (Chmiel, 1997) as well as ingredients in cosmetics particularly for babies (Negishi, 1997).

Table 3.9 Whey protein applications in foods (adapted from de Wit (1989b) and Fox and McSweeney (1998)).

Used in:	*Effect:*
Bakery products	
Bread, cakes, muffins, croissants	Nutritional, emulsifier, egg replacer, dough formation, heat setting
Dairy products	
Yoghurt, quarg, ricotta cheese	Yield, nutritional, consistency, curd cohesiveness
Cream cheeses, cream cheese spreads, sliceable/squeezable cheeses, cheeses fillings and dips	Emulsifier, gelling, sensory properties
Beverages	
Soft drinks, fruit juices, powdered or frozen orange beverages	Nutritional, solubility
Milk-based flavoured beverages	Viscosity, colloidal stability
Chocolate drink (pH 6.5)	Colloidal stability
Dessert products	
Ice-cream, frozen juice bars, frozen dessert coatings	Skim milk solids replacement, whipping properties, emulsifying, body/texture
Whipped topping	Whipping ability with fat
Dressings	
Salad dressing	Emulsifying ability at pH 4.0
Confectionary	
Aerated candy mixes, meringues, sponge cakes	Whipping properties, emulsifier
Meringue	Foam stability at high temperature
Meat products	
Frankfurters, luncheon meats	Pre-emulsion, gelation
Ham	High solubility at low viscosity
Convenience and textured foods	
Wide range of foods	Various functional and nutritional properties
Nutritional foods	
Special dietary preparations for athletes, dieting patients/persons, etc	Nutritional, physiological, pharmaceutical
Infant formulae	Nutritional, physiological

4.1.1.5α-lactalbumin

Composition and structure of α-lactalbumin

α-lactalbumin is the principal whey protein in human milk comprising about 42% of total whey protein though it is only the second most prevalent whey protein in bovine milk behind β-lactoglobulin containing about one fifth of total whey protein (Table 3.2). Its biological function is as a coenzyme in the synthesis of lactose (Walstra et al, 1999). It is a calcium metalloprotein and has a molecular weight of 14,176 and consists of some 123 amino acids. It contains 4 disulfide linkages but no phosphate groups. Two genetic variants exist; type B contains one arginine residue and is the only variant secreted by western cattle. Type A has a glutamic acid residue replacing the arginine and is far less common (Fox and McSweeney, 1998). The primary structure of the α-lactalbumin molecule is shown in Fig. 3.3.

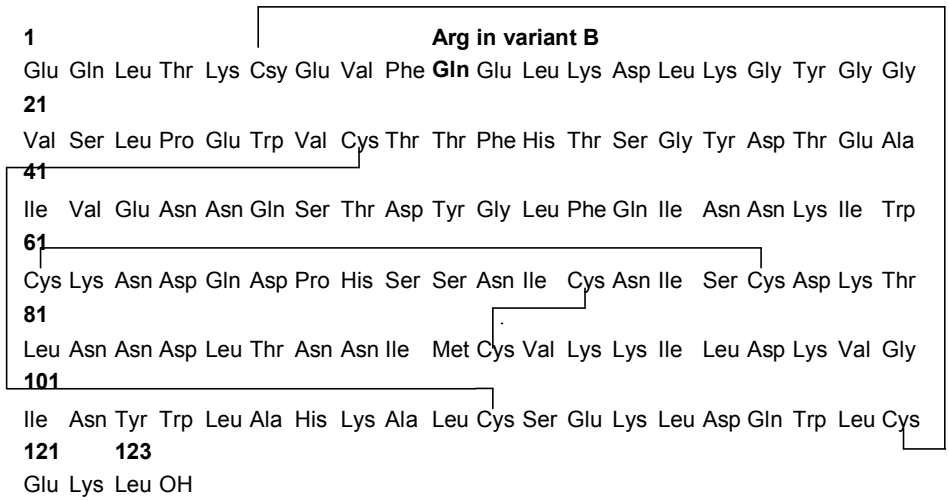

Figure 3.3 Primary structure of α-lactalbumin including disulphide bonds (from Brew and Grobler, 1992).

α-lactalbumin has a compact near spherical tertiary structure as can be seen from Fig. 3.4.

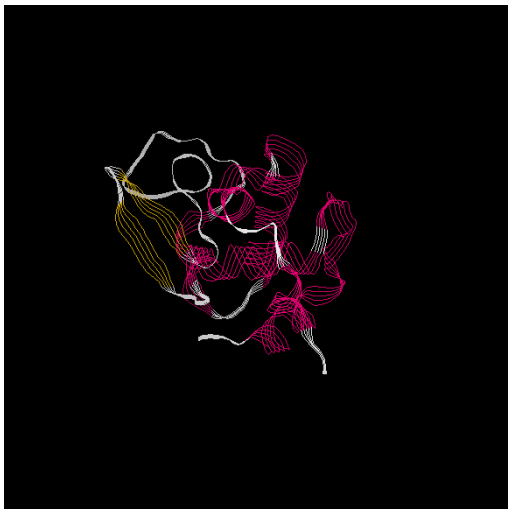

Figure 3.4 The globular tertiary structure of α-lactalbumin reproduced from Vogel (2000) (with author's permission).

Functional and nutritional properties of α-lactalbumin

The α-lactalbumin molecule is rich in the essential amino acids tryptophan (4 residues per mole), threonine (7 per mole) and isoleucine (8 per mole) (Swaisgood, 1982), all of which are typically present in lower relative proportions in bovine milk than in human milk (Coultate, 1996) and has an amino acid profile similar to that of human milk (Heine et al, 1996). It is therefore an ideal ingredient in infant formulae (Heine et al, 1991; de Wit, 1998; Chatterton et al, 1999) as well as nutritional fortification formulae, athlete training formulae and sports drinks. It may also find use as an ingredient in therapeutic medical foods (Maubois and Ollivier, 1997). α-lactalbumin also has good emulsification and foaming properties (de Wit, 1989a). Tossavainen et al (1998) reviewed the functional properties of α-lactalbumin against β-lactoglobulin fractions produced at pilot scale from a number of studies. They found the solubility of α-lactalbumin to be lower than β-lactoglobulin at pH 6.7, α-lactalbumin emulsion stability was lower (at 0.15% protein concentration) but the apparent viscosity of α-lactalbumin was higher than β-lactoglobulin.

Thermal denaturation of α-lactalbumin

The thermal partial denaturation of α-lactalbumin accompanied by precipitation and aggregation around its isoelectric point is a widely employed technique used to separate an α-lactalbumin rich precipitate fraction from a β-lactoglobulin rich fraction during whey protein fractionation. α-lactalbumin is an extremely soluble protein and remains in solution in the pH range 3.0-9.0 under 50°C (Pearce, 1983b). However as α-lactalbumin is a calcium metalloprotein, the removal of the calcium ion at temperatures above about 55°C results in a reversibly denatured form known as apo α-lactalbumin. (Bernal and Jelen, 1984). Pearce (1989) surveys a number of studies which investigate the temperature at which α-lactalbumin begins to partially denature over a range of pH values around and above its isoelectric point at 4.2. The midpoint transition temperatures are reported variously as 65.2°C at pH 6.7, 62-63°C at pH 6.5, 61°C between pH 4.5 and 6.5 and decreasing to 58.6°C at pH 3.5. This protein is very heat stable in that irreversible thermal denaturation does not occur until temperatures of up to 77°C and beyond (Pearce, 1989).

4.1.1.6β-lactoglobulin

Composition and structure of β-lactoglobulin

β-lactoglobulin is the most abundant whey protein in bovine milk comprising about half the total whey proteins present. It is unique to ruminants (though a closely related protein occurs in pigs, kangaroos, dolphins, etc. (Fox and McSweeney, 1998)) and is only present in negligible quantities in human milk. It has a residue sequence similar to that of retinol-binding proteins (Papiz et al, 1986) and is present in species which transport high levels of immunoglobulins during the formation of colostrum. Its biological function is thought to be that of retinol bearer from parent to offspring (de Wit, 1998). β-lactoglobulin contains 162 amino acids and has a molecular weight of about 18,283 depending on the genetic variant. Most bovine milk contains four principal genetic variants (A,B,C,D) though Eigel et al (1984) identified an additional four. β-lactoglobulin exists as a dimer between about pH 5.2 and 6.7, as an octamer between about pH 3.5

and 5.2 and as a monomer below 3.5 and above 6.7 (de Wit, 1989a). The protein is strongly hydrophobic and has a very compact globular tertiary structure. Fig 3.5 shows the primary structure of β-lactoglobulin.

Figure 4.5 Primary structure of β-lactoglobulin including disulphide bond between Cys 66-160 and dynamic disulphide bond between Cys 119-106 and 106-121 (from Swaisgood, 1982).

Functional and nutritional properties of β-lactoglobulin

β-lactoglobulin is present in negligible quantities in human milk and is the protein most commonly held responsible for the allergies that a small proportion of babies suffer from cows' milk. The protein is responsible for the excellent gelation properties of whey proteins (Maubois and Ollivier, 1992) and has found uses, among other things, as a fat replacer in processed meats (Pearce et al, 1997) or in edible films. It is also an excellent emulsifier. Both α-lactalbumin and β-lactoglobulin are responsible for the good foaming

properties of WPC though β-lactoglobulin is the better of the two (de Wit, 1989a) and is an ideal foaming agent in frozen deserts (Rantamaki at al, 1997). Like α-lactalbumin, β-lactoglobulin exhibits good solubility aver a broad pH range and particularly under acidic conditions (>97% at pH 3.0) and is thus suitable for use in protein fortified fruit juice drinks and sports beverages (Smithers et al, 1996).

Thermal denaturation of β-lactoglobulin

Reversible denaturation of β-lactoglobulin occurs at above about 65°C and this is followed by the onset of irreversible denaturation of the protein above about 70°C (Fox and McSweeney, 1998). Bernal and Jelen (1985) report denaturation temperatures of 75.9°C at pH 6.5, 77.8°C at pH 5.5, 81.2°C at pH 4.5, 81.9°C at pH 3.5 and 78.7°C at pH 2.5. Since reversible denaturation of β-lactoglobulin occurs at temperatures above that at which apo α-lactalbumin forms, this allows for the selective precipitation of an α-lactalbumin rich precipitate phase from WPC and its subsequent fractionation from a soluble β-lactoglobulin rich phase.

4.1.1.7Other whey proteins

Bovine serum albumin

The Bovine Serum Albumin (BSA) found in milk is as a result of leakage of the BSA present in blood where it is a carrier of free fatty acids. Thus the molecule is not synthesised in the mammary gland and it probably has little functional use in milk. It is a rather large elongated molecule of about 3 x 12 nm in size (Walstra et al, 1999) of molecular weight approximately 66,000 Da. This corresponds to a molecule diameter of about 5nm which compares with about 4nm for β-lactoglobulin, 3nm for α-lactalbumin and 0.3nm for water (Hobman, 1992). It has been suggested that the presence of bovine BSA in infant formulae may be in part responsible for precipitating type I diabetes in a small proportion of infants (Marincic, 1999). As a food ingredient it has good emulsification properties (Waniska et al, 1981) and solubility (de Wit, 1989a). BSA is

partially denatured to form a precipitate between 42°C and 50°C (de Wit, 1989a), but full denaturation does not occur until around 72-74°C (Bernal and Jelen, 1985).

Immunoglobulins

Immunoglobulins (Ig) are a large heterogeneous group of antibody proteins synthesized in the bloodstream and are part of the passive immunity transported to the neonate via colostrum in many species until the young is able to synthesise its own antibodies. Because of this they are present in much lower concentrations in milk than in colostrum and falls from about 10% to about 0.1% of bovine protein in the first week post partum (Mulvihill, 1994). Human infants do not require Ig's from milk as they've already received it *in utero* and indeed are not capable of ingesting Ig's through the intestine (Fox and McSweeney, 1998). The immunoglobulins present in bovine milk include IgG_1, IgG_2, IgA and IgM. All have a similar basic structure being composed of 2 light chains with molecular weights of 20,000-25,000 Da with two heavy chain each having molecular weights of between 50,000 and 70,000 Da. Those present in bovine milk range in size from about 150,000 Da to 900,000 Da. In terms of functional properties, immunoglobulins are best noted for their gel strength which is far superior to α-lactalbumin but inferior to β-lactoglobulin (de Wit, 1989a).

Proteose peptones

Proteose peptones (pp) are defined as the mixture of phospho(glyco)peptides remaining in solution after milk has been heated at 95°C for 20 minutes and then acidified to pH 4.6, which can then be precipitated with 12% trichloroacetic acid (de Wit, 1989a). The majority of proteose peptones comprise the debris of β-casein degradation during rennet induced coagulation, otherwise known as glycomacropeptides (GMP). These include proteose peptone 5 (pp5), proteose peptone 8 fast (pp8f) and proteose peptone 8 slow (pp8s). An unusual feature of proteose peptones is that they contain no aromatic amino acids and thus are nutritionally suited to patients suffering from phenylketonuria

(Mulvihill, 1994). The proteose peptones are by definition resistant to heating and are good emulsifiers (Huffman, 1997).

Other Milk Proteins

Lactoferrin (Lf) is an iron binding protein with antibacterial properties. It is present in very large quantities in human milk (it is actually the principal whey protein) but is normally a minor protein in bovine milk. It has thus found an increasing market as a natural antibiotic (with potential uses in mouthwash solutions or in chewing gum (Maubois and Ollivier, 1997)) and as an ingredient in infant formulae (Smithers et al, 1996).

Lactoperoxidase (LPO) is another protein with significant antibacterial activity, but which occurs at higher concentration in bovine milk than in human milk.

Other minor bovine whey proteins include indigenous enzymes, vitamin binding proteins (for vitamins A, B_2, B_{12}, D and folate) and various growth factors including bifidus factors which promote the growth of bifidobacteria.

4.1.2 Whey protein precipitation and fractionation

4.1.2.1Composition of whey protein concentrate

Size exclusion high performance liquid chromatography (HPLC) is commonly used to identify and quantify the individual protein fractions in WPC where individual proteins are identified by elution time which exhibits an inverse relationship with protein molecular weight (Dimenna and Segall (1981), Pearce (1983a), Kinghorn et al, (1995)). The relative concentration of the two major whey proteins, β-lactoglobulin and α-lactalbumin is typically somewhere around 2.5 (Pearce, 1989) for rennet whey though this can vary substantially and there can be a huge variation in concentrations of individual proteins throughout the season, from season to season and between breeds. Regester and Smithers (1991) found that while the β-lactoglobulin content in WPC increased

throughout the season, and especially towards the end of lactation α-lactalbumin reached its peak mid-season and fell off thereafter. They also found levels of proteose peptones (casein derived peptides) varying from 10.6% to 27.4% of total whey proteins in milk, the latter figure being recorded four months into lactation during mid season when overall milk yield is maximum. Other large variations were reported for the α-lactalbumin content (9.4%-19.5%) and β-lactoglobulin (49.3%-59.7%). Moreover, in an earlier study, Larson and Kendall (1957) found considerable differences in whey protein content between breeds of cattle finding, for example, that the β-lg/α-la ratio was consistently considerably lower for say, Holsteins than for Guernsey cows as was the percentage by weight of immunoglobulins present. Gray and Mackenzie (1987) reported a reduction in both α-lactalbumin and β-lactoglobulin following a reduction in pasture intake of cows, as might be expected, though they found no significant decrease in non-mammary synthesised whey proteins such as BSA and the immunoglobulins.

4.1.2.2WPC fractionation

The exploitation of the individual whey proteins to date has not been fully realised. Apart from poor marketing by the dairy industry of the potential uses of individual whey proteins in non-food areas such as biotechnology, healthcare and veterinary medicine, and the sometimes inconsistent and unreliable physical functional performance of whey proteins in food systems, Smithers el al (1996) identified a lack of 'viable industrial technologies' to effect the isolation of individual whey proteins as a key reason for this under utilisation. Large scale production of α-lactalbumin and β-lactoglobulin fractions does not currently exist, though a small number of companies globally are reported to produce a α-lactalbumin rich fractions on a 'pre-commerial' basis (Jost et al, 1999). To the author's knowledge, there is only one such producer of an α-lactalbumin rich whey protein fraction in Ireland at present and this also is at pilot scale. However, a number of processes have been proposed, one of which has been adapted at both laboratory and pilot scale in this study.

4.1.2.3WPC isoelectric precipitation

The method of whey protein precipitation used here, has been described as probably the most commercially amenable technique available (Mulvihill, 1994) and is based on that described by Pearce (1983b, 1987). It involves pH and temperature adjustment in a batch agitation vessel to perform isoelectric precipitation. This results in the formation of precipitates rich in α-lactalbumin, BSA and immunoglobulins which can then be separated from the supernatant phase containing β-lactoglobulin and proteose peptones.

pH, temperature and concentration effects

Pearce (1983b) showed it was possible to selectively precipitate an α-lactalbumin rich fraction by adjusting pH of a WPC solution to around the isoelectric point of α-lactalbumin (pH 4.2-4.5) while heating to within the temperature range at which α-lactalbumin begins to partially denature (55°C-65°C) which is also below the denaturation temperature of β-lactoglobulin (72°C). Each α-lactalbumin molecule is attached to a single calcium ion which serves to stabilize the tertiary structure of the metalloprotein. α-lactalbumin forms an intermediate and reversible 'apo' form between 55°C and 65°C and around its isoelectric point, which may be related to the dissociation of the calcium ion (Bramaud et al, 1995). The partial denaturation and resultant precipitation of α-lactalbumin under these conditions facilitates separation ('fractionation') from a β-lactoglobulin rich supernatant by, for example, centrifugation or ultrafiltration (see section 3.1.3) which may be followed by subsequent dissolution and recovery of native α-lactalbumin by means of temperature and pH readjustment.

Optimal pH and temperature conditions for the preferential precipitation of α-lactalbumin have been recommended by various authors. Pearce (1983b) found optimum pH varied depending on the concentration of whey protein concentrate in solution. Using HCl to reduce pH and heating to a temperature of 65°C for 30 minutes, he suggested optimum pH of 4.3, 4.0 and 3.8 for cheese whey concentrations of 7, 14 and 21% (total solids in

solution) respectively and suggested 14% as an optimum for precipitation and separation by centrifugation. Pearce (1983b) further suggested that the 21% concentration might be too high due to increased density and viscosity which would hinder sedimentation of the particles during centrifugation. Pierre & Fauquant (1986) used clarified whey and suggested an optimum pH of 3.8 at an α-lactalbumin concentration greater than 12 g/kg, and pH 4.2 at α-lactalbumin concentration less than 12 g/kg while holding at 55°C for 30 minutes. Bramaud at al (1995) confirmed the reduction in optimum pH as WPC concentration increased in the range 6 to 60g/L. Pierre & Fauquant (1986) also noted that a higher α-lactalbumin content resulted in higher levels of precipitation in the range 6-21 g/kg α-la at 65°C for 30 minutes ageing. Gésan-Guiziou et al (1999) concurred with this as did Bramaud at al (1995) noting a sharp decline in the precipitated fraction of α-lactalbumin below an α-lactalbumin concentration of 3 g/L when concentrations from 0.5 - 9 g/L were investigated at 60°C for 150 minutes.

Pearce (1987) carried out protein fractionation at pilot plant scale using 12% total solids content by heating to 64°C for 5 minutes at pH 4.2 as did Gésan-Guiziou et al (1999) using both defatted Gouda WPC and acid WPC. Acid WPC was found to yield higher purity β-lactoglobulin fractions due to the absence of proteose peptones in acid WPC. Bramaud et al (1995) using defatted WPC with total solids content 6 g/L and increased the ionic strength of the solution tenfold by adding NaCl and found that the optimum pH fell from about 4.1 to around 3.8 at 60°C. They also noted that although almost all precipitation occurred during the first 30 minutes, equilibrium is reached only after 150 minutes of heat treatment though Gésan-Guiziou et al (1999) found no further precipitation at very high initial protein concentrations for clarified acid whey (146 g/L). Bramaud et al (1997a) suggested using citric acid and sodium citrate as a calcium complexation agents to reduce the free calcium concentration in WPC. Bramaud et al (1997b) further noted that the addition of citrates (at pH 3.9 for 150 minutes) enables preferential precipitation of α-lactalbumin at lower temperatures. This resulted in higher

precipitation efficiencies but only at protein concentrations < 65 g/L (Gésan-Guiziou et al, 1999). Preferential precipitation of α-lactalbumin is possible because the rate of increase in precipitation of co-precipitates such as BSA and the immunoglobulins at lower temperatures is not as great as that of α-lactalbumin when citrate is added.

Shear effects

Pierre and Fauquant (1986) mentioned stirring the solution during a 30 minute ageing period, though neither the extent nor effect of agitation were considered. Shear effects during precipitation and ageing of other proteins (e.g. soya) have been studied and reported on by a number of authors (section 3.3). Agitation of the WPC solution during conditions conducive to the partial denaturation and precipitation of α-lactalbumin increases opportunities for collision and structured aggregation. Conversely, aggregates aged under quiescent conditions tend to be larger and less dense than aggregates which are exposed to shear during precipitate formation and ageing. The size and nature of particles formed during these formative stages may affect their ability to withstand exposure to higher shear-rates during subsequent pilot or production scale processing and ultimately on the efficiency of centrifugal separation of phases.

4.1.2.4Whey protein separation

Fractionation of the individual whey proteins is completed by separating the α-lactalbumin rich precipitates from the supernatant rich in β-lactoglobulin. This can be achieved by a number of methods including centrifugal separation and membrane technology (e.g. microfiltration).

Centrifugal separation

Centrifugal separation has been used a means of separating precipitates rich in α-lactalbumin from a β-lactoglobulin rich supernatant in the processes of Pearce (1987), Fauquant et al (1985), Pierre and Fauquant (1986), Bramaud et al. (1997a), Maubois et

al (1987) and by Amundson et al (1982) and is the usual technology used to effect recovery of protein precipitates (Twineham et al, 1984). Efficient centrifugal separation of precipitates requires feed particles of reasonable size and capable of withstanding the considerable turbulence and shear experienced during processing through pumps, pipes and, in particular, at the inlet zone of a disc stack centrifuge where precipitates experience rapid acceleration (Virkar et al, 1981; Bell and Dunnill, 1982b; Bell, 1982; Bell et al, 1983; Twineham et al, 1984; Hoare et al, 1987; Clarkson et al, 1994).

Other techniques for precipitate separation

Microfiltration (retains particles in the range 0.1 to about 5 microns), ultrafiltration (range 0.001-0.02 microns (Cheryan, 1998)) and diafiltration or a combination these technologies are alternative methods used to separate α-lactalbumin precipitates from β-lactoglobulin. Diafiltration involves the addition of extra water to wash the membranes to which larger macromolecules adhere (i.e. repeated ultrafiltration) and is necessary when protein concentration is greater than 60-65% (Hobman, 1992). Bramaud (1995) used diafiltration but reported that low transmission of β-lactoglobulin limited separation efficiency. Gésan-Guiziou et al (1999) used diafiltration for the separation of the soluble β-lactoglobulin enriched fraction and ultrafiltration for the final purification of α-lactalbumin. These methods were employed at laboratory scale and at pilot scale on both acid and Gouda rennet whey resulting in yields in the range 52-83% and 85-94% for α-lactalbumin and β-lactoglobulin respectively. The authors acknowledged that there was room for optimisation with respect to the final separation of α-lactalbumin.

4.1.2.5Other techniques used for WPC fractionation

Apart from whey protein fractionation on the basis of isoelectric precipitation, a number of other whey protein separation techniques have been described in the literature. Aschaffenburg and Drewry proposed a salting out procedure as far back as 1957 where Na_2SO_4 addition followed by pH adjustment to 2.0 was used to precipitate out all proteins except β-lactoglobulin. Fox et al. (1967) suggested adding trichloroacetic acid to

cause all proteins bar β-lactoglobulin to precipitate. Processes involving the salting out at low pH of an α-lactalbumin rich precipitate have been proposed by Kaneko (1985) (with $FeCl_3$), Kuwata et al (1985) (with $FeCl_3$), Maillard and Ribadeau-Dumas (1988) (with NaCl), Maté and Krochta (1994) (with NaCl) and by Al-Mashikhi and Nakai (1987) (with sodium hexametaphosphate). A variation of the process undertaken in this study involves the readjustment of calcium ion levels using citric acid to effect calcium chelation in order to encourage the precipitation of α-lactalbumin (Fauquant et al, 1985; Pierre and Fauquant, 1986; Bramaud et al, 1995; Bramaud et al, 1997). Amundson et al (1982) developed an alternative fractionation process in which pre-concentrated whey is demineralised by electrodialysis at pH 4.65 (the optimum pH for whey protein demineralisation and for β-lactoglobulin precipitation). Slack et al (1986) developed this method at pilot scale. Ion exchange chromatography methods have been proposed by Manii et al (1985), Yoshida (1990), Carrère et al (1994) and Ohtomo and Kuwata (1994) and a number of industrial scale ion exchangers (e.g. Spherosil, Vistec, Indion) more commonly used to produce whey protein isolate can also be used to fractionate whey proteins for commercial use (Donnelly and Mehra, 1990). All proteins are absorbed initially on the resin but as throughput increases with time β-lactoglobulin, which has a greater affinity with the gel, displaces α-lactalbumin and BSA giving an eluent rich in these proteins (Mulvihill, 1994). However these techniques would seem to have very limited commercial potential in terms of large scale production of individual whey protein fractions (Pearce, 1992a). Other separation methods involve the use of ion exchange beads in stirred tanks (Etzel, 1995) and ion exchange membranes as described by Weinbrenner and Etzel (1994), and by Etzel (1995) who suggested that this may ultimately be a more efficient and economical method than the other ion exchange methods available.

4.1.3 Protein precipitate growth and breakage under shear conditions

The application of shear, for example due to impeller agitation, during and after protein precipitation can play an important role in influencing a number of aggregate properties including size, density or compactness and strength. This is significant as these properties contribute to the separation efficiency during any subsequent centrifugal operation.

4.1.3.1Aggregate growth

Precipitation of whey proteins may be considered a three stage process: the first stage is the partial denaturation and unfolding of α-lactalbumin which occurs optimally at its isoelectric pH and around temperature 60°C as described in detail in section 3.1.5.3. The second stage is the aggregation of the unfolded protein with other similarly unfolded proteins to form small primary particles and the third stage involves primary particles colliding with each other and form larger aggregates. The first two stages occur rapidly, Bell (1982) suggests up to 1 second for protein molecules in stirred tanks with low molecular weight precipitation agents, while aggregation of primary particles takes place on a larger time scale (Petenate and Glatz, 1983).

The kinetics involved in the isoelectric precipitation and growth of protein aggregates have been widely reported (Hoare, 1982; Virkar et al, 1982; Bell et al, 1983, Petenate and Glatz, 1983, Nelson and Glatz, 1985, Fisher and Glatz, 1988) and broadly follow the theory first propounded by Smoluchowski (1917). This describes initial formation of small primary particles when diffusional effects dominate (in a process known as perikinetic growth) which then collide and aggregate as a result of convectional and fluid shear forces to form much larger precipitate particles (orthokinetic growth). A simple model for perikinetic growth with mono-sized spherical particles can be described according to Smoluchowski's theory in terms of the initial rate of decrease in particle number concentration:

$$-\frac{dN}{dt} = 8\pi\Delta dN^2 \qquad 3.1$$

A more comprehensive from of this model is required to encompass a range of particle size distributions and the following general rate equation has been used to model perikinetic growth:

$$\frac{dN_k}{dt} = \frac{1}{2}\alpha\left\{\sum_{i=1}^{i=k-1} 2\pi(d_i + d_j)(\Delta_i + \Delta_j)N_i N_j\right\} - \alpha N_k\left\{\sum_{i=1}^{\infty} 2\pi(d_i + d_k)(\Delta_i + \Delta_k)N_i\right\} + \frac{1}{2}\alpha\left\{8\pi d_k \Delta_k N_k^2\right\} \qquad 3.2$$

Moreover the rate of decrease in particle number concentration by spherical mono-sized particles in a field with uniform shear rate, G, for orthokinetic growth reads:

$$-\frac{dN}{dt} = \frac{2}{3}\alpha G d^3 N^2 \qquad 3.3$$

This can also be expanded to an expression analogous to 3.2 for orthokinetic growth:

$$\frac{dN_k}{dt} = \frac{1}{2}\alpha\left\{\sum_{i=1}^{i=k-1}\frac{1}{6}(d_i + d_j)^3 G N_i N_j\right\} - \alpha N_k\left\{\sum_{i=1}^{\infty}\frac{1}{6}(d_i + d_k)^3 G N_i\right\} + \frac{1}{2}\alpha\left\{\frac{4}{3}d_k^3 G N_k^2\right\} \qquad 3.4$$

On the right hand side of equations 3.2 and 3.4 the first term describes the rate of formation of particles of diameter d_k by collisions of smaller particles while the second term is the rate of loss of particles of diameter d_k by collision, and the final term takes into account collisions between similar particles in the second term having been counted twice. Smoluchowski's growth theory has been experimentally tested on a number of

aggregating particles providing reasonable agreement including precipitating casein aggregates (Hoare, 1982) and reportedly on latex particles and colloidal metal dispersions (Bell et al, 1983).

The size of primary particles plays a significant role in the properties of the aggregates they comprise. Nelson and Glatz (1985) showed how smaller primary particles may lead to larger aggregate size. In addition, Bell (1982) suggested that smaller primary particles contribute to denser more compact particles and ultimately stronger particles. In turbulent fluid shear environments, Bell (1982) proposed, on the basis that primary particles grow by diffusional perikinetic growth within respective turbulent eddys, that the limiting size attained by primary particles depends upon the amount of protein within a given eddy and the degree of mixing and hence is a function of both protein concentration and micromixing time (i.e. the characteristic time for micromixing based on molecular diffusion between eddys and the bulk fluid). Micromixing time is itself a function of the turbulent microscale and hence of impeller shear-rate. Nelson and Glatz (1985) however suggested primary particle growth may be solely diffusional and proposed a model involving homogeneous nucleation based on expressions first proposed by Nielsen (1964). Such a model disregards the presence of fluid eddys and was used to satisfactorily model primary particle size of soy protein precipitate as a function of concentration only.

In any case, primary particles are generally of sub micron diameter, typically between 0.2 - 0.5 μm, (Steventon, 1992) though this can vary depending on the species involved (Hoare, 1982) and may be as high as 10μm in low shear environments (Bell et al, 1983). Above this size orthokinetic growth becomes more important. Under conditions of ideal temperature and pH, precipitation occurs rapidly and growth involves the supplementation of growing aggregates with primary particles rather than the union of larger aggregates (Glatz et al, 1986). Freshly aggregated particles comprise a strong inner core of strongly bound proteins surrounded by a very porous network of loosely bound primary particles (Ayazi Shamlou et al, 1996a).

4.1.3.2Aggregate breakage

Agitation introduces an opposing force to growth. Particle breakage or 'de-aggregation' accompanies aggregate growth and the two occur concurrently until a period of equilibrium is eventually reached between the two opposing effects (Ayazi Shamlou et al, 1996b). In an agitation vessel, there exists a relation between maximum aggregate size and power dissipation per unit volume and hence between maximum aggregate size and the turbulent microscale or eddy size (Tomi and Bagster, 1978) (see equation 4.6). Aggregates equal to or larger than eddy size suffer breakage from inertial forces due to particle-particle or particle-solid collisions or hydrodynamic shear whereas aggregates smaller than eddy size are exposed predominantly to viscous fluid induced shear stresses leading to rupture or 'bulgy deformation' (Bell and Dunnill, 1982a, Petenate and Glatz, 1983, Tambo and Hozumi, 1979, Ayazi Shamlou et al, 1994b, Spicer et al, 1996, Ayazi Shamlou et al, 1996a, Ayazi Shamlou et al, 1996b). Ayazi Shamlou and Titchener-Hooker (1993) suggest however that viscous stresses continue to play an important role in breakage for up to ten times the turbulent microscale.

In addition the fluid induced stresses which cause erosion of the aggregates are up to 100 times greater in the small zone immediately around the impeller blade, where flow is strongly accelerating, than in the slower moving bulk fluid (Ayazi Shamlou et al, 1994a). Breakage of aggregates substantially larger than the turbulent microscale here is mainly due to normal hydrodynamic shear due to the large pressure differences which prevail, whereas disruption is due to tangential shear stresses for aggregates well below the turbulent microscale and a combination of both for aggregates of about the same size (Ayazi Shamlou et al, 1994a). Thus maximum inertial shear effects occur where particles are approximately equal to eddy size (Hoare, 1982). Particle-particle and particle-solid collisions are thought to cause a relatively insignificant amount of breakage even for comparatively large particles due to the relatively small density difference between particles and solution as a result of the porous nature of protein aggregates (Ayazi Shamlou et al, 1996a).

Numerous models have been proposed to describe how increased energy input results in breakage (Glasgow and Luecke, 1980; Petenate and Glatz, 1983; Twineham et al, 1984; Brown and Glatz, 1987; Ayazi Shamlou et al, 1994b; Ayazi Shamlou et al, 1996a).

Agitation affects both particle size and composition as loosely bound particle fragments are removed by erosion from the larger particles to be replaced by other primary particles to 'fill in' the spaces and form a smaller though stronger more compact structure (Bell and Dunnill, 1982a, Spicer et al, 1996). Stronger particles will be less susceptible to breakage during subsequent exposure to higher shear-rates during processing (Bell et al, 1983). From a process design perspective, therefore, it is thus important to integrate protein precipitation and ageing with subsequent process operations which involve exposure to elevated shear-rates. This is because subsequent efficient centrifugal separation of precipitates requires feed particles be of a reasonable size and capable of withstanding considerable turbulent shear. Such shear is typically experienced during processing through pumps, pipes and, in particular, at the inlet zone of a disc stack centrifuge where precipitates experience rapid radial and tangential acceleration (Virkar et al, 1981, Bell and Dunnill, 1982b, Twineham et al, 1984, Hoare at al, 1987, Clarkson et al, 1994) where shear-rates are of the order 10^5 s^{-1} (Bell, 1982). Previous studies on the formation of kaolinite clay-aluminium aggregates have found inverse relationships between particle size and density (Tambo and Watanabe, 1979b) and proportional relationships between density and particle strength (Tambo and Hozumi, 1979).

4.1.4 Chapter conclusions

Chapter 3 provides a context for the work undertaken in subsequent chapters. It details the composition and functionality of whey and outlines the means by which whey is produced and its global importance. The optimum conditions for the fractionation of the principal whey proteins are detailed as described in the literature, as are the growth and

breakage mechanisms for protein aggregates under shear conditions. Armed with an awareness of the optimum fractionation conditions and aggregate growth and breakage mechanisms, whey protein fractionation in a batch agitation vessel was undertaken at laboratory scale in the first instance. This work is described in the following chapter.

Chapter 5 Laboratory scale protein precipitation and fractionation

5.1.1 Theory

5.1.1.1Agitation vessel shear-rate

Agitator intensity should be vigorous enough to provide good mixing in order to prevent localized high concentrations of precipitation agent without being so high as to produce small precipitate particles which would be difficult to recover subsequently (Hoare, 1982). For a fluid of kinematic viscosity, ν, the average spatial shear-rate due to impeller agitation, G, within a standard configuration stirred-tank is given as (Camp and Stein, 1941):

$$G = \left(\frac{\varepsilon}{\nu}\right)^{1/2} \qquad 4.1$$

where ε is the average rate of turbulent energy dissipation per unit mass in a standard configuration batch agitation vessel and is given by:

$$\varepsilon = \left(\frac{N_P N^3 D^5}{V}\right) \qquad 4.2$$

While G is merely indicative of an average shear-rate, and should not be taken too literally for design purposes (Bell et al, 1983), it is nevertheless useful for comparing the effects of energy input on particle size and during process scale up. The average turbulent energy dissipation rate is matched by the impeller power input, P:

$$P = \rho N_p N^3 D^5 \qquad 4.3$$

where N_p may be taken as equal to 5 for a Ruston impeller in a standard configuration vessel at an impeller Re greater than 10^4 (Bates et al, 1963). Thus average spatial shear rate in a vessel of effective volume, V (m^3) can be estimated by combining 4.1 and 4.2:

$$G = \left(\frac{N_P N^3 D^5}{\nu V} \right)^{1/2} \qquad 4.4$$

Turbulent flow is characterised as having a Reynolds' number of greater than 10,000 (Geankoplis, 1993) where in an agitation vessel:

$$\mathrm{Re} = \frac{ND^2}{\nu} \qquad 4.5$$

For turbulent agitated systems, the turbulent microscale (or Kolmogorov length), η provides the diameter of turbulent eddies in the fluid. Aggregates are often smaller than this dimension at least in the early stages of protein precipitation (Bell et al, 1983):

$$\eta = \left(\frac{\nu^3}{\varepsilon} \right)^{1/4} \qquad 4.6$$

Finally, the mean particle circulation time can characterised by:

$$t_c = \frac{V}{N_q N D^3} \qquad 4.7$$

5.1.1.2Laminar capillary shear-rate

For laminar flow the shear-rate of a Newtonian solution being passed through a capillary pipe ranges from 0 s^{-1} at the tube centre to a maximum at the tube wall, γ_w. The wall shear-rate can be determined by combining the Hagen-Poisseuille equation for laminar flow of Newtonian fluid:

$$Q = \frac{\pi R_t^4 \Delta P}{8 \mu L} \qquad 4.8$$

with the velocity profile equation for laminar flow differentiated with respect to r across the tube radius (from r = 0 to r = R_t):

$$u_x = \frac{\Delta P}{4 \mu L}\left(R_t^2 - r^2\right) \qquad 4.9$$

This yields the following:

$$\left.\frac{du_x}{dr}\right|_{@\,wall} = \gamma_w = \frac{4Q}{\pi R_t^3} \qquad 4.10$$

Given that for a Newtonian fluid, viscosity is constant, and for any type of fluid or flow, wall shear rate is given by:

$$\gamma_w = \frac{\tau_w}{\mu} = \frac{\Delta P R_t}{2 \mu L} \qquad 4.11$$

the mass average shear rate for a Newtonian fluid, $\overline{\gamma}_m$ can be found for laminar flow by integration from the pipe centreline (r = 0) to the pipe wall (r = R_t):

$$\bar{\gamma}_m = \frac{\bar{\tau}_w}{\mu} = \frac{1}{\mu Q}\int_0^{R_t}\tau\int_0^{R_t}A\int_0^{R_t}u_x = \frac{\Delta P}{2QL}\int_0^{R_t}rdr.2\pi\int_0^{R_t}rdr.\frac{\Delta P}{4\mu L}\int_0^{R_t}\left(R^2 - r^2\right)dr \qquad 4.12$$

Solving 4.12 yields;

$$\bar{\gamma}_m = \frac{\pi\Delta P^2 R_t^5}{30\mu^2 QL^2} \qquad 4.13$$

and inserting the Hagen-Poisseuille equation (4.8) instead of Q gives:

$$\bar{\gamma}_m = \frac{4\Delta P R_t}{15\mu L} \qquad 4.14$$

Equations 4.8 and 4.11 can be inserted in 4.14 to yield the following expression for the mass average shear rate in terms of the wall shear rate:

$$\bar{\gamma}_m = \frac{32Q}{15\pi R_t^3} = \frac{8}{15}\gamma_w \qquad 4.15$$

If the actual pressure drop is measured over the length of capillary pipe, the actual friction factor, f for laminar flow of Newtonian fluid can be estimated from the definition of friction factor:

$$f = \frac{\Delta P R_t}{L\rho\bar{u}_x^2} = \frac{C}{\mathrm{Re}} \qquad 4.16$$

The actual Reynolds' number, based on the fluid flowrate can be inserted in equation 4.16 to yield a value for the constant C. This will equal 16 for laminar flow of the Newtonian fluid. Once the Reynolds' number increases to a point where flow begins to become transitional, C will no longer be constant and will deviate upwards from 16 as

the fluid velocity profile changes. At this point equations 4.8 to 4.10 and 4.12 to 4.15 cease to apply and consequently equation 4.15 ceases to provide an accurate estimate of the mass average shear rate experienced by fluid.

5.1.1.3Particle size

Isoelectric protein aggregates are composed of a very large number of precipitate primary particles which adhere together in a non-uniform manner thus forming aggregates which are not of regular shape. Particle size is thus not a clearly defined parameter and can be measured in terms of volume, surface area, projected area or on any number of other criteria. A laser diffraction particle sizer is used in this study (Malvern Instruments, Malvern, Worcestershire, England) and it measures particle size in terms of the diameter of a sphere of equivalent volume by the application of Mie theory (Mie, 1908).

The full range of particles in a given sample can be represented by a single size in a number of ways. The diameter of a sphere with a volume equivalent to the average particle volume for a full range of particles in a sample is known as the volume mean diameter, D(4,3) (Coulson and Richardson, 1991):

$$D(4,3) = \frac{\sum d^4}{\sum d^3} \qquad 4.17$$

The size of the particle of the median (volume based) diameter, d_{50}, is that size below which 50% of particles in a sample exist on an equivalent sphere volume basis. Since the shape of the particle size distribution curve does not change appreciably with shear conditions throughout this study, the d_{50} is used as a representative measure of particle size.

5.1.2 Materials and methods

5.1.2.1Feed material composition

The whey protein concentrate used in this study was a high gel rennet WPC 30 powder supplied by Dairygold, Mitchelstown, Co. Cork, Ireland (company product code: 1044 177P). Table 4.1 outlines the WPC composition as detailed on the certificate of analysis for the batch used in this study. Size exclusion high performance liquid chromatography (HPLC) (TosoHaas TSK-Gel G2000 SW_{XL}, TosoHaas GmbH, Stuttgart, Germany) was used to identify the individual protein fractions in Fig. 4.1. Table 4.2 lists the components and relative peak areas of the proteins in Fig. 4.1. Note that relative peak areas do not directly correspond to relative proportions of proteins present. These can only be ascertained by passing protein standards through the HPLC column and determining the peak area which corresponds to a given protein concentration. β-lactalbumin (L-0130) and α-lactalbumin (L-6010) standards were obtained from Sigma-Aldrich Corp (St. Louis, MO, USA) and were used to determine the concentration of the two main proteins present.

Table 4.1 Composition of rennet whey protein concentrate (WPC30).

WPC component	*% Composition (w/w)*
Lactose	57.3
Protein	31.0
Fat	1.70
Moisture	3.37
Ash	6.63
Nitrates (ppm)	< 50
Nitrites (ppm)	< 0.5

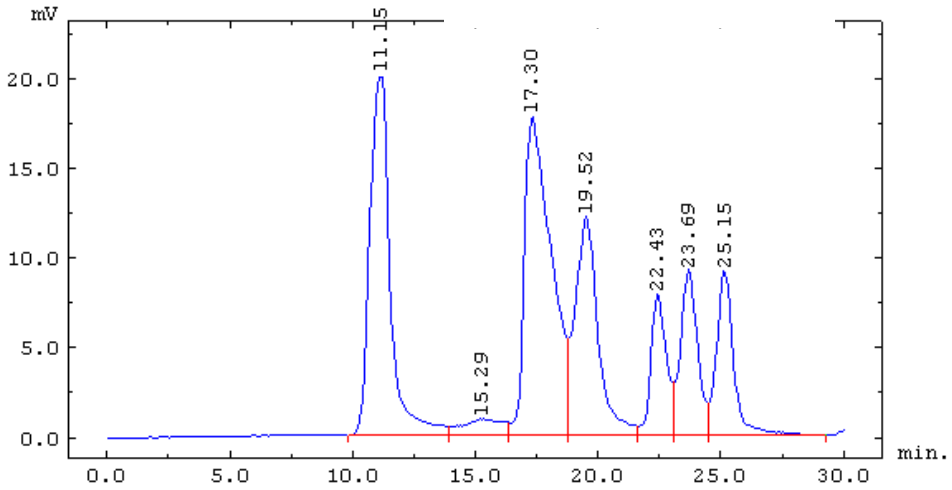

Figure 4.1 HPLC Elution profile for WPC 30.

The WPC solution shown in Fig. 4.1 has a β-lactoglobulin concentration of 18.4 g/L and an α-lactalbumin concentration of 5.2 g/L for a 10% (w/w) solution. This corresponds to a β-lactoglobulin/α-lactalbumin ratio of 3.56. This is a typical ratio for the WPC used in this study which ranges between about 3.3 and 3.6. This ratio is somewhat higher than previous reported work (Pearce, 1989) for rennet whey. This can be attributed to factors such as the cows breed, plane of nutrition, stage of lactation and season (Gray and Mackenzie, 1987) and the relatively high β-lactoglobulin content suggests that the WPC may have been processed from late lactation milk (Regester and Smithers, 1991).

Table 4.2 WPC 30 composition and component retention times.

Peak No. (wrt time)	*Protein*	*Retention time (min.)*	*Area (%)*
1	Immunoglobulins	11.15	25.03
2	Bovine Serum Albumin	15.29	2.13
3	β-lactoglobulin	17.30	29.11
4	α-lactalbumin	19.52	17.08
5	Proteose peptones	22.43	7.53
6	"	23.69	9.53
7	"	25.15	9.58

5.1.2.2Precipitate formation and ageing

Sample preparation

A 10% (w/w) whey protein concentrate solution was made up by adding distilled water to 140 g of 30% high gel rennet whey protein concentrate powder (Dairygold, Mitchelstown, Co. Cork, Ireland) to create 1400 g of feed solution in a 2 litre vessel. Full dissolution of the whey powder, which tends to form sticky lumps upon initial addition of the water, was effected by gentle stirring of a 6 bladed Rushton impeller driven by an IKA Eurostar digi-visc mechanical stirrer motor (IKA-Werke GmbH & Co. KG, Staufen, Germany) at 300 rpm for about 1200 s while placed at an angle to prevent the formation of energy dissipating vortices in the vessel. Precipitation of the dissolved whey solution could then be effected by adjusting temperature and pH to the appropriate values.

The temperature of the dissolved solution was raised from ambient (~ 20°C) to about 60°C by placing the solution in a microwave oven (Hotpoint ME21, Peterborough, England) and heating at full power (900 W) for a total of 300 seconds consisting of two periods of 180 and 120 seconds respectively. This was done so that the solution could be stirred between microwave heating periods to promote homogeneous heating within the solution.

The heated solution was then transferred to a glass jacketed vessel which had been pre-heated to 60°C using a water bath connected by rubber tubing to the vessel jacket. The cylindrical vessel had a diameter of 123 mm and thus an effective standard configuration volume of approximately 1.4 L when baffles and agitator were in place (Fig. 4.2). Four baffles of 13 mm width were inserted into the vessel and the IKA stirrer motor powered 6 bladed Rushton impeller of diameter 40.2 mm was positioned the same distance above the bottom of the vessel rendering the configuration standard.

Figure 4.2 Standard configuration laboratory scale baffled jacketed vessel

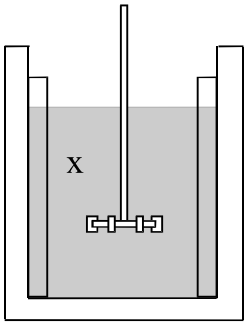

with 6-bladed Rushton impeller (effective volume approx. 1.4L).

Protein precipitation and aggregation

Protein precipitation and aggregation was initiated by the lowering of the whey solution pH from an initial pH of about 6.8 to around the isoelectric pH of α-lactalbumin at 4.0-4.2 causing selective protein precipitation yielding α-lactalbumin rich precipitates. This was achieved by the addition of some 34 cm^3 of 2M hydrochloric acid (HCl) as a precipitation agent at a constant rate of 0.2 cm^3s^{-1} over a period of 170 s. A constant rate of acid addition was chosen since the rate of acid addition is an important factor in determining the nature and size distribution of aggregates formed (Virkar et al, 1982, Fisher et al., 1986). The acid was added at the surface of the solution while the impeller rotated at a pre-selected speed; this speed determines the shear rate at which solution and forming precipitates are subject to during acid addition and is hugely significant in determining the properties of aggregates being formed (Fisher et al, 1986). Temperature and pH probes attached to a Jenway 3310 pH meter (Jenway Ltd., Essex, England) were inserted into the vessel to monitor these properties during acid addition and ageing. Acid was added using a Stepdos 08 S peristaltic pump (KNF Flodos AG., Sursee, Switzerland). Fig. 4.3 shows the vessel agitation and acid addition rig.

Once the acid had been added to the solution and the pH had fallen to about 4.1, the impeller speed was adjusted to the appropriate agitation speed for ageing and aggregates were aged at this impeller speed for up to 3000 seconds. A sample was

taken immediately after acid addition (ageing time = 0 seconds) and additional samples were taken at ageing times of 120, 600, 1800, and 3000 seconds. 15 ml samples were taken at a point mid-way between the top of the impeller and the solution surface and mid-way between the impeller shaft and the vessel inner wall (point X on Fig. 4.2). Samples were taken with a purpose built sampling pipette with a wide orifice to minimise potential shear damage of aggregates during sampling. They were immediately quenched in chilled distilled water (4°C - 5°C) at a sample to water weight ratio 1:2 to prevent further particle growth or aggregation before being sized. This left a bulk solution containing 3.33% whey protein concentrate.

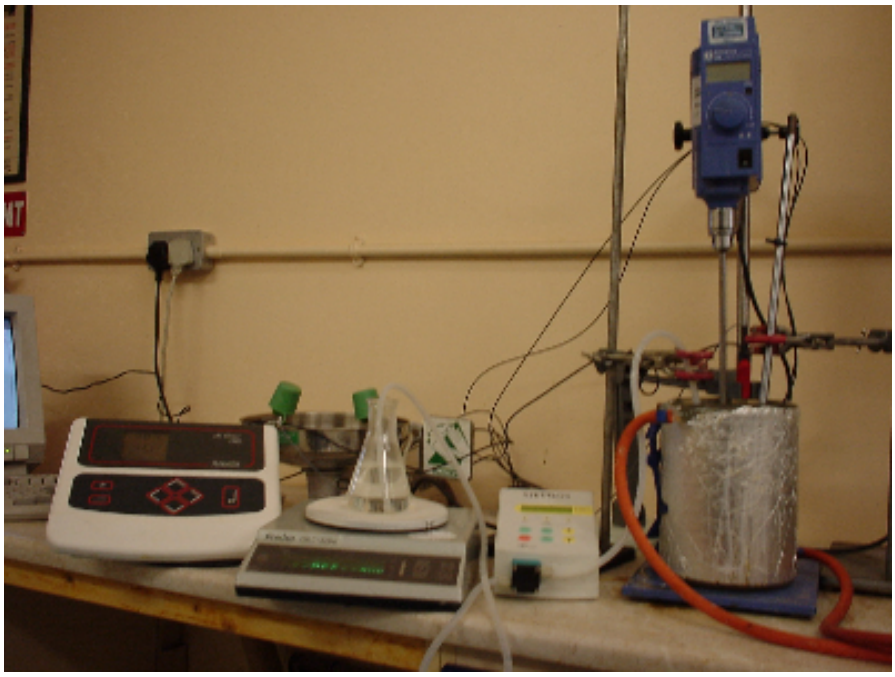

Figure 4.3 Agitation and acid addition rig shows jacketed vessel (bottom right), IKA stirrer motor (top right), HCl being added by peristaltic pump (centre) and Jenway pH and temperature meter (left).

Impeller speeds were chosen based on initial trial runs. Acid addition impeller speeds might be characterised as ranging from ‘very low’ (200 rpm), ‘low’ (350 rpm), ‘medium-low’ (450 rpm), ‘medium’, (550 rpm), ‘medium-high, (650 rpm), ‘high’ (750 rpm) and ‘very

high' (900 rpm). This broad range of impeller speeds reflects the importance of shear-rate during the acid addition period. Moreover ageing impeller speeds can be characterised as either 'low' (400 rpm) or 'high' (700 rpm).

The solution, which contained roughly 3% whey protein concentrate, exhibits Newtonian flow properties over the range of shear rates encountered in the vessel (Qingnong et al, 1990; Alizadehfard and Wiley, 1996) and had a measured density of 1050 kg/m^3. The dynamic viscosity of the suspending fluid (water) at 60°C is 4.71*10^{-7} Nsm^{-2} (Rogers and Mayhew, 1988). This information can be used in the equations presented in section 4.1.1 to determine mass average shear-rates and other properties based on impeller speeds employed in a standard configuration vessel. This is done in Table 4.3 which makes use of equations 4.1 - 4.2 and 4.5 - 4.7 to determine Reynolds' number, average turbulent energy dissipation per unit mass, average spatial shear-rate, average particle circulation time and the turbulent microscale dimension (a measure of eddy vortex diameter) respectively.

Table 5.3 Laboratory scale agitation vessel calculated properties.

Fluid properties;

ρ =	1050 kg/m^3	N_p (Turbulent flow):	5
ν =	4.71E-07 m^2/s	N_q (Rushton impeller):	0.9
D =	0.0402 M	V =	1.40E-03 m^3

Impeller speed *rev/min*	**N** *rev/s*	**Re**	**ε** *W/kg*	**G** *s^{-1}*	**t_c** *s*	**η** μm
200	3.33	11,440	0.014	172	7.18	52.4
350	5.83	20,020	0.074	398	4.10	34.4
400	6.67	22,880	0.111	486	3.59	31.1
450	7.50	25,740	0.158	580	3.19	28.5
550	9.17	31,460	0.289	783	2.61	24.5
650	10.83	37,180	0.477	1006	2.21	21.6
700	11.67	40,040	0.595	1124	2.05	20.5
750	12.50	42,900	0.732	1247	1.92	19.4
900	15.00	51,480	1.265	1639	1.60	16.9

Thus the average imparted fluid shear-rates under consideration lie in the range 1.7×10^2 s^{-1} to 1.7×10^3 s^{-1} (for impeller speeds in the range 200 rpm - 900 rpm).

5.1.2.3Exposure to high shear-rates during processing of aggregates

In any industrial separation process, precipitates are typically exposed to relatively high levels of shear during processing through pipes, pumps and in centrifugal separation equipment, especially at the centrifuge feed zone (Bell, 1982, Clarkson et al, 1994). This has implications with respect to the ease of centrifugal recovery, for example if there are changes in particle size and/or density. In this study, aggregates were 'processed' by being exposed to shear-rates greater than they had previously experienced in the agitation vessel to see how shear exposure in the agitation vessel affects particle strength.

Two shear processing regimes were employed. The first regime involved passing aggregates through a capillary pipe while the second involved exposing aggregates to more extreme levels of turbulent shear by passing aggregate solution through a partially open ball-valve. Particle sizing was carried out both before and after exposure to process shear for both regimes.

In all cases, samples taken from the agitation vessel were further diluted with 2⅓ times their mass of distilled water at 20°C to yield a 1% whey protein concentrate (w/w) Newtonian solution before processing.

Capillary shear

Compressed air was used to pump aggregates through a capillary pipe as shown in Fig. 4.4. Pressure drop across the capillary tube was measured using a Honeywell ST 3000 pressure transmitter (Honeywell, Amiens, France). The capillary shearing rig comprised an on/off regulating valve followed by over a metre of type 316 stainless steel pipe of 0.929 mm inner diameter (both Tubesales (UK) Ltd., Southampton, England). Solution was held in a cylindrical reservoir before being pumped through the capillary pipe with compressed air at various pressures up to about 9 bar (Fig. 4.5). A pressure transducer with a 4-20 mA output range was used to measure the pressure drop across 1.01

metres of the pipe. This allowed one to determine when flow had become steady (flow must be allowed become steady before a sample can be taken) and to monitor the level of turbulence in the flow.

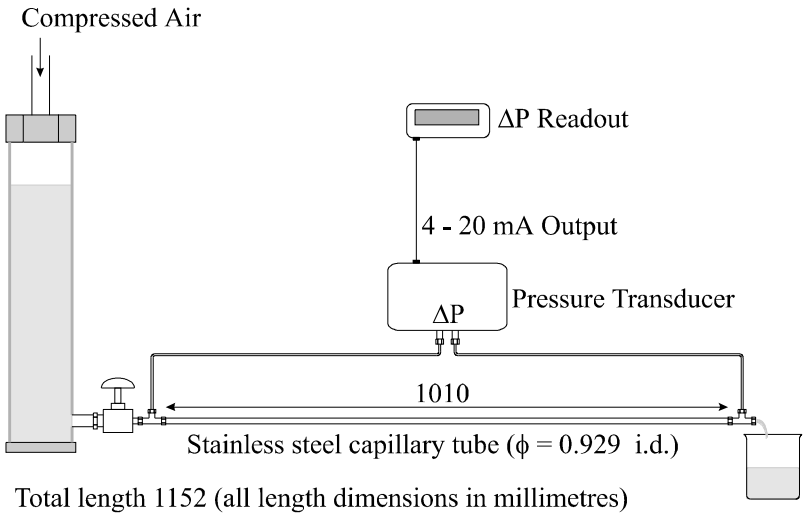

Figure 4.4 Capillary shearing rig and dimensions.

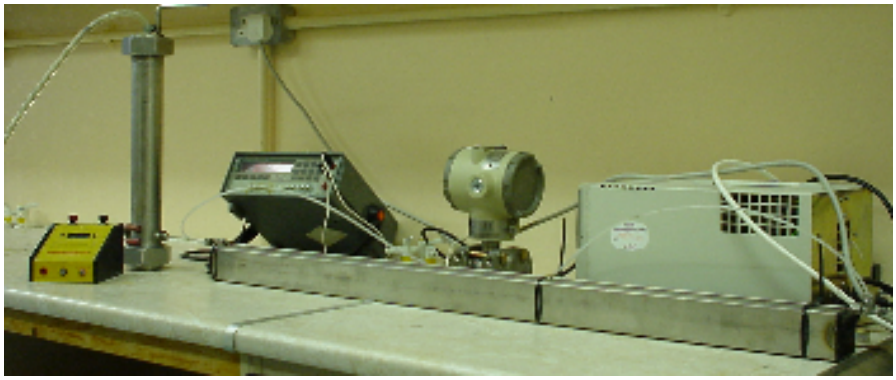

Figure 4.5 Capillary shearing rig (including pressure transducer and monitor) with timer.

This configuration allows both laminar and transitional/turbulent flow to be employed and their effects considered under controlled conditions, mimicking the moderate shear-rates that precipitates would encounter during routine industrial processing through pipes and pumps with moderate shear. Laminar flow occurs when the product of the Reynolds'

number and the Fanning friction factor equals 16 (equation 4.16) and under these flow conditions mass average shear rates can be determined from equation 4.14. Fig. 4.6 plots the actual friction factor (from equation 4.16) against Re. The curve on the chart gives the predicted friction factor assuming laminar flow (f = 16/Re). Predicted and actual friction factors show good agreement up to a Reynolds' number of about 1,800. Thereafter actual and predicted values begin to deviate indicating the onset of transitional flow.

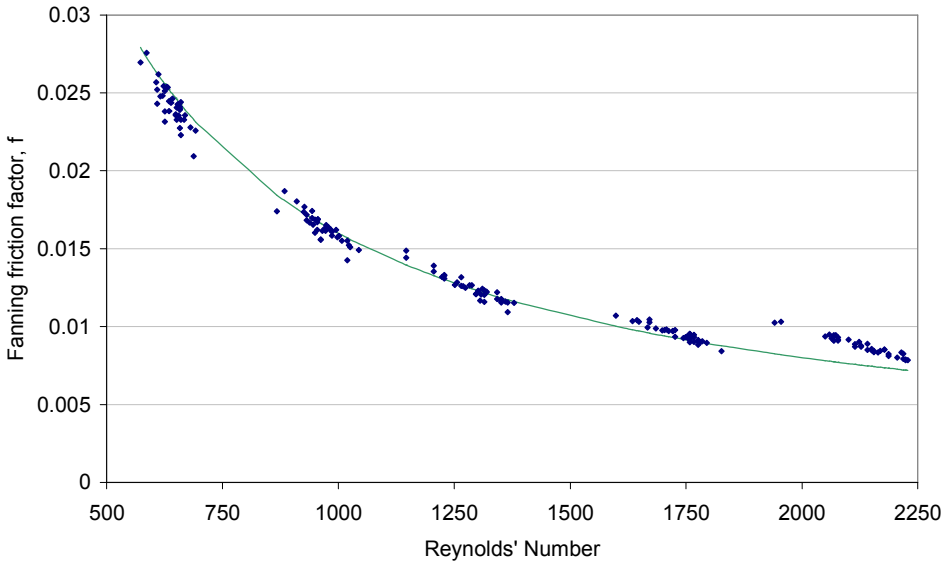

Figure 4.6 Actual Fanning friction factors and Reynolds' numbers for Newtonian 1% protein aggregate solution pumped through a 0.929 mm diameter pipe (curve represents relationship between Re and f for ideal laminar flow; f = 16/Re).

Similarly for laminar flow the shear-rate profile, including the maximum shear-rate (at the pipe wall) and mass average shear-rate experienced in the pipe can be accurately predicted from equation 4.14 though not as the velocity profile changes due to turbulence. Fig. 4.7 shows how predicted mass average shear-rate closely relates to Reynolds' number when flow is laminar, providing a mass average shear-rate of up to

about 9,100 s^{-1} at Re = 1,800 (corresponding wall shear-rate of about 17,000s^{-1}) but for more turbulent flow than this equation 4.14 can provide neither an accurate nor meaningful estimate of average shear-rate. Since capillary Reynolds' numbers of up to and well above 5,000 were achieved during this work, capillary shear levels are thus expressed in terms of Reynolds' number.

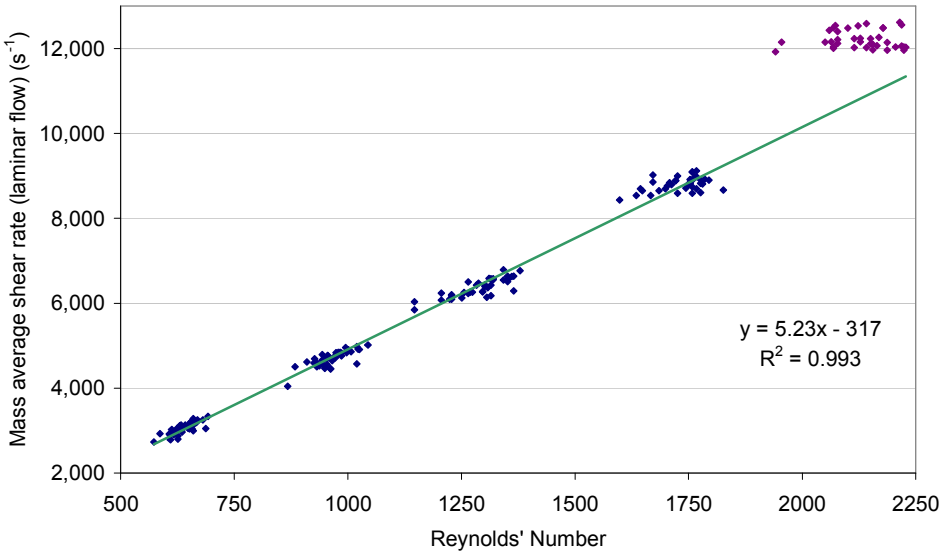

Figure 4.7 Predicted mass average shear-rate for laminar flow of a Newtonian 1% protein aggregate solution pumped through a 0.929 mm diameter pipe versus Reynolds' number.

Compressed air at a range of compressed air pressures was used to pump solution through the capillary pipe. Runs were carried out in duplicate and three samples were taken per run. Samples were collected over either periods of 20, 30 or 60 seconds depending on flowrate and volumetric flowrates were calculated before sample aggregates were sized by laser diffraction to allow comparison with pre-sheared aggregates and assess the degree of particle breakage and compression. Residence time of the solution in the 1.01 m long capillary pipe ranged from 0.17 seconds to 1.6

seconds for the flowrates under investigation which ranged from around 3.4×10^{-6} m^3/s to 4.3×10 m^3/s as shown in Fig. 4.8.

Figure 4.8 Range of shear exposure times for a 1% protein aggregate solution pumped through a 0.929 mm diameter pipe.

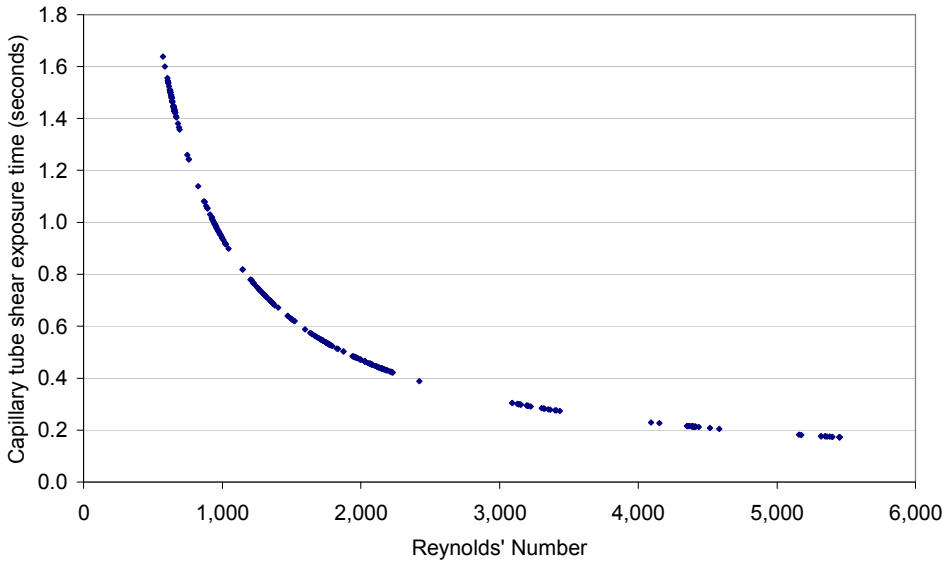

Table 4.4 shows solution capillary flowrates and turbulence as well and the accompanying effects on aggregate size for some example aggregate solutions produced under various agitation vessel conditions.

Table 4.4 Changing size profile for aggregates subject to various levels of capillary shear formed at agitator vessel shear-rate of $783s^{-1}$ (med) during acid addition followed by 3000 seconds of ageing at either $486s^{-1}$ (low) or $1124s^{-1}$ (high).

Pipe diameter (m)			9.295E-04			Fluid density (kg/m^3)			1003	
Effect. pipe length (m)			1.01			Rheol. n-value			1	
						Rheol. K-value			1.00E-03	
Rig measurements		3. Sample				7.Exposure	(median)	10% u'size	90% u'size	(Vol. mean)
1.ΔP	2. Vol.	time	4. Q	5. v_{avge}	6. Re(pipe)	time	d_{50}	d_{10}	d_{90}	D(4,3)
bar	m^3	s	m^{3}s^{-1}	ms^{-1}		s	μm	μm	μm	μm
WPC ppt. Acid addn 550rpm, aged 400rpm, 50 min, @ 60°C (1% solr										
0.0							15.44	7.09	28.44	16.74
0.6	1.949E-05	30	6.497E-07	0.96	893	1.05	14.64	6.78	26.52	15.72
1.0	3.216E-05	30	1.072E-06	1.58	1,473	0.64	14.37	6.74	25.85	15.4
1.5	4.092E-05	30	1.364E-06	2.01	1,874	0.50	13.75	6.5	24.59	14.72
4.0	7.004E-05	30	2.335E-06	3.44	3,208	0.29	10.99	5.2	19.46	11.7
6.5	9.539E-05	30	3.180E-06	4.69	4,369	0.22	8.66	3.95	15.52	9.22
9.0	7.785E-05	20	3.893E-06	5.74	5,348	0.18	7.25	3.17	13.17	7.7
WPC ppt. Acid addn 550rpm, aged 700rpm, 50 min, @ 60°C (1% solr										
0.0							15.52	7.22	28.07	16.69
0.6	1.655E-05	30	5.517E-07	0.81	758	1.24	15.01	7.09	27.05	16.13
1.0	3.287E-05	30	1.096E-06	1.61	1,505	0.63	14.85	7.13	26.29	15.85
2.0	4.358E-05	30	1.453E-06	2.14	1,996	0.47	14.09	6.75	24.96	15.04
4.0	6.982E-05	30	2.327E-06	3.43	3,198	0.29	11.73	5.59	20.79	12.51
6.5	9.591E-05	30	3.197E-06	4.71	4,393	0.21	9.11	4.17	16.32	9.7
9.0	7.858E-05	20	3.929E-06	5.79	5,398	0.17	7.56	3.33	13.71	8.06

Ball-valve shear

If the capillary tube is replaced by a partially opened ball-valve, higher levels of turbulence can be achieved which compare well with the extreme levels of turbulent shear experienced at the feed zone of a disc stack centrifuge which are typically about 10^4 - 10^5 s^{-1} (Bell, 1982; Bell and Dunnill, 1982a) for about 10^{-3} seconds (Bell, 1982). This is evidenced by the similar degree of shear damage imparted on ball-valve processed particles and disc stack centrifuged particles as measured by changes in particle size distribution. The turbulent flow patterns through a partially opened ball-valve cannot be easily characterised by some average shear-rate unlike for laminar flow and thus exposure through the ball-valve is instead characterised by volumetric flowrate.

This ball-valve rig also consists of a 0.929 mm diameter ball-valve (Tubesales (UK) Ltd., Southampton, England). Aggregates in solution are pumped through it with compressed air through a cylindrical reservoir and flow is controlled with an on/off regulatory ball-valve (Fig. 4.9). In addition the ball-valve is followed by a short length of capillary pipe which is merely employed to direct the sample solution towards a collecting receptacle.

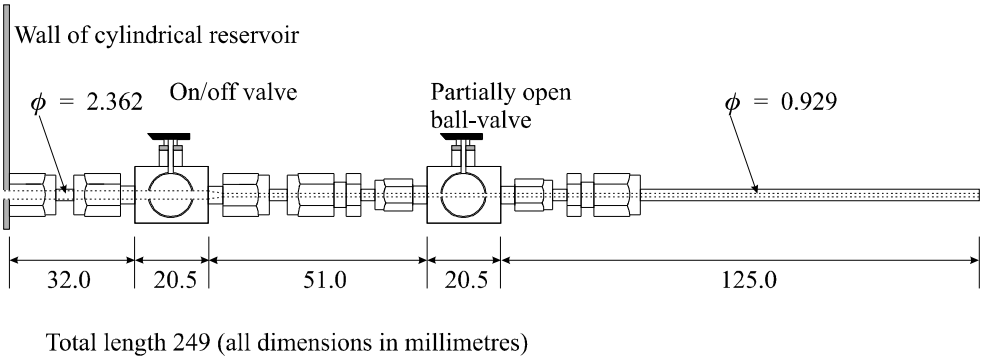

Figure 4.9 Ball-valve shearing rig and dimensions.

Compressed air at 8 bar was used to propel solution through the rig, the critical point being the ball-valve which was kept at a 40° angle from the closed position. This created a highly turbulent flow regime around the valve with low volumetric flowrate (of about 7×10^{-7} m^3s^{-1} or about 37% of that if the valve were fully open), capable of imposing substantial shear damage on particles. Total computed head losses across the ball-valve amount to some 80.5 m, which correspond to an energy dissipation rate of 0.554 W. This is equal to power loss in the ball-valve of 39,734 W kg^{-1} for a throughput of 7.02 $\times$ 10^{-4} kg/s. Runs were carried out in duplicate and three samples were taken per run. Samples were taken over a 60 second period. Particles were sized by laser diffraction to ascertain the effects of high shear exposure to aggregates (formed under various agitation vessel shear conditions) on particle size distribution and compactness.

This configuration facilitates the imposition of shear-rates far in excess of those attained in the capillary-rig under flow conditions of extreme turbulence as fluid traverses the partially open ball-valve. Thus this regime facilitates the imposition of extreme turbulent processing and associated shear-rates (through the sharp geometrical transitions of the partially open ball-valve) comparable with but under more controlled conditions than would be experienced by precipitates on an industrial scale, for example at the feed-zone of a disc stack centrifuge or in a high shear centrifugal pump.

5.1.2.4Particle characterisation

Particle size distribution was measured by laser diffraction using a Malvern Mastersizer S laser particle sizer (Malvern Instruments, Malvern, Worcestershire, England).

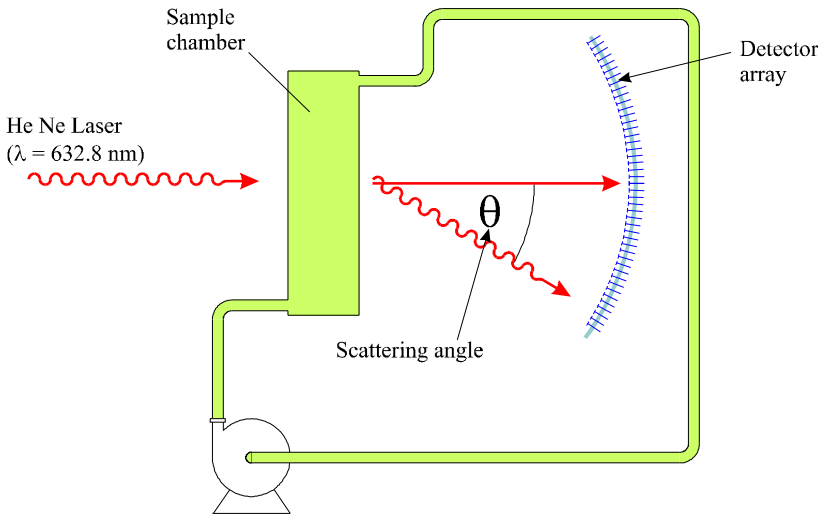

Figure 5.10 Schematic representation of light scattering and detection by Malvern.

Circulating particles were pumped through a flow cell through which a helium-neon (He-Ne) laser light (wavelength 632.8 nm) is passed. The laser light is scattered by the particles to a greater or lesser degree depending on their size and configuration (scattered angle is greater for smaller particles) and scattered light is then captured by a series of 42 detectors placed at various angles around the cell in such a way that each detector collects the light scattered from a particular range of angles (Fig. 4.10). A 300RF (reverse Fourier) lens was used to facilitate the measurement of particles in the size range 0.05 μm - 880 μm. The in-built Malvern software uses the information gathered by the detector cells to model particle size distribution based on Mie theory, as developed by the German physicist Gustav Mie (1908) to predict particle size distribution based on the way light is refracted or absorbed by spherical particles.

A representative aliquot was taken from each sample to be sized and added to the carrier solvent (distilled water) via the 'small volume sample presentation unit' which acts as a pump and promotes circulation and mixing of the sample and solvent. Fig. 4.11 shows the Malvern presentation software displayed alongside the Mastersizer. Samples were measured in duplicate.

Figure 4.11 Malvern Mastersizer S optical unit connected to small volume sample presentation unit (pump) in front.

Laser diffraction data from the Malvern Mastersizer S was also used to calculate the fractal dimension of particles.

5.1.2.5Precipitate separation

Precipitates were separated from the supernatant phase using a Hettich Universal 16R bench top centrifuge (Hettich GmbH, Stuttgart, Germany). 10ml aliquots were spun at 2710g (4920rpm) for 3000 seconds at 20°C. At the end of each run tubes contained a compact white precipitate at the bottom (rich in α-lactalbumin) and in excess of 9ml of clear supernatant (rich in β-lactoglobulin). A small amount of the supernatant was taken from the top of the centrifuge tube and filtered through a 0.2μm cellulose acetate filter (Sartorius, Goettingen, Germany) into a 1.5ml micro-test tube (Eppendorf Vertrieb

Deutschland GmbH, Cologne, Germany) receptacle in preparation for liquid chromatography to determine the protein composition of the supernatant.

5.1.2.6Size exclusion high performance liquid chromatography

Size exclusion chromatography (SEC) is the chosen form of high performance liquid chromatography (HPLC) to estimate feed and separated product supernatant protein composition as examined by Dimenna and Segall (1981) for dairy proteins. A significant feature of SEC is that it provides low interaction between gel and sample and thus it facilitates high retention of bimolecular enzymatic activity and enables separation of components which may not be achieved by other chromatographic methods.

Supernatant composition was determined by eluting filtered supernatant through a TosoHaas TSKgel G2000SW_{XL} column (TosoHaas GmbH, Stuttgart, Germany) of dimensions 30cm $\times$ 7.8mm inner diameter with a silica based packing of spheres of diameter 5μm and pore size 125Å capable of separating globular proteins of molecular weight in the range 5,000-150,000 Da. The column is protected by a TosoHaas guard column of dimensions 7.5cm $\times$ 7.5mm inner diameter with silica based gel packing of diameter 10μm.

Elution of the supernatant was carried out with a 0.05M Phosphate buffer solution (pH 6.80) as proposed by Dimenna and Segall (1981) to separate dairy proteins. The buffer solution flowed through the guard and column at 1 ml/min with typical operating pressure drop in the range 275-285 psi.

The aqueous buffer solution consisted of the following chemicals all of which were purchased from BDH laboratory supplies (Poole, England):

0.05M Potassium di-hydrogen orthophosphate (KH_2PO_4, MW: 136.09 Da); HiPerSolv for HPLC, minimum assay 99.5%

0.05M Di-potassium hydrogen orthophosphate 3-hydrate ($K_2HPO_4.3H_2O$, MW: 228.23 Da); HiPerSolv for HPLC, minimum assay 99.0%

0.1M Sodium sulphate anhydrous (Na_2SO_4 ,MW: 142.02); Analar, minimum assay 99%

A tincture of Sodium Azide (NaN_3 ,MW: 65) (bacteriostat).

Distilled water was added to the respective salts to make up the buffer solution and were fully dissolved in an ultrasonic bath before being filtered through a 0.2μm cellulose acetate filter (Sartorius, Goettingen, Germany). The buffer solution was pumped through the column by two Spectra Series P100 Isocratic pumps (Thermo Separation Products, Riviera Beach, Florida, USA) which were aligned in series to provide a steady flow. Eluted components were detected with a Spectra Series UV100 variable wavelength ultra violet detector (Thermo Separation Products, Riviera Beach, Florida, USA) set at 280nm. Filtered supernatant samples of volume 2 μl were injected at the manual injection port and total elution time was about 45 minutes. The HPLC system is shown in Fig. 4.12.

The data system used to gather and present elution data is the WINner on Windows Data System (Thermo Separation Products, Riviera Beach, Florida, USA).

Fig 4.12 SE HPLC system: includes isocratic pumps (left), manual injection port (left of centre), guard column (on bench), separation column (centre) and UV detector (right).

5.1.3 Results

5.1.3.1Effect of agitation during acid addition and ageing on aggregate size

Effect of agitation on PSD profile

Protein precipitation and aggregation occurs rapidly and aggregates rich in α-lactalbumin, BSA and immunoglobulins form during the 170 seconds as the precipitation agent (HCl) is added to the whey protein solution reducing pH from about 6.8 to 4.1. By the end of this period, a characteristic particle size distribution (PSD) profile has emerged in conditions of moderate or high impeller shear (certainly at shear-rates in excess of 580 s^{-1}). This characteristic PSD profile incorporates a bimodal PSD curve for whey protein precipitates as is illustrated in Fig. 4.13 for aggregates formed subject to a vessel shear-rate of 1247s^{-1}.

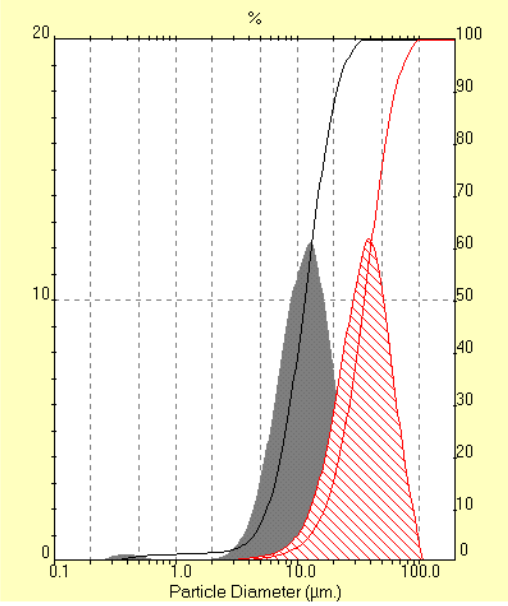

Result: Analysis Table

ID: 750-000-00-4.11-59.6	Run No: 1	Measured: 24/6/99 12:38
File: AP21JUNE	Rec. No: 49	Analysed: 24/6/99 12:38
Path: C:\SIZERS\DATA\ERIN\		Source: Analysed

Range: 300RF mm	Beam: 2.40 mm	Sampler: MS1
Presentation: 3NHD	Analysis: Polydisperse	Obs': 14.9 %
Modifications: None		Residual: 0.249 %

Conc. = 0.0193 %Vol	Density = 1.000 g/cm^3	S.S.A.= 0.8204 m^2/g
Distribution: Volume	D[4, 3] = 12.51 um	D[3, 2] = 7.31 um
D(v, 0.1) = 5.60 um	D(v, 0.5) = 11.52 um	D(v, 0.9) = 21.07 um
Span = 1.344E+00	Uniformity = 4.188E-01	

Size (um)	Volume Under%	Size (um)	Volume Under%	Size (um)	Volume Under%	Size (um)	Volume Under%
0.05	0.00	0.67	1.32	9.00	32.18	120.67	100.00
0.06	0.00	0.78	1.37	10.48	42.88	140.58	100.00
0.07	0.00	0.91	1.42	12.21	54.55	163.77	100.00
0.08	0.00	1.06	1.47	14.22	66.69	190.80	100.00
0.09	0.00	1.24	1.52	16.57	77.43	222.28	100.00
0.11	0.00	1.44	1.59	19.31	86.09	258.95	100.00
0.13	0.00	1.68	1.66	22.49	92.43	301.68	100.00
0.15	0.00	1.95	1.74	26.20	96.57	351.46	100.00
0.17	0.00	2.28	1.85	30.53	98.93	409.46	100.00
0.20	0.01	2.65	2.06	35.56	100.00	477.01	100.00
0.23	0.03	3.09	2.46	41.43	100.00	555.71	100.00
0.27	0.10	3.60	3.21	48.27	100.00	647.41	100.00
0.31	0.26	4.19	4.57	56.23	100.00	754.23	100.00
0.36	0.50	4.88	6.84	65.51	100.00	878.67	100.00
0.42	0.78	5.69	10.46	76.32	100.00		
0.49	1.02	6.63	15.77	88.91	100.00		
0.58	1.21	7.72	23.02	103.58	100.00		

Figure 4.13 Above: PSD of whey protein precipitates subject to average agitation vessel shear-rate of (a) 1247s^{-1} (high) (fill) and (b) 398s^{-1} (low) (hatch) at the end of acid addition period (170 seconds); Below: Analysis size table for (a).

The filled PSD plot in Fig. 4.13 (corresponding data in the accompanying table) clearly shows that the vast majority (over 98% by volume) of particles lie in the size range with

(equivalent spherical) diameters between 2 μm and 35 μm while a relatively tiny (in terms of volume) yet significant group of far smaller particles also exist a couple of orders of magnitude smaller, chiefly in the sub micron range. This phenomenon is evident at impeller shear-rates at or above 783s^{-1} (550 rpm) during acid addition and the number and volume of primary particles increase with increased applied shear-rate.

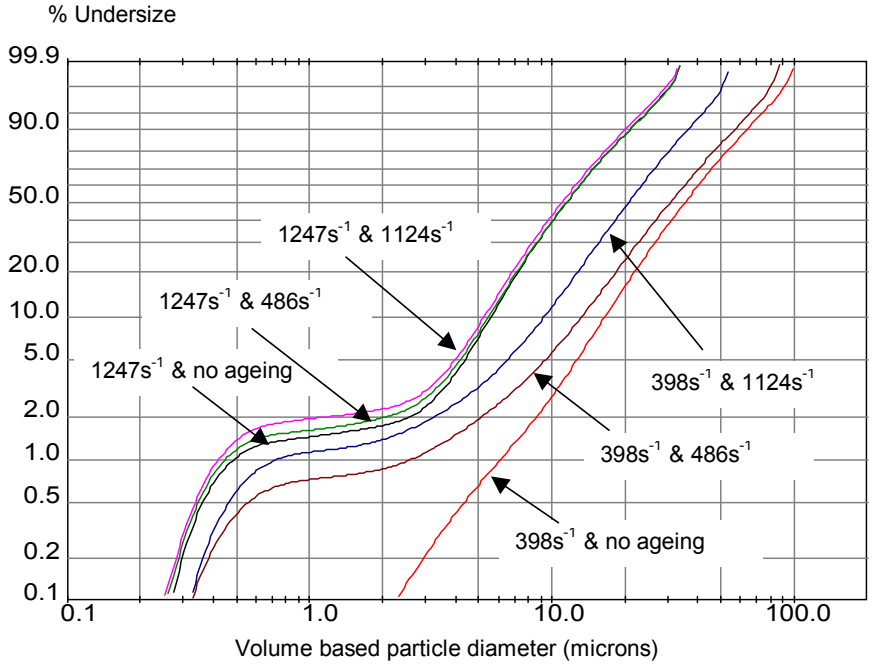

Figure 4.14 Effect of impeller shear-rates of 398s^{-1} (low) and 1247s^{-1} (high) on PSD of whey protein precipitates after 170 seconds of acid addition followed by various ageing regimes; none, 486s^{-1} (low) for 3000 seconds and 1124s^{-1} (high) for 3000 seconds.

However, at or below 580s^{-1} (450 rpm), no sub micron particles are evident at the end of the acid addition period and a mono-modal PSD curve is evident as illustrated in Fig. 4.14. This result indicates that the presence of a substantial number of sub micron particles at the end of the period of precipitation agent addition is essentially due to breakage effects associated with increased impeller agitation. This is further supported by Fig. 4.14 which shows that the application of both 'high' (1124s^{-1}) and 'low' (486s^{-1})

impeller shear-rates during a subsequent 3000 second ageing period results in the appearance of fragment particles among aggregates formed at $398s^{-1}$ while causing further size reduction and an increase in sub micron particles for the precipitates formed at a higher acid-addition shear-rate. Thus clearly by the end of the acid addition period aggregates have already reached their largest size and particle breakage due to erosion has taken hold at all but low shear environments.

A good level of reproducibility was achieved throughout and median diameters presented in this chapter represent average values. Variation in aggregate size is very small after vessel agitation and standard deviations are thus not presented, unlike after high shear processing where they are routinely appreciable.

Effect of agitation on aggregate size

Fig. 4.15 compares median particle diameters (d_{50}) for precipitates formed subject to various impeller shear-rates during acid-addition and ageing. The greater the applied shear-rate during acid-addition, the smaller the precipitate particles produced. Impeller shear-rates during ageing have little affect on the PSD of precipitates formed with high impeller shear-rates during acid-addition. On the other hand, precipitates exposed to lower impeller shear-rates during acid addition show an appreciable reduction in particle size during ageing, particularly when subjected to high shear-rates.

However, when a relatively low acid addition impeller shear-rate is followed by a very high impeller shear-rate during ageing, the eventual particle size is not nearly as small as for particles which have been subjected to higher shear-rates initially during acid-addition. Thus shear history of aggregates does affect their size. Bell and Dunnill (1982a) attributes this to rearrangement as a result of deaggregation or erosion of primary particles followed by a more stable and compact restructuring or ‘infilling’ during the formative stages of aggregation. Particle size does not increase during ageing even

when small particles produced during high shear acid addition are subsequently exposed to gentle agitation during ageing.

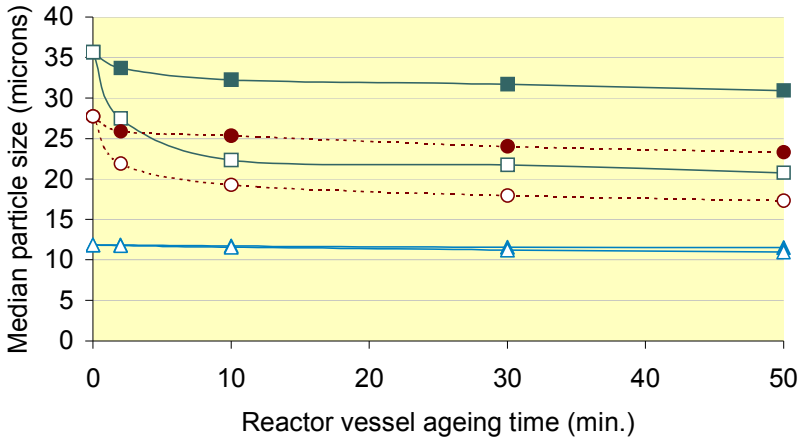

Figure 4.15 Effect of impeller shear-rate during acid addition and during ageing on median particle size in a 1.4 L agitation vessel (squares represent an acid addition impeller shear-rate of 398s^{-1} (low), circles are 580s^{-1} (med-low), triangles are 1247s^{-1} (high); filled symbols represent an ageing impeller shear-rate of 486s^{-1} (low), open symbols represent an ageing impeller shear-rate of 1124s^{-1} (high)).

Fig. 4.16 and Fig. 4.17 show the effect of two ageing shear-rate regimes on aggregates which have been subject to a common range of shear-rates during the initial acid addition period. Fig. 4.16 relates to aggregates subject to ageing at shear-rate 486 s^{-1} while Fig. 4.17 represents aggregates aged at 1124 s^{-1}. Comparison of the two show that high ageing shear rates have a greater effect on particle size when aggregates have been exposed to lower shear-rates during formative stages.

Figs. 4.15 - 4.17 each show that in general, when aggregate sizes are reduced due to ageing, most size reduction occurs during the first 600 seconds of ageing.

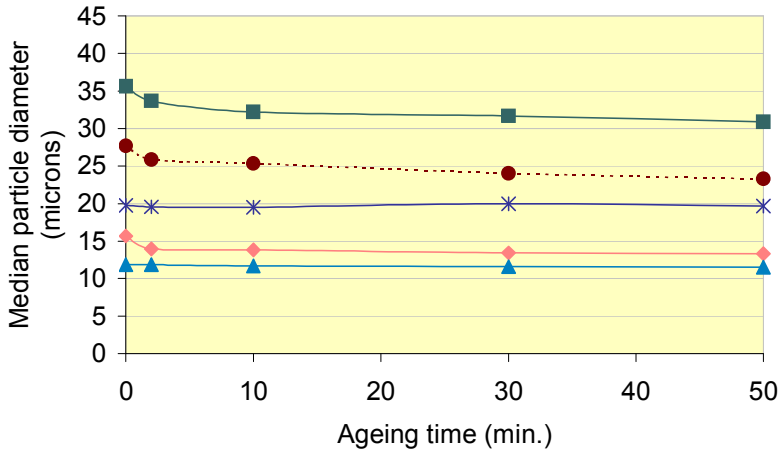

Figure 4.16 Effect of impeller shear-rate on median precipitate size in a 1.4 L agitation vessel for an ageing period of up to 3000 seconds at 486 s^{-1} (low) following various acid addition impeller shear-rates (squares 398 s^{-1} (low); circles 580 s^{-1} (med-low); crosses 783 s^{-1} (med); diamonds 1006 s^{-1} (med-high); triangles 1247 s^{-1} (high)).

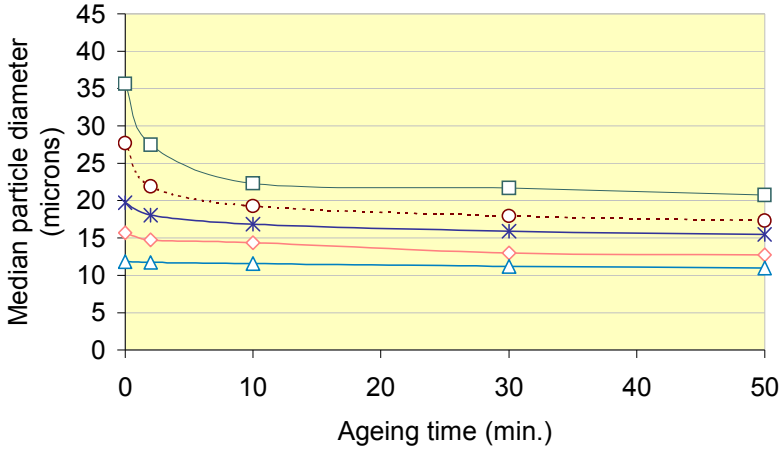

Figure 4.17 Effect of impeller shear-rate on median precipitate size in a 1.4 L agitation vessel for an ageing period of up to 3000 seconds at 1124 s^{-1} (high) following various acid addition impeller shear-rates (squares 398 s^{-1} (low); circles 580 s^{-1} (med-low); crosses 783 s^{-1} (med); diamonds 1006 s^{-1} (med-high); triangles 1247 s^{-1} (high)).

This is in agreement with similar studies on other protein precipitates (Brown and Glatz, 1987; Ayazi Shamlou et al, 1994b; Ayazi Shamlou et al, 1996b).

The relationship between aggregate size and turbulent microscale

Sub micron particles are continuously formed by two means: α-lactalbumin molecules precipitate and aggregate along with immunoglobulins by diffusional forces to form sub-micron primary particles, which in turn aggregate to form larger coarse particles as described in section 3.3.1. Erosion of these particles then takes place, either through hydrodynamic shear or particle-particle or particle-solid collisions or through viscous shear induced forces depending on the size of aggregates relative to the turbulent microscale dimension (as described in section 3.3.2) yielding more sub micron particles, their prevalence increasing with applied shear-rate (Fig. 4.14). In many systems involving protein precipitates, aggregate size is smaller than the microscale dimension and thus viscous shear forces are thought to provide the dominant destructive forces (Bell et al, 1983), though these forces may continue to be important up to ten times the microscale dimension (Ayazi Shamlou and Titchener Hooker, 1983).

Table 4.5 Volume fraction of particles below average turbulent microscale dimension at end of acid addition period (170 seconds).

HCl add γ (s^{-1})	η (μm)	% vol. < η
398	34.4	47.3
580	28.5	43.2
783	24.5	66.3
1006	21.6	74.0
1247	19.4	86.3

Table 4.5 presents turbulent microscale lengths and compares them with the volume percentage of aggregates lying below respective microscale dimensions extracted from

PSD plots for precipitates formed at a variety of agitation vessel shear-rates. This shows a substantial amount of aggregates above the turbulent microscale dimension particularly at low applied impeller shear-rates. Indeed most aggregates formed at shear-rates less than or equal to 580 s^{-1} are greater than the turbulent microscale on a volume basis. This is reversed at higher shear-rates and aggregates fall below the turbulent microscale length increasingly with ascending shear-rate, despite the reduction in eddy size.

It should be remembered however that the particle size data in Table 4.5 is presented on a volume basis and this affords a distorted perception of actual particle numbers; in fact the vast majority of particles are of size smaller than the turbulent microscale -it takes just a few large particles to take up a relatively large proportional volume. Moreover, even though maximum shear is experienced around the microscale length (Hoare, 1982) the maximum shear at low shear-rates is considerably lower than that experienced at higher vessel shear-rates and the lower agitation shear-rates presented here ($\leq$ 580 s^{-1}) correspond to regimes of relatively gentle agitation. This may help explain the apparently low percentage of aggregates by volume below the turbulent microscale at lower shear-rates. Also turbulent microscale dimensions are merely average values and actual eddy size can vary from a minimum around the impeller blades to over twice that in the bulk fluid (Bell et al, 1983). Thus the range of turbulent microscale lengths present in a vessel gets bigger with decreasing impeller induced shear. If one combines this fact with two additional observations; 1. the impeller zone occupies just about 5% of the vessel volume (Ayazi Shamlou et al, 1996) and thus aggregates spend most of their time in the bulk fluid and 2. the circulation rate through the impeller region plays a leading role in the extent of particle breakage (Reuss, 1988), then one can conceive a situation where in vessels with low impeller speed, conditions might be more conducive to the growth and survival of a significant number of particles of a size above the average microscale dimension by virtue of having little contact with the impeller zone region especially in the early precipitation stages.

Table 4.6 Volume fraction of particles below average turbulent microscale dimension at selected ageing times during ageing at average shear-rates of 486^{-1} (low) and 1124s^{-1} (high).

HCl add γ (s^{-1})	Ageing γ (s^{-1})	Ageing η (μm)	% vol. < η @ 120 s.	% vol. < η @ 600 s.	% vol. < η @ 1800 s.	% vol. < η @ 3000 s.
398	486	31.1	44.1	45.8	48.8	50.6
580	486	31.1	64.0	65.2	69.4	71.3
783	486	31.1	82.1	82.3	81.2	81.5
1006	486	31.1	95.7	95.9	96.7	96.8
1247	486	31.1	98.9	98.9	98.9	99.0
398	1124	20.5	28.7	43.4	44.9	49.0
580	1124	20.5	44.9	57.7	60.7	63.6
783	1124	20.5	59.8	65.0	70.0	72.3
1006	1124	20.5	74.9	76.2	83.1	84.6
1247	1124	20.5	87.4	88.4	89.4	90.3

Table 4.6 presents size data for aggregates formed subject to a range of shear-rates during acid addition for 170 seconds are then subjected to either a relatively high (1124s^{-1}) or relatively low (486s^{-1}) shear-rate during subsequent ageing periods ranging from 120 to 3000 seconds. It illustrates a couple of points; Firstly, ageing generally results in a reduction in particle size (though effect is minimal when the rate of shear ageing is far less than that during acid addition). Secondly, it illustrates the importance of agitation vessel shear-rate during the acid addition period in determining ultimate particle size - even when the levels of turbulence are increased appreciably in the vessel during ageing there is not a huge increase in the volume fraction below the average eddy size over ageing time and even these values do not converge between aggregates formed at various shear-rates even after 3000 seconds ageing. For example, aggregates aged at 1124 s^{-1} for 120 seconds differ by about 60% in terms of the volume percent of aggregates which are below the turbulent microscale depending on their (acid

addition) shear histories (28.7% for 398 s^{-1} versus 87.4% for 1247 s^{-1}) but this has only been reduced to about 50% (49.0% versus 90.3%) after a full 3000 seconds ageing at this vigorous agitation speed. This highlights the importance of initial shear on ultimate aggregate size.

5.1.3.2Effect of shear exposure and ageing time on the degree of α-lactalbumin precipitation

The yield of α-lactalbumin in the precipitate phase increases substantially with ageing. Fig. 4.18 shows the protein profile of the supernatant phase eluted through HPLC after acid addition at shear-rate 1124 s^{-1} followed by 3000 seconds of ageing at 486 s^{-1}. This is a typical profile after 3000 seconds ageing for all vessel shear conditions. The peak representing α-lactalbumin (19.41 minutes) has fallen considerably when compared with its concentration in the feed solution (Fig. 4.1), while the proportion of β-lactoglobulin present (17.18 minutes) has risen substantially providing a β-lg/α-la ratio of 13.59. Fig. 4.19 illustrates the precipitation of α-lactalbumin over ageing time in the agitation vessel for various acid addition shear-rates. Between 20 and 30% of the α-lactalbumin precipitates out during the initial 170 seconds of acid addition. This precipitation continues at a progressively slower rate during ageing, until about 70 to 80% of the α-lactalbumin is in the precipitate phase after 3000 seconds.

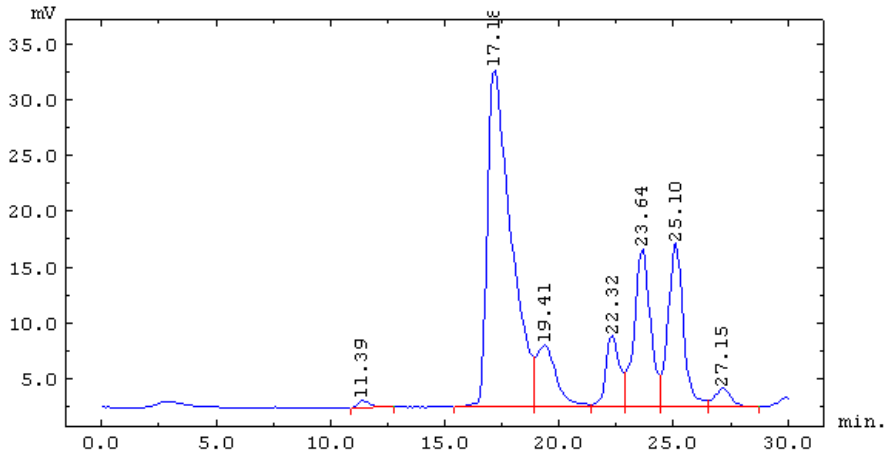

Figure 4.18 Typical HPLC profile of supernatant after 50 minutes ageing in agitation vessel.

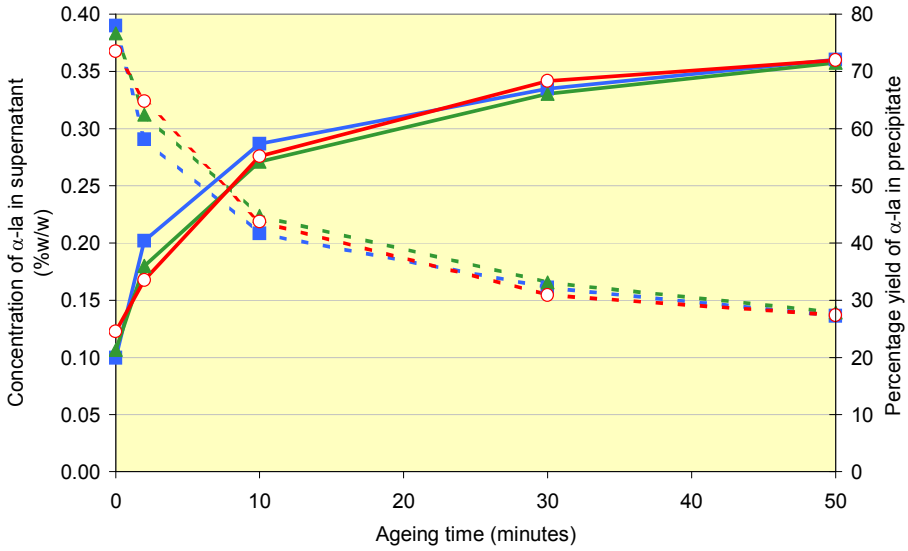

Figure 4.19 Absolute concentration (broken line) and percentage yield (filled line) of α-lactalbumin in supernatant and precipitate phases respectively during ageing at impeller shear-rate 486s^{-1} (low) following acid addition at impeller shear-rates 398s^{-1} (low) (squares), 783 s^{-1} (med) (triangles) and 1247 s^{-1} (high) (open circles).

This clearly shows the role played by ageing in precipitating proteins quite apart from any beneficial effects ageing may have on strengthening particles. It demonstrates the presence of a substantial amount of mass transfer during ageing. There is no net increase in aggregate size throughout the ageing period while the α-lactalbumin concentration increases substantially. This indicates considerable mass transfer takes place incorporating the mechanisms of aggregate erosion and restructuring, as well as the growth of smaller aggregates.

In contrast to the important role played by ageing time on precipitation of proteins, the application of various shear-rates during acid-addition and ageing have little effect on the rate of α-lactalbumin precipitation over time, as demonstrated in Fig. 4.19. Similar plots are obtained for different ageing shear rates. Moreover, HPLC analysis of the supernatant phase separated from precipitates before and after exposure to turbulent flow both through the capillary rig and through the ball-valve rig shows that there is no significant change in the α-lactalbumin content of the precipitate phase even where there is substantial aggregate breakage.

5.1.3.3Effect of agitation during acid addition and ageing on aggregate strength

Change in precipitate PSD leaving the capillary rig

Initial capillary shearing tests were undertaken on aggregate solutions with both 3.33% and 1% (w/w) whey protein concentration solution at high pressure to see if the higher concentration aggregate solution with corresponding higher level of particle-particle interaction suffers a significant amount of increased breakage in comparison with the 1% solution. These trials found a very slightly but consistently lower PSD profile in aggregates in the more concentrated solution after capillary shearing. Given the tiny difference in effect, a 1% solution was used for all subsequent runs since this resulted in minimum particle-particle interaction in comparison with particle-fluid and particle-wall effects and had rheological and density properties similar to that of water.

The solutions were processed through the capillary pipe to ascertain the effects of moderate levels of process shear on aggregates formed and aged under various agitation vessel shear conditions. A solution containing stronger, more compact aggregates, capable of resisting breakage during routine short term moderate shear processing is a more suitable feedstock for subsequent efficient centrifugal recovery of aggregates. Solutions were subject to both laminar (Re ≤ 1,800) and transitional/turbulent flow at Reynolds' number up to about 5,000 for times ranging from 1.6 seconds to 0.17 seconds depending on flowrate.

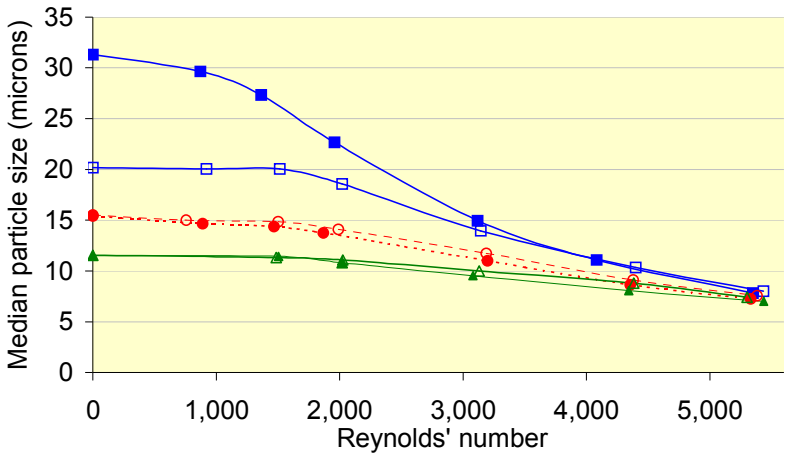

Figure 4.20 Effect of capillary shear on median particle size of aggregates with various shear histories aged for 3000 s (squares represent an acid addition impeller shear-rate of 398s^{-1} (low), circles are 783s^{-1} (med), triangles are 1247s^{-1} (high); closed symbols represent an ageing impeller shear-rate of 486s^{-1} (low), open symbols represent an ageing impeller shear-rate of 1124s^{-1} (high)).

Fig. 4.20 demonstrates the effects of capillary shear on aggregates with various formative and ageing shear histories. Particles subject to mild agitation during formation (precipitation and aggregation) and ageing (e.g. 398 s^{-1} & 486 s^{-1}) are much bigger than those produced under intense agitation (e.g. 1247 s^{-1} & 1124 s^{-1}). However, these

particles are not very robust and are readily broken down when exposed to turbulent capillary flow. The degree of turbulence exhibited by the flow in the tube has a significant effect on the degree of particle breakage. Laminar flow, even at mass average capillary shear-rates of up to about 9,000 s^{-1}, causes minimum shear disruption to all but the largest most delicate aggregates. However, as flow begins to become transitional above a Reynolds' number of about 1,800, breakage is accelerated. Particles formed at higher shear-rates in the stirred-tank suffer a lesser degree of breakage when exposed to high capillary shear. However, irrespective of shear history, median particle diameters appear to converge at turbulent flow, particularly when particles are exposed to the maximum Reynolds' number of 5,400 achieved in the capillary rig, roughly corresponding to the moderately high turbulent environment that might be encountered during routine processing through pipes and bends.

So why this apparent convergence? PSD plots show that increased turbulence in the capillary tube causes the volume of fragmented sub micron particles to increase substantially.

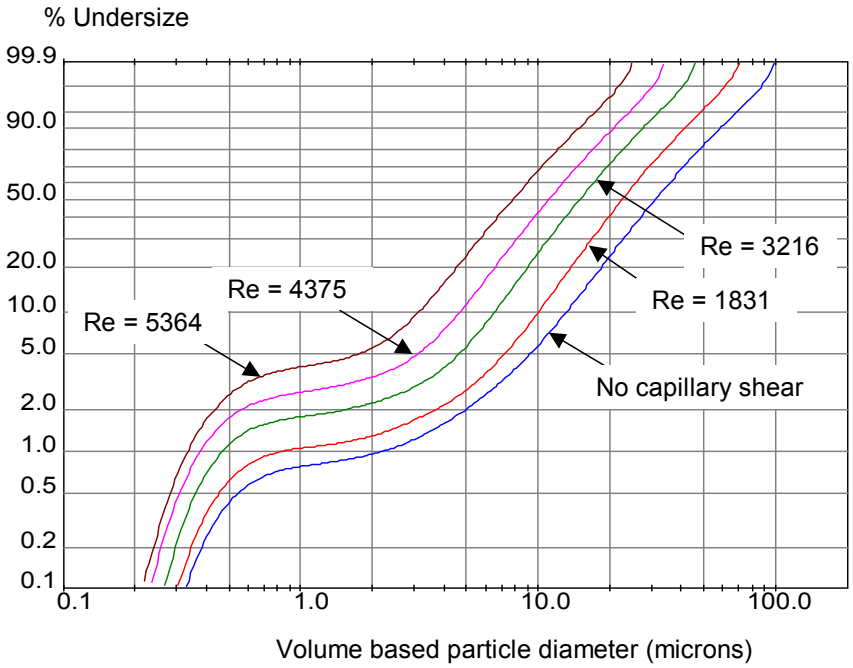

Figure 4.21 Effect of capillary shear on PSD of aggregates formed at agitator vessel shear-rate of 398s^{-1} (low) during acid addition followed by 3000 seconds of ageing at 486s^{-1} (low).

Fig. 4.21 shows a greater than five fold increase in the volume of sub micron particles when a precipitate solution, formed subject to mass average impeller shear-rate of 398 s^{-1} and aged at 486 s^{-1} for 3000 seconds, is subjected to Re of 5,364 for 0.175 seconds as it flows through the capillary tube. Moreover, the actual number of fragmented particles present increases substantially as the smallest particle diameter dips to 0.2 μm from 0.3 μm as a result of capillary processing. Hence it appears that PSD reduction in larger particles is principally due to erosion of primary particles from the relatively weak outer layers leaving a cohort of particles pared down to a relatively compact inner core and a substantial increase in sub micron particles. The smaller more compact aggregates formed under higher agitation vessel shear-rates however, suffer comparatively less erosion as there is less of the looser outer layer described by Ayazi

Shamlou et al (1996a) since the aggregates are fractal in nature (see chapter 5) and exhibit progressively looser structures as radial distance increases.

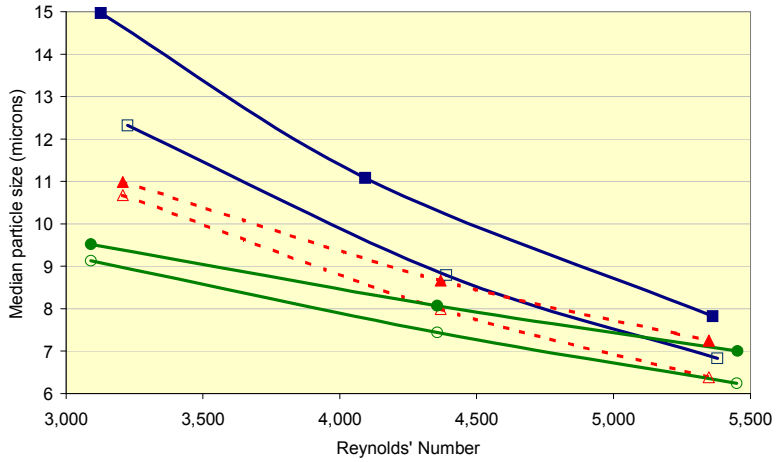

Figure 4.22 Effect of ageing time and capillary shear on median diameter of aggregates with various shear histories (squares represent an acid addition impeller shear-rate of 398 s^{-1} (low), triangles are 783 s^{-1} (med), circles are 1247 s^{-1} (high); open symbols represent a subsequent ageing time of 600 s; closed symbols represent an ageing time of 3,000 s). Ageing impeller shear-rate is 486 s^{-1} (low) throughout.

Ageing time also has an effect on aggregate strength. Fig. 4.22 shows the effect of capillary shear on the size of aggregates formed at various average acid addition shear-rates followed by ageing at 486 s^{-1} for either 600 seconds or 3000 seconds. Invariably aggregates aged for greater duration were better able to resist destruction when subject to moderately high turbulent flow in the capillary rig. This suggests aggregate restructuring takes place during ageing resulting in the evolution of smaller more compact aggregates better able to withstand subsequent harsher shear conditions.

Change in precipitate PSD leaving the ball-valve rig

The preceding section examined the effects of shear stresses associated with laminar and transitional capillary flow on protein precipitates and observed that shear history

seemed to have little effect on the ultimate size of particles since particle diameters tended to converge when subject to Reynolds' numbers up to about 5,000. However, at particular points in a separation process, far higher shear-rates may be experienced by particles, for example, during certain types of pumping or at the feed zone of a disc stack centrifuge. A ball-valve rig was constructed to investigate the effects of exposure to highly turbulent flow of this type.

Fig. 4.23 shows how this highly turbulent flow through the ball-valve affects the median particle size of aggregates formed under various mass average impeller shear-rates in the agitation vessel. In all cases, flow through the ball-valve produced a significantly greater reduction in particle size than flow through the capillary and aggregates are effectively shattered by this regime.

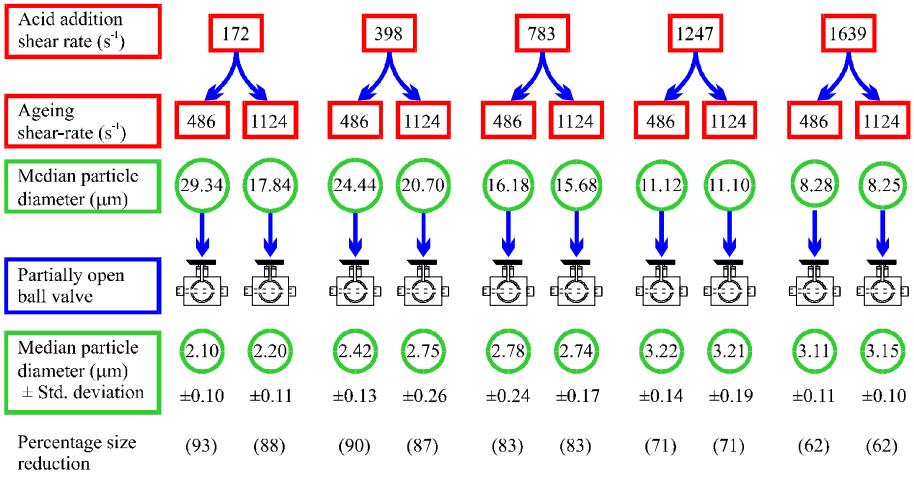

Figure 4.23 Effect of highly turbulent processing through a partially open ball-valve on particle size for whey protein precipitates subject to various impeller shear-rates during acid addition and ageing in a 1.4 L batch agitation vessel.

Impeller shear-rates during acid-addition in the stirred-tank have a significant effect on the size of particles leaving the ball-valve. Aggregates formed subject to high shear-rates (1247 s^{-1} and 1639 s^{-1}) are broken down upon leaving the ball-valve to form

particles of greater size than those formed under medium shear-rates (398 s^{-1} and 783 s^{-1}), which in turn are greater than those formed under very low shear-rates (172 s^{-1}). A final aggregate average median diameter of 3 microns may not appear substantially greater than 2 microns in absolute value, but it does represent a 50% increase in diameter and over 3 times larger in volume. These results suggest that application of higher shear-rates during acid-addition result in the formation of a stronger more compact aggregate that has a higher resistance to break-up when exposed to highly turbulent conditions as prevalent in the ball-valve rig. There may however be an optimum agitation vessel shear-rate depending on subsequent shear processing conditions. For example, in this process aggregates formed under the maximum acid addition shear-rate of 1639 s^{-1} suffer the least reduction in size by percentage but their product particles after ball-valve shearing are still marginally smaller than the corresponding particles emanating from aggregates formed at 1247 s^{-1}. Increased agitation intensity during aggregate formative stages increases aggregate strength in general but above a certain shear level this increase may become marginal.

The huge drop in particle size experienced by aggregates of all shear histories suggests a different and more robust mechanism involved in aggregate breakage than mere erosion. Just as the ostensibly converging aggregate size due to capillary shear suggests erosion of outer layers of aggreagtes leaving particles of broadly similar size made up of a compact core, the absence of such during ball-valve shearing and the variable post ball-valve sizes and relatively large standard deviations associated with them suggests a more brutal and random type of breakage.

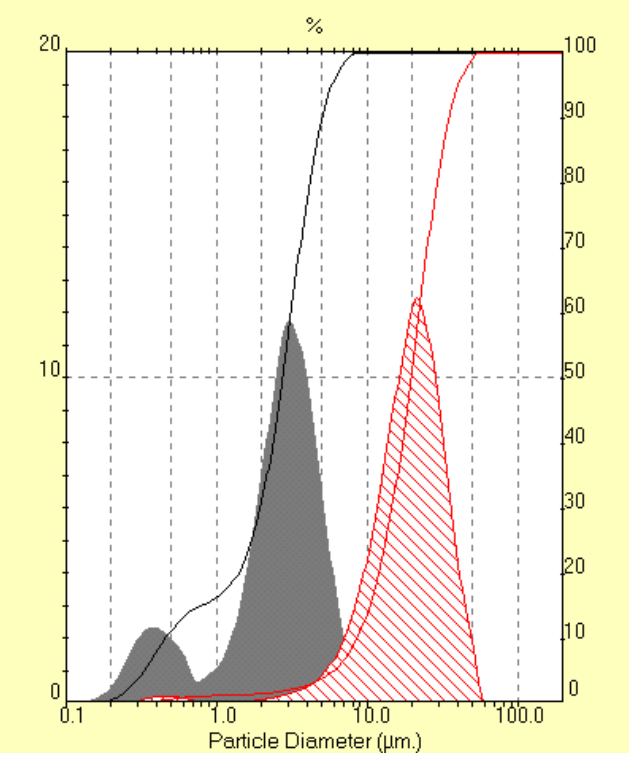

Figure 4.24 Effect of ball-valve shear on PSD of aggregates previously subject to an agitation vessel acid addition shear-rate of 398 s^{-1} (low) followed by 3000 seconds ageing at 1124 s^{-1} (high) (hatched represents pre-shear PSD, filled is post-shear).

Fig. 4.24 shows how PSD profile of aggregates is radically changed as a result of ball-valve shear. The number of sub micron particles have increased substantially and account for some 15% of aggregates by volume from just over 1% before shear exposure in this instance. In addition larger aggregates have decreased in size from diameters of tens of microns to 2-3 microns typically. This is not the stuff of mere erosion, fracture of aggregates into a number of smaller aggregates is likely. Such a process would also involve erosion but only as a secondary breakage mechanism where fragment particles are eroded from the newly formed fragment particles under condition of severe turbulent fluid stresses. This feature was also recognised by Bell and Dunnill (1982a) and Bell (1982) suggests that while erosion may be the dominant mechanism

for aggregate breakage in the initial stages of precipitation, fragmentation of groups of primary particles is more likely after ageing.

5.1.4 Chapter conclusions

The application of higher shear-rates in an agitation vessel during the isoelectric precipitation of proteins results in smaller aggregates. Impeller agitation during the aggregate formative period when the precipitation agent is being added has greatest influence on size though the application of shear during a subsequent ageing period may contribute to further size reduction particularly if the shear-rate during ageing is higher than that experienced during the addition of the precipitation agent.

The appearance of a characteristic bimodal particle size distribution curve at moderate to high agitation vessel impeller shear-rates suggests a significant amount of aggregate erosion takes place producing a large number of sub micron particles. This effect is noted as early as the end of the acid addition period and is the dominant mode during any subsequent ageing period.

Ageing time has a significant effect on the degree of precipitation of α-lactalbumin. 20 – 30% of α-lactalbumin precipitates out during acid addition with a further 50% over 3000 seconds of ageing.

Particle size does not increase during ageing over the shear regimes considered and any major decreases occur during the first 600 seconds after which there is a slow decrease in particle size. Particles become stronger with increased ageing time and this is most likely due to the particles becoming more compact through restructuring, erosion and infilling with α-lactalbumin rich primary particles.

Capillary processing under a laminar flow regime does not result in shear-rates capable of causing much size reduction in aggregates, this is especially true for smaller

aggregates formed at higher agitation vessel shear conditions. However, as capillary flow becomes more turbulent, there is a substantial increase in the degree of particle breakage, particularly among larger aggregates formed under mild impeller shear. This results in converging median aggregate sizes after turbulent capillary shear, irrespective of agitation vessel shear history. This implies that an erosion mechanism takes place whereby sub micron particles are eroded from a loose outer layer of variable thickness (depending on agitation vessel shear history) which surrounds a dense inner core with a diameter common to all aggregates.

Aggregates subject to still higher levels of turbulent shear during ball-valve processing break down to even smaller particles and median particle size again diverges but with less consistency or repeatability. This suggests size reduction is due to aggregate fracture, which even involves the dense inner core, to produce smaller fragments. In this case however, shear history in the agitation vessel has a significant effect on ultimate particle size after ball-valve processing as aggregates formed under more intense agitation result in significantly larger particles after ball-valve processing. Aggregates subject to intense vessel agitation would thus appear to be stronger and better able to resist further breakage. Such aggregates should be better suited to centrifugal separation on an industrial scale where shear associated with the centrifuge feed zone might also cause substantial breakage.

Aggregate size and strength are important parameters in determining ease of ultimate centrifugal separation. However, another factor which impinges on separation efficiency is the degree of aggregate compactness. This is explored in terms of fractal dimension in Chapter 6. Hindered settling is also undertaken in order to gain a better understanding of separation patterns and compare with predicted settling velocities.

Chapter 6 Particle settling and fractal properties

6.1.1 Theory

6.1.1.1Free settling

Free settling of particles is a term used to describe gravity settling of particles in a fluid where the only opposing forces are those due to the drag of the surrounding fluid on the surface of the particle. Stokes (1851) found the total drag force on a spherical particle falling slowly (in the laminar or Stokes region) at its terminal velocity in a Newtonian fluid by solving the relevant Navier-Stokes equations:

$$F = 3\pi\mu d V_t \qquad 5.1$$

This is balanced by an opposing and equal gravitational force on the particle:

$$F = \frac{\pi d^3(\rho_p - \rho)g}{6} \qquad 5.2$$

A force balance involving the preceding two relations gives the Stokes terminal velocity:

$$V_t = \frac{d^2(\rho_p - \rho)g}{18\mu} \qquad 5.3$$

This equation describes particle terminal velocity in an ideal situation where a solid particle of density ρ_p falls through an infinite expanse of fluid of density ρ. However, in real terms it works well at particle concentrations below about 0.5% by volume as at these concentration levels particle-particle interactions are minimal (Svarovsky, 1981).

6.1.1.2Hindered settling

For most industrial separation processes, concentrations in excess of 0.5% typically exist and the effects of particle-particle and to a lesser extent particle-wall interactions

must also be considered. This type of particle settling is known as hindered settling. Hindered settling has a number of distinguishing features which result in the settling velocity being slower than for free settling. The relative speed of settling is a function of the particle concentration in solution and falls rapidly with increasing concentration. Where there are settling particles spanning a range of sizes, larger particles fall more quickly than the others dragging smaller particle in their wake but in doing so they displace fine particles with the suspending fluid through smaller available cross sectional area which then creates a greater upward drag on the settling particles due to 1) higher upward velocity and 2) greater effective viscosity of the suspending fluid (Geankoplis, 1983). Furthermore, the relative closeness of particles leads to particle-particle interactions which may adhere to each other forming loose larger aggregates (Svarovsky, 1981). Typically there is an initial brief period of particle acceleration during which time an interface layer is formed (Coulson and Richardson, 1991). Thereafter this layer gradually settles as particles fall. If the range of particle size is not greater than 6:1, all the particles in a concentrated solution settle at the same velocity (Svarovsky, 1981; Coulson and Richardson, 1991). Particle-wall interactions are thought not to be significant if particle diameters are less than 1% of settling vessel diameter (Coulson and Richardson, 1991).

6.1.1.3Fractal geometry of particles

Particle separation properties; size and fractal dimension

Particle size is the most important factor determining the separation efficiency of precipitates from a suspended fluid during gravity settling or centrifugation as illustrated in equation 5.3. Equation 5.3 shows that particle density is another important factor governing the ease of separation of particles from the supernatant. Protein precipitates however are neither of uniform density nor are they perfect spheres and indeed neighbouring precipitates may form loose inter-particle aggregates during hindered gravity settling or centrifugation. Indeed, to characterise protein precipitates by a single density value is somewhat misleading as, in common with many other aggregates, they

typically comprise a dense inner core surrounded by progressively looser, less strongly bound outer layers, exhibiting a reduction in density proportional to distance from the centre (Ayazi Shamlou et al, 1996a; Sonntag and Russell, 1987). Tambo and Watanabe (1979b) experimentally showed how bulk density decreases with increasing aggregate size. Such aggregates are said to have fractal characteristics and protein aggregates typically fall into this category (Ayazi Shamlou et al, 1994b; Feder, 1998). Accordingly, more useful insights into the behaviour of particles during centrifugal or gravitational settling might be gained from a study of the fractal geometry of the aggregates.

What is fractal dimension?

Benoit Mandelbrot proposed and pioneered the study of fractals and has published a number of standard references, which explore how fractal geometry can be applied to a diverse range of fields (1975, 1977, 1982). Mandelbrot has reportedly proposed the following succinct definition of a fractal (Feder, 1998):

> "A shape made of parts similar to the whole in some way"

An aggregate in three-dimensional space may be considered fractal if its density decreases with radial distance, r from the origin such that $\rho(r) \propto r^{D_f - 3}$ where D_f is known as the fractal dimension in three-dimensional space and is less than the Euclidean dimension (i.e. three) (Feder, 1988; Ross 1994). If the three-dimensional fractal dimension is less than two then it has the same value as the fractal dimension in two-dimensional space (Meakin, 1988). An aggregate with a fractal dimension of three will have a completely compact structure and its density will correspond to the density of the primary particles from which it is composed. On the other hand, an aggregate with a fractal dimension less than three will exhibit a porous structure with a progressive reduction in the number of primary particles present per unit volume with increasing radial distance from the aggregate centre and a corresponding decrease in bulk density as volume defined by radial distance increases. For example, if a spherical aggregate,

comprising a large number of primary particles packed uniformly and compactly and each of radius, r_0, has a radius, r, the number of primary particles in the aggregate can be expressed:

$$N_o \propto \left(\frac{r}{r_0}\right)^3, N_o \to \infty \qquad 5.4$$

If the particle is fractal, the number of primary particles present per unit volume decreases with respect to radial distance from the aggregate centre, r, the rate of fall off depending on the fractal dimension:

$$N_o(r) \propto \left(\frac{r}{r_0}\right)^{D_f}, N_o \to \infty \qquad 5.5$$

Moreover, if each primary particle is assumed to have the same density, ρ_o, the number of primary particles is directly proportional to the mass of the aggregate particle and particle density in three-dimensional space can be written:

$$\rho_{D_f}(r) = \frac{M(r)}{V_p(r)} = \frac{m_o N_o(r)}{V_p(r)} = \frac{\rho_o V_o r^{D_f}}{V_p(r) r_o^{D_f}} = \rho_o \left(\frac{r}{r_o}\right)^{D_f - 3} \propto r^{D_f - 3} \qquad 5.6$$

Similarly, in two-dimensional space, D_f is less than 2:

$$\rho_{D_f}(r) \propto r^{D_f - 2} \qquad 5.7$$

and in general:

$$\rho_{D_f}(r) \propto r^{D_f - E} \qquad 5.8$$

where E is the Euclidean dimension of the space being considered. Thus a perfect sphere has a fractal dimension of 3, whereas a two-dimensional circular disc has a fractal dimension of 2 and a straight line has a fractal dimension of 1. Similarly a branched porous fractal structure when measured in three-dimensional space has a fractal dimension approaching three as its compactness increases.

Equation 5.6 estimates density of a spherical aggregate as a function of its fractal dimension assuming the free space in the fractal aggregate contributes nothing to overall density. In reality this space is occupied by interstitial fluid and the bulk aggregate density, ρ_p, lies somewhere between the density of the solid protein (of density ρ_s) and that of the interstitial fluid (density ρ_f) which combine to make up the aggregate:

$$\rho_p = \left(\frac{\rho_{D_f}}{\rho_s}\right)\rho_s + \left(1 - \frac{\rho_{D_f}}{\rho_s}\right)\rho_f = \rho_{D_f} + \left(1 - \frac{\rho_{D_f}}{\rho_s}\right)\rho_f \qquad 5.9$$

where ρ_{Df} is the density of a fractal aggregate (equation 5.6). In order to estimate the fractal dimension of a number of aggregate particles of various radii, r, equation 5.5, with proportionality constant k, can be rearranged in log-log form:

$$Log_{10}N_o(r) = Log_{10}k + D_f Log_{10}(r/r_0) \qquad 5.10$$

Protein precipitate aggregates are typically scale invariant fractals (Feder, 1998; Ayazi Shamlou at al, 1994b) albeit with little experimental data available on their fractal geometry (Ayazi Shamlou at al (1994b; 1996a). Moreover, the bulk of literature studies on fractal aggregates have been confined to spherical particles which are monodisperse in both size and shape (Bushel and Amal, 2000).

Determination of fractal dimension

In practice, it is impossible to count directly the number of primary particles that make up an aggregate particle of a given size as would be required to solve for D_f in equation 5.10. However, this can be overcome by using laser light scattering data to determine fractal dimension. Indeed, the use of cumulative size distribution to calculate the fractal dimension of aggregates is probably the best method in terms of producing accurate estimates (Logan and Kilps, 1995). Data produced by the Malvern Mastersizer S laser particle sizer (Malvern Instruments, Malvern, Worcestershire, England) is thus used for this purpose.

Laser light is projected through the sample chamber of the Malvern Mastersizer S (see Fig. 4.10). An array of detectors placed at the far side of the chamber at various scattering angles, θ are used to construct a profile of the particles. When incident laser light falls on a particle it is deflected, the angle of deflection increasing as particles become smaller. The Malvern Mastersizer S has diameter limits 0.05 - 880μm, well within the limits of particle diameters sampled in this study. This device consists 42 detectors where each detector is placed at a unique scattering angle and thus only detects particles in a particular size range. The scattering wave vector, q is a function of detector scattering angle and is defined:

$$q = \frac{4\pi n_i}{\lambda} \sin\left(\frac{\theta}{2}\right) \qquad 5.11$$

Thus each defined value for q corresponds to (the inverse of) some particle radius r. The intensity of light, I, scattered at each arbitrary scattering angle is a function of both the number of aggregate particles at the corresponding particle size present and of the structure of these particles. The latter is measured in terms of what is known as the "structure factor", which is in turn a function of fractal dimension (Lin et al, 1990). By definition, the number of primary particles present in each of these aggregates is a function of fractal dimension. Thus the deflected laser light intensity at each scattering

angle, I, is ultimately a function (among other things) of N_o and just as r may be measured in terms of q, equation 5.10 can in fact be written in the following quantifiable terms:

$$Log_{10} I = k_1 - D_f Log_{10} q \qquad 5.12$$

The negative slope of a plot of Log I vs. Log q at various scattering angles provides an overall estimate of the fractal dimension of the aggregate particles.

One caveat which applies to equation 5.12 is that, in order to obtain a reliable estimate of D_f, $r_{o\ min} < q^{-1} < r_{min}$ must be satisfied, where r_{min} is the radius of the smallest aggregate present and $r_{o\ min}$ is the radius of a single primary particle. At scattering wave vectors outside these limits, scattering is either isotropic and independent of q for primary particles or the phase difference between scattered fields from different smaller fractal sub-units within an aggregate is greater than unity and the phases add incoherently so that the total intensity is the sum of the intensities scattered from each sub-unit (Lin et al, 1990).

6.1.2 Materials and Methods

6.1.2.1Surface properties

Fractal geometry measurement

Aggregate fractal geometry was estimated by plotting equation 5.12 with laser diffraction data obtained from the Malvern Mastersizer. PSD profiles generated from the same equipment show the smallest primary particles have radii of about 0.1 μm though they can attain radii of up to 0.4 μm while aggregate radii (of sheared aggregates) can be as low as 0.5 μm. The chosen limits for estimating q^{-1} were based on these theoretical considerations as well as on practical considerations of the detector geometry and correspond with q^{-1} values in the range 0.112 to 0.355 μm. An example plot is shown in Fig. 5.1 from which D_f is estimated from the negative slope between the designated limits of q with 95% confidence limits.

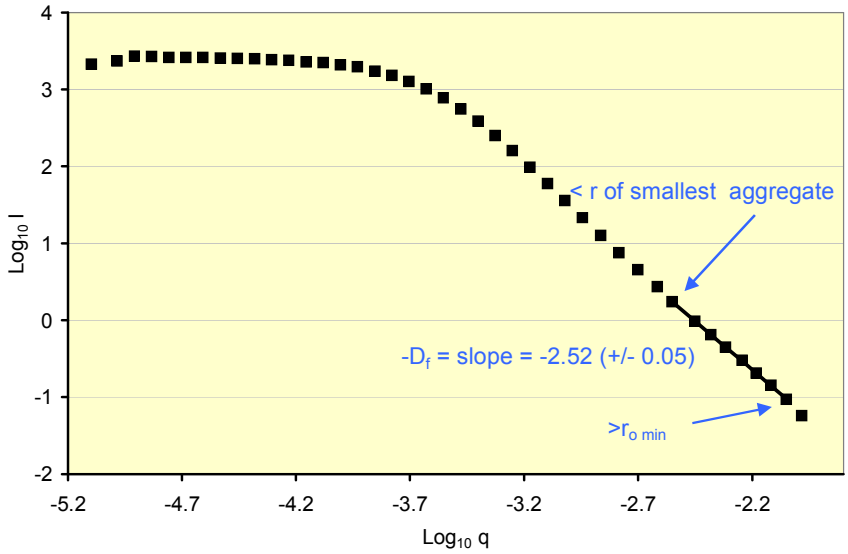

Figure 5.1 Log-log plot constructed to estimate fractal dimension using laser scattering data for precipitates subject to impeller shear-rate during acid addition of 783s^{-1} (med) followed by 3000 seconds of ageing at 486s^{-1} (low) in a 1.4L batch agitation vessel.

6.1.2.2Hindered settling studies

A laboratory centrifuge was used (Hettich Universal 16R bench top centrifuge (Hettich GmbH, Stuttgart, Germany)) to separate aggregates from supernatant. 10ml samples were prepared in centrifuge tubes from a 1:1 composition of whey protein aggregate solution and distilled water (effectively a 5% WPC concentration) made up from samples

taken at ageing times from 120 to 3,000 seconds with agitation vessel (acid addition and ageing) shear-rates ranging from $374s^{-1}$ to $1058s^{-1}$. The tubes were spun at 2000 rpm (equivalent to centrifugal force of 680 g) at 20°C for 300 seconds exclusive of run up and run down times (at 60 seconds and 220 seconds respectively) before being checked for the presence and height of an interface layer. This procedure was repeated a further five times in order to establish a profile of the rate of aggregate settling over time. This procedure effectively provided accelerated hindered settling as the height of the interface layer progressively decreased with centrifugation time.

6.1.3 Results

6.1.3.1Effect of agitation during acid addition and ageing on fractal geometry of aggregates

Fig. 5.2 shows the effects of vessel impeller shear (both during acid addition and subsequent ageing) on fractal dimension and size of protein aggregates formed by isoelectric precipitation. Smaller particles subject to higher impeller shear-rates during the formative acid addition period exhibit more compact structures and possess higher fractal dimensions. Ageing at elevated shear-rates also results in a slightly more compact structure except for precipitates subject to the highest acid addition shear rates.

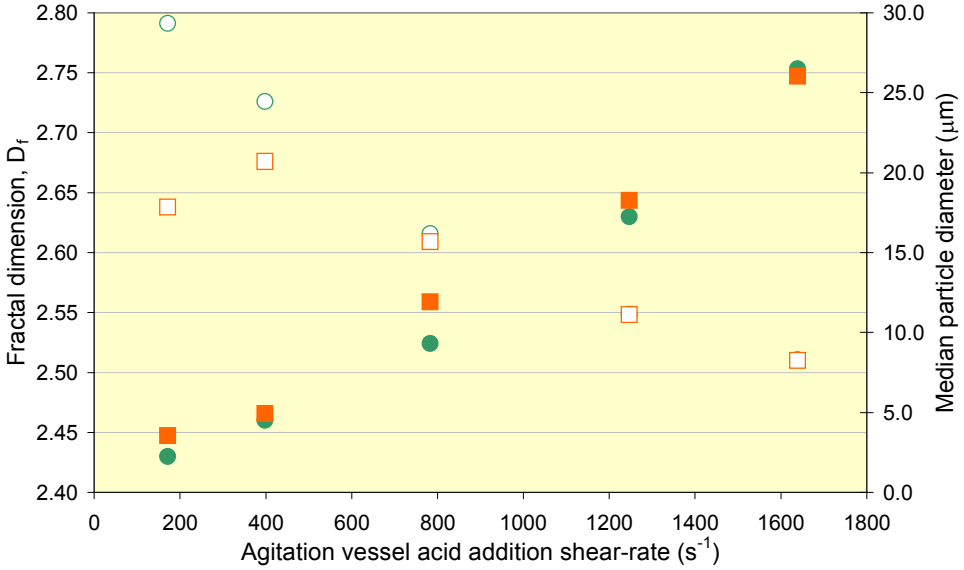

Figure 5.2 Fractal dimension (filled symbols) and size (open symbols) of aggregates formed by precipitation in a 1.4L batch agitation vessel subject to various impeller acid addition shear-rates followed by ageing at 486s^{-1} (low) (circles) and 1124s^{-1} (high)(squares) respectively for 3000 seconds.

This supports the model of aggregate erosion and restructuring during ageing presented earlier. A second mechanism might also be occurring concurrently during ageing as suggested by Lin et al (1990) who postulated that the application of shear causes loose ends to bend or deform particularly on larger fractal aggregates resulting in the formation of additional bonds and loops and an altogether stronger more compact structure. This restructuring is particularly evident at high impeller speeds. Logan and Klips (1995) reported that more compact structures with higher fractal dimensions are formed in agitation vessels with high shear environments especially around the impeller zone.

Aggregates formed by isoelectric protein precipitation are largely spherical as evidenced by optical microscope photographs (Bell and Dunnill, 1982b) and so aggregate density can be estimated using equations 5.7 and 5.10 and hence the relative Stokes settling velocities from equation 5.3. These data are presented in Table 5.1 where the density of

the solvent and interstitial fluid (water) at 20°C is taken as 998.2 kg/m^3 (Rogers and Mayhew, 1988) and the density of the solid protein phase (which also represents the primary particle density) is taken as 1300 kg/m^3 i.e. within the density range 1280 to 1366 kg/m^3 for solvated proteins as suggested by Bell et al (1983). PSD data of aggregates subject to various shear conditions suggest that the mode of primary particle diameters is about 0.4μm (Fig. 4.13; Fig. 4.14; Fig. 4.21, Fig. 4.24) and this is taken as representative of primary particle diameter for the purpose of estimating density. Stokes settling velocities show similar trends to hindered settling velocities as estimated by Richardson-Zaki relation (1954):

$$\frac{V(C)}{V_t} = (1 - C)^n \qquad 5.13$$

Perry's Handbook (1997) shows n to be about 4.5 for spherical particles settling at Re < 1.

Table 5.1 Particle size, fractal dimension and derived densities and settling velocities of aggregates subject to various impeller shear-rates during acid addition and ageing for 3000 seconds in a 1.4L batch agitation vessel.

Vessel shear rate (s^{-1})		Post vessel agitation			Aggreg. ρ	Rel. Stokes
acid add'n	ageing	d_{50} (μm)	D_f	Stand. Dev.	(kg/ m^3)	velocity
172	486	27.59	2.43	0.025	1025	1.00
172	1124	18.29	2.45	0.027	1035	0.59
398	486	24.36	2.46	0.024	1031	0.95
398	1124	19.54	2.47	0.025	1036	0.70
783	486	16.25	2.52	0.027	1050	0.66
783	1124	14.42	2.56	0.027	1060	0.63
1247	486	11.45	2.63	0.025	1085	0.56
1247	1124	10.89	2.64	0.027	1091	0.54
1639	486	8.02	2.75	0.018	1142	0.45
1639	1124	8.11	2.75	0.015	1139	0.45

Over the wide range of shear conditions studied, the fractal dimensions of aggregates range from 2.43 to 2.75, resulting in the bulk density of the smallest aggregates being over 10 percent greater than that of the largest. However the predicted settling velocity

of the larger looser aggregates remains higher, even without taking into account the higher sticking probability that is inherent in aggregates with lower fractal dimensions (Ross, 1994) which would favour further loose aggregation of particles during hindered separation. Table 5.1 shows that acid addition shear-rate is the dominant factor in determining fractal dimension just as it is in determining particle size. Ageing shear-rate has little effect on the settling properties of aggregates which have been subject to high shear-rates during acid addition though it does have a considerable effect on predicted settling velocities of aggregates subject to very low acid addition shear-rates.

Ageing also has some effect on fractal dimension. Table 5.2 shows aggregates which have been subject to a common acid addition and ageing shear rate of 866 s^{-1} become slightly more compact in addition to becoming smaller. Table 5.2 also predicts relative Stokes settling velocities for aggregates subject to various ageing periods and suggests that the larger particles with slightly lower fractal dimensions should settle faster than smaller aggregates which have been aged for longer.

Table 5.2 Particle size, fractal dimension and derived settling properties of aggregates subject to impeller shear-rate of 866s^{-1} during acid addition and ageing for various ageing times in a 1.4L batch agitation vessel.

Shear-rate (s^{-1})	Ageing time (s)	Post vessel agitation d_{50} (μm)	D_f	Aggreg. ρ (kg/m^3)	Rel. Stokes velocity
866	120	18.53	2.43	1032	1.00
"	600	16.51	2.45	1037	0.91
"	1800	15.30	2.47	1042	0.88
"	3000	14.63	2.48	1045	0.85

6.1.3.2Effect of vessel agitation and subsequent turbulent processing on the fractal geometry of aggregates

The previous section found that aggregates subject to lower shear-rates during acid addition and ageing, though less compact were significantly larger and thus predicted that they would separate more quickly during free settling. However this scenario assumes that particles are not exposed to the high shear conditions one might expect during industrial scale processing, through pipes, pumps, valves and upon entering a centrifuge. To this end the fractal dimensions of aggregates subject to highly turbulent

ball-valve shearing under the conditions described in section 4.2.2.2 were evaluated. Fig. 5.4 shows the effect of high shear processing on fractal dimension and size.

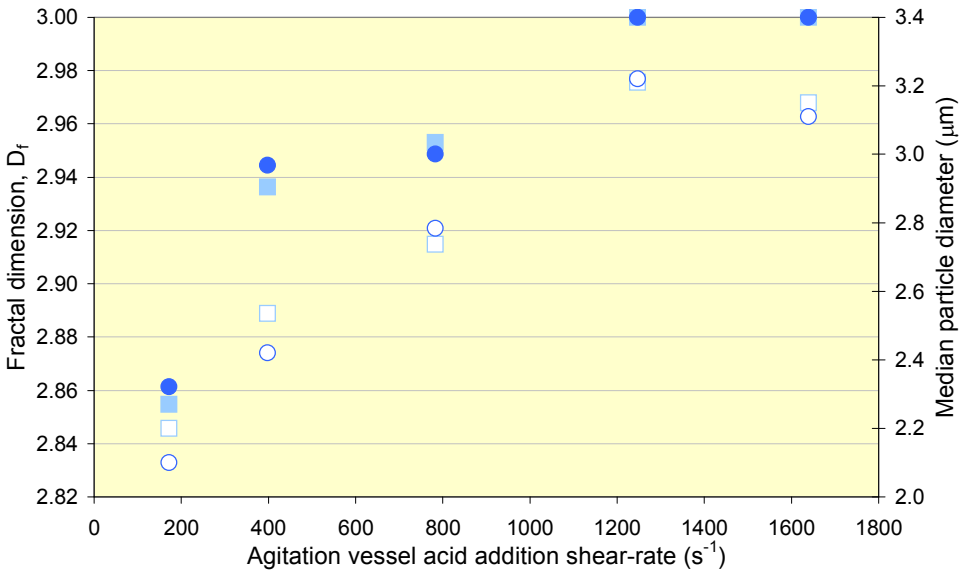

Figure 5.4 Fractal dimension (filled symbols) and size (open symbols) of aggregates subject to turbulent processing in a ball-valve rig after 1.4L batch agitation vessel precipitation at various acid addition impeller shear-rates followed by ageing at 486s^{-1} (low) (circles) and 1124s^{-1} (high) (squares) respectively for 3000 seconds.

The fractal dimension of aggregates increases appreciably upon passing through the ball-valve as they are broken down into smaller fragment particles. Indeed the larger fragmented particles formed from aggregates previously subject to impeller shear rates during acid addition of 1247s^{-1} or above appear to be so compact that they can no longer be described as fractal as their fractal dimension approaches three. This suggests that the compactness and strength of the aggregate inner core increases with increasing acid addition shear rate. There appears to be little difference in terms of post ball-valve fractal dimension and aggregate size for aggregates formed at acid addition shear-rates of 1247 s^{-1} and 1639 s^{-1}. This suggests there may be a limiting acid addition shear-rate above which there is no improvement in aggregate core strength and degree

of compactness. The intensity of agitation during acid addition has a significant effect on their fractal dimension apart from being highly important in determining the size of particles leaving the ball-valve.

Table 5.3 Particle size, fractal dimension and derived densities and settling velocities of aggregates subject to turbulent processing in ball-valve rig after 1.4L batch agitation vessel precipitation at various impeller shear-rates during acid addition and ageing for 3000 seconds.

Vessel shear rate (s^{-1})		Post ball-valve turbulent shear			Aggreg. ρ	Rel. Stokes
acid add'n	ageing	d_{50} (μm)	D_f	Stand. Dev.	(kg/ m^3)	velocity
172	486	2.14	2.86	0.011	1237	0.05
172	1124	2.19	2.85	0.011	1234	0.06
398	486	2.32	2.94	0.010	1272	0.07
398	1124	2.48	2.94	0.005	1267	0.08
783	486	2.6	2.95	0.009	1272	0.09
783	1124	2.89	2.95	0.007	1273	0.11
1247	486	3.26	3.00	0.009	1300	0.16
1247	1124	3.07	3.00	0.007	1300	0.14
1639	486	3.18	3.00	0.006	1300	0.15
1639	1124	3.24	3.00	0.005	1300	0.15

Table 5.3 estimates aggregate densities and relative Stokes settling velocities for ball-valve sheared aggregates previously subject to a wide range of agitation vessel impeller shear regimes. Higher acid addition shear results in stronger more compact aggregates which are better equipped to withstand subsequent elevated shear-rates and suffer less breakage and remain more compact during ball-valve processing. Such particles exhibit substantially higher free settling velocities and by extension should present a solution more suitable for more efficient (hindered) separation in a centrifuge.

6.1.3.3Centrifugal hindered settling of aggregates

Table 5.4 displays the settling rate of protein aggregate solutions formed and aged at a range of shear-rates and times through centrifugal separation. Shear-rates employed during acid addition were also employed during a subsequent ageing period. Dashes indicate the presence of no visible interface. Centrifuge tubes of 10cm volume were used. Some of these data are represented in graphical form in Fig. 5.5 and Fig 5.6.

Table 5.4 Rate of laboratory centrifugal settling of protein precipitate phase for aggregate solutions which have been subject to various agitation vessel shear-rates and ageing times.

Shear-rate (s^{-1})	Ageing time (s)	D(v,0.5) (μm)	Interface height (cm) after respective centrifugal spin times (min.) 5	10	15	20	25	30
$374s^{-1}$	120	25.80	4.25	3.10	2.75	2.50	2.40	2.20
"	600	25.34	4.00	2.90	2.50	2.30	2.10	2.00
"	1800	24.58	3.70	2.70	2.50	2.30	2.10	2.00
"	3000	23.56	3.60	2.50	2.40	2.25	2.10	2.00
$523s^{-1}$	120	24.35	4.60	3.20	2.80	2.50	2.35	2.20
"	600	22.66	4.30	3.00	2.70	2.50	2.30	2.20
"	1800	21.73	4.00	2.60	2.45	2.20	2.05	2.00
"	3000	20.99	4.00	2.50	2.30	2.10	2.05	2.00
$687s^{-1}$	120	22.26	4.80	3.48	3.00	2.65	2.50	2.35
"	600	20.27	-	3.38	2.85	2.50	2.43	2.28
"	1800	18.86	-	2.90	2.40	2.20	2.05	2.00
"	3000	18.18	-	2.65	2.20	2.05	1.98	1.95
$866s^{-1}$	120	18.53	-	3.85	3.25	2.83	2.55	2.50
"	600	16.51	-	3.45	2.55	2.33	2.15	2.00
"	1800	15.30	-	-	2.13	1.98	1.90	1.75
"	3000	14.63	-	-	2.05	1.95	1.88	1.75
$1058s^{-1}$	120	16.59	-	3.90	3.08	2.83	2.60	2.48
"	600	14.16	-	-	2.90	2.13	2.00	1.98
"	1800	13.18	-	-	2.00	1.88	1.75	1.65
"	3000	12.70	-	-	1.90	1.75	1.65	1.55

Fig. 5.5 shows how improved separation is obtained when aggregates have been subject to longer ageing times. This is not necessarily in contradiction to the predicted relative Stokes settling velocities presented in Table 5.2. Aggregates aged for a shorter time do tend to settle faster initially when conditions closest to free settling prevails as is evidenced by the quicker formation of an interface layer for aggregates formed and aged at 687 s^{-1} and above (Table 5.4). However ultimately the smaller but more compact aggregates formed after greater ageing settle more compactly. The same is true for aggregates which have been formed and aged at higher shear-rates. Fig. 5.5 shows that aggregates subject to lower agitation vessel shear-rates settle faster initially and quickly form an interface layer, though those subject to higher vessel agitation shear-rates eventually catch up and ultimately settle more compactly.

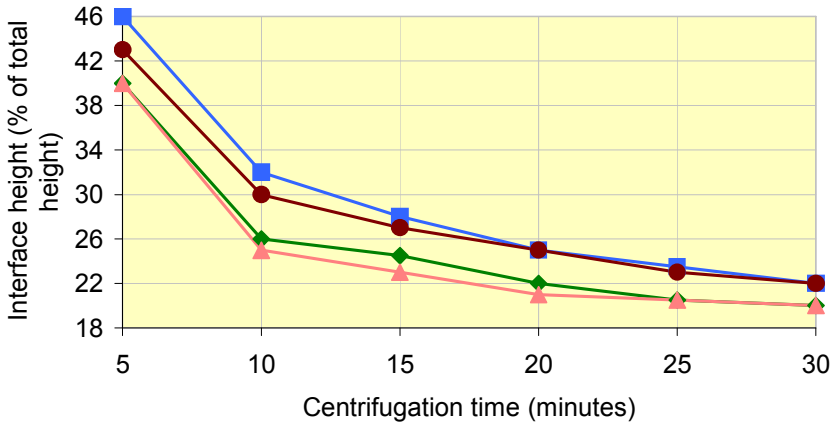

Figure 5.5 Rate of laboratory centrifugal settling of protein precipitate phase for aggregate solutions which have been subject to agitation vessel acid addition and ageing shear-rate of 523 s^{-1} for various ageing times: squares 120 s; circles 600 s; diamonds 1800 s; triangles 3000 s.

Figure 5.6 Rate of laboratory centrifugal settling of protein precipitate

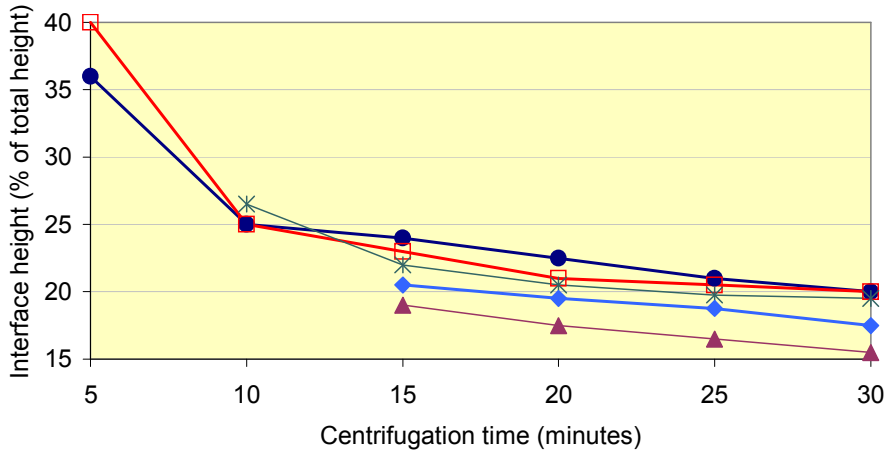

phase for aggregate solutions which have been aged for 3000 seconds at various shear-rates: squares 374 s^{-1}; circles 523 s^{-1}; crosses 687 s^{-1}; diamonds 866 s^{-1}; triangles 1058 s^{-1}.

In general smaller aggregates, whether due to longer ageing or more intense agitation shear, ultimately settle more compactly. This is due to the more efficient packing that can be achieved with smaller particles and also since they are likely to exhibit greater sphericity due to increased erosion and restructuring. Such particles also exhibit higher fractal dimensions which are associated with reduced sticking probability and hence reduced likelihood of forming loose aggregate-aggregate bonds during hindered settling.

Two contrasting settling regimes emerge. These are presented schematically in Fig 5.7.

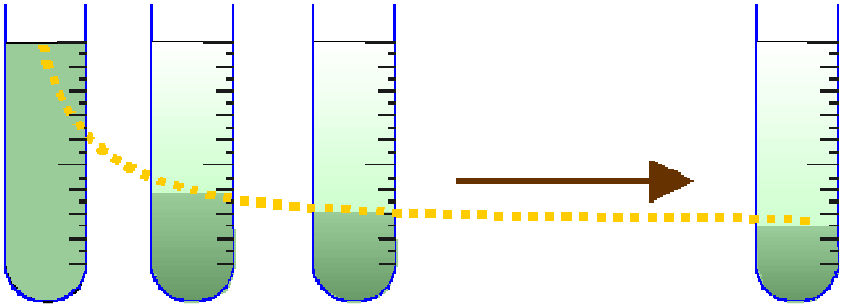

(a) Solutions containing larger aggregates settle quickly initially before slowing but do not ultimately provide a compact supernatant phase.

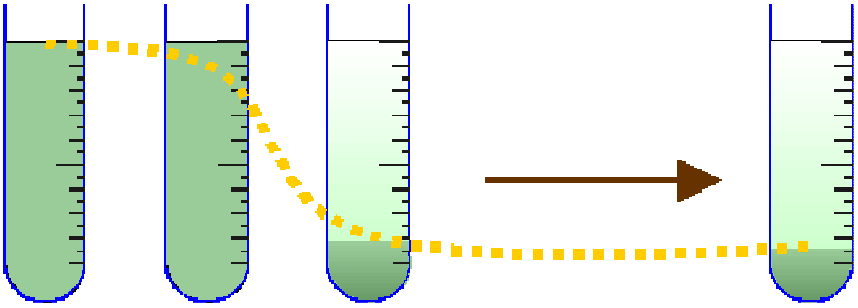

(b) Solutions with smaller aggregates do not quickly form an interface layer, instead settling slowly together initially but ultimately provide a more compact supernatant.

Figure 5.7 Hindered settling regimes for protein aggregates.

Larger aggregates formed and aged at lower shear-rates settle quickly initially before slowing down while smaller aggregates which have been exposed to higher shear-rates

and/or longer ageing times take a lot longer to form an interface layer though when it does it forms at a lower height. The latter aggregates eventually settle more compactly and take up less volume, thus ultimately separating more effectively.

Though all settling is hindered it is less so during the initial stages of centrifugal settling before the formation of an interface layer. The initial fast settling of larger particles is as predicted in the previous sections for the free settling velocity of such particles. Larger particles are also more likely in turn to form loose aggregates with neighbouring particles accelerating the initial settling rate still further. This is likely for two reasons: Firstly, larger aggregates are more likely to collide with other aggregates simply due to the space they occupy and greater settling speeds and secondly, when they do collide larger aggregates possess lower fractal dimensions and thus greater sticking probability. This also helps explain the poorer eventual compactness of centrifuged precipitates containing larger particles. Large loose multi-aggregates with non-descript shapes will not pack as well as smaller rounder more compact single aggregates. Smaller aggregates formed at higher shear-rates and/or extended ageing times settle more slowly initially though when the interface layer does form it is generally lower than for larger aggregates. This is due to the fact that denser particles take up less space and thus settling is less hindered, hence particles are more likely to settle independently for longer. Moreover aggregate solutions containing smaller aggregates have a smaller PSD range and the settling regime would be closer to that which pertains in cases where the particle size range is less than 6:1 i.e. all the particles settle at the same velocity.

In terms of the implications this has for centrifugal separation efficiency at pilot or industrial scale, it is clear that ultimately improved clarification is achieved for more rounded particles with higher fractal dimensions but that sufficiently high centrifugal force and/or residence time must be allowed.

6.1.4 Chapter conclusions

Protein aggregates formed by isoelectric precipitation are fractal in structure. A knowledge of the fractal geometry of these aggregates can thus provide a better understanding of their structure and can be used to predict their separation characteristics. Aggregates with higher fractal dimensions exhibit more compact and denser structures. Impeller agitation intensity affects fractal dimension and both shear-rate and ageing time have a positive effect on fractal dimension as increasing either leads to the development of more compact particles. As is the case with particle size and strength, impeller shear-rate during the period of acid addition is most important in determining ultimate particle structure. Higher shear-rates during this period lead to more compact aggregates though subsequent shear during ageing and ageing time also have important roles to play, particularly for aggregates subject to low shear-rates during acid addition.

Aggregates subject to high agitation vessel shear-rates during acid addition followed by 3000 seconds of ageing resulted in the most compact aggregates being produced after highly turbulent flow through the ball-valve rig ($D_f \rightarrow 3$). This result coupled with their greater size (chapter 4) suggest that higher shear-rates during acid addition should help improve centrifugal separation efficiency as these particles should be most resilient to the highly turbulent flow conditions prevalent around the centrifuge feed zone. There appears to be a critical acid addition shear-rate (~1247 s^{-1}) above which fractal dimension and size of particles fragmented in the ball-valve remain largely unaffected since aggregate core compactness has reached its maximum, breaking down into non-fractal dense particles. Increasing the acid addition shear-rate above this level would thus seem futile.

Chapters 4 and 5 have considered whey protein aggregates formed in a batch agitation vessel at laboratory scale and their corresponding separation characteristics. Similar aggregates produced at pilot scale are considered in the following chapter and separated in a disc stack centrifuge. The size of aggregates and their ease of separation

having been subject to various shear histories are compared at pilot scale with size and predicted separation efficiencies at laboratory scale to establish the effects of scale-up.

Chapter 7 Pilot scale protein precipitation and fractionation

7.1.1 Theory

7.1.1.1Agitation vessel scale-up

Geometric similarity is preserved during scale-up of a standard configuration vessel from laboratory to pilot scale. Scale-up based on providing fluid with constant power per unit volume, and hence constant spatial average shear-rate, is regularly used during batch vessel scale up as the average turbulent energy dissipation rate per unit mass, ε is the main determinant of microscale shearing effects (Oldshue, 1985). Moreover a number of authors have suggested a direct correlation between maximum particle diameter formed during precipitation and rate of turbulent energy dissipation (Tambo and Hozumi, 1979, Ayazi Shamlou et al, 1996a). Scale up preserving both geometric similarity and power per unit mass was thus employed in this study. This strategy does not however result in the maximum shear-rate to which aggregates are exposed being preserved. A comparison of the values in Table 4.3 (laboratory scale conditions) and Table 6.1 (pilot scale) bears this out. Table 4.3 depicts the flow conditions in the laboratory scale vessel computed from the relevant relations outlined in chapter 4 while Table 6.1 does the same for the pilot scale vessel. The pilot scale vessel had a volume 19.3 times greater than the lab scale vessel. This resulted in impeller speed decreasing by about 49% with constant power input upon scale up, though actual tip speed increased by 39% and hence maximum vessel shear-rate increased. Some other parameters were affected also. While fluid and particles experienced greater shear around the impeller in the larger vessel, they take longer to circulate since the mean particle circulation time, t_c (equation 4.7) also increased by some 92%. In addition, while flow is turbulent for all conditions chosen, the Reynolds' number increases by a factor of 3.73 in the larger vessel. Fig. 6.1 shows the laboratory scale and pilot scale vessels and their respective dimensions drawn to scale.

Table 6.1 Pilot scale agitation vessel calculated properties.

Fluid properties;						
ρ =	1050 kg/m^3		Np (Turbulent flow):	5		
ν =	4.71E-07 m^2/s		Nq (Rushton impeller):	0.9		
$D_{(impeller)}$ =	0.1083 m		V =	2.70E-02 m^3		
Impeller speed	**N**	**Re**	**ε**	**G**	**t_c**	**η**
rev/min	*rev/s*		*W/kg*	*s^{-1}*	*s*	μm
180	3.00	74,739	0.075	398	7.87	34.4
206	3.43	85,376	0.111	486	6.89	31.1
231	3.86	96,049	0.158	580	6.12	28.5
283	4.71	117,396	0.289	783	5.01	24.5
334	5.57	138,738	0.477	1006	4.24	21.6
360	6.00	149,409	0.595	1124	3.94	20.5
386	6.43	160,111	0.733	1247	3.67	19.4

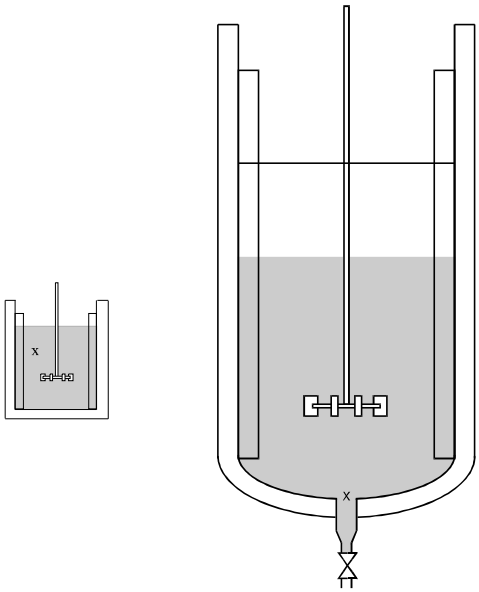

	Laboratory scale	Pilot plant scale
Configuration:	Standard	Standard
Internal diameter (m):	0.122	0.324
Effective Volume (l):	1.4	27
Sampling points denoted by X.		

Figure 6.1 Laboratory and pilot scale agitation vessels drawn to scale.

7.1.1.2Centrifugal separation

The terminal settling velocity of a particle under centrifugal acceleration can be assessed by replacing the gravity term, g in equation 5.3 with the centrifugal acceleration term, $\omega^2 r_c$, where ω is the centrifugal angular velocity and equals $2\pi N_c$:

$$V_t = \frac{d^2(\rho_p - \rho)\omega^2 r_c}{18\mu} \qquad 6.1$$

Centrifugation is used instead of gravity settling to speed up the separation process by increasing the driving force behind separation usually by a number of orders of magnitude. The ratio of centrifugal to gravitational separation speeds is known as the relative centrifugal force, RCF:

$$RCF = \frac{\omega^2 r_c}{g} \qquad 6.2$$

RCF is a function of both centrifugal speed and effective centrifugal radius as described by the following relation (Moir, 1988):

$$RCF = 11.22 \times 10^{-4} N_c{}^2 r_c \qquad 6.3$$

One important difference exists between gravitational and centrifugal settling; in the latter the driving force is not constant for a given particle, it increases with radial distance as the particle settles. As with gravitational settling, centrifugal separation times are extended by higher particle concentrations due to hindering effects (Svarovsky, 1981)

The sigma factor, Σ is a useful concept in centrifuge design and operation and indicates the required area of a gravitational settling tank which would have the same separating capacity as a centrifuge subject to given centrifugal speed. It is useful in comparing the

performance of different types of centrifuges and for scale-up on the basis of its relationship with flowrate through the centrifuge, Q/Σ. This ratio gives an indication of settling velocity. The sigma factor is a function of the geometry and design of a given centrifuge and for a disc stack centrifuge is given as (Records, 1977):

$$\Sigma = \frac{2}{3g}\pi Z_S \varpi^2 \cot\theta (r_o^{\ 3} - r_i^{\ 3}) F_1 \qquad 6.4$$

where F_1 is a correction factor to account for the presence of spacer ribs which support and separate the centrifuge discs;

$$F_1 = 1 - \frac{3Z_c b_c}{4\pi r_O} \cdot \frac{\left(1 - \left[\frac{r_i}{r_o}\right]^2\right)}{\left(1 - \left[\frac{r_i}{r_o}\right]^3\right)} \qquad 6.5$$

The clarification efficiency of a continuous disc stack centrifuge can be found if feed and supernatant optical density (OD) are known and compared against the OD of some clarified reference sample:

$$\%Clarification = \left(\frac{(OD_{feed} - OD_{ref}) - (OD_{\sup ernat} - OD_{ref})}{(OD_{feed} - OD_{ref})}\right) \times 100 \qquad 6.6$$

Clarification efficiencies at different feed flowrates can then be combined to create plots of clarification efficiency versus flowrate enabling the centrifugal separation efficiencies of precipitates formed and aged at various impeller shear-rates to be compared.

7.1.2 Materials and methods

Pilot scale protein precipitation and fractionation were undertaken at the Advanced Centre for Biochemical Engineering (ACBE), Department of Biochemical Engineering, University College London, England. This involved scale up of the laboratory scale precipitation and fractionation process described in previous chapters (carried out at the Department of Process Engineering, University College Cork, Ireland).

7.1.2.1Precipitate formation and ageing

Sample preparation

A batch standard configuration jacketed stainless steel fermentation vessel of effective volume 27 L was used to effect precipitation (Fig. 6.1). The vessel was fitted with 4 baffles and a 6-bladed Rushton impeller. 20 kg of reverse osmosis (RO) water was added to the vessel and preheated to 60°C via the vessel jacket which is supplied with process steam. 2.7 kg WPC was added to this while the impeller gently rotated at 180 rpm. 4.3 kg of water was then added to make up a 10% (w/w) protein solution. The impeller continued to rotate at 180rpm until the solution temperature had again risen to 60°C and protein dissolution was complete.

Protein precipitation and aggregation

585g of 2M Orthophosphoric acid (H_3PO_4) was added at a rate of 3.25g/s over 180 seconds as precipitation agent to reduce the pH of the solution to about 4.1. Orthophosphoric acid was chosen in preference to HCl due to its lower corrosive properties on stainless steel. The acid was added at the liquid surface of the solution with a Watson Marlow 605 DI peristaltic pump (Watson-Marlow Limited, Falmouth, Cornwall, England).

Impeller speeds were varied both during acid-addition and a subsequent ageing period of up to 3000 seconds. These were chosen to preserve the average spatial shear-rates

observed at laboratory scale upon scale-up. Applied impeller speeds and accompanying average shear-rates are listed in Table 6.1.

After acid addition, the impeller speed was adjusted to the appropriate agitation speed for ageing and aggregate solution samples of about 10-15ml were taken after 0, 120, 600, 1800 and 3000 seconds of ageing. Samples were immediately added to twice their volume of chilled RO water (4°C - 5°C) to disperse aggregates, adjust temperature, and prevent further potential aggregation. They were immediately placed in ice. Samples were taken at a sampling port at the base of the vessel (point X on the pilot vessel in Fig. 6.1) after excess residual solution had been flushed through.

7.1.2.2Particle characterisation

Particle size distribution was measured by laser diffraction with a Malvern 3600Ec laser particle sizer (Malvern Instruments, Malvern, Worcestershire, England). Aggregate sizes were measured from agitation vessel samples taken after ageing times of 120, 600, 1800 and 3000 seconds. Aggregates were also sized after disc stack centrifugation to measure the effects of centrifugal separation on particle size. An accurate measure of particle size was difficult to obtain however due to a considerable amount of clumping and re-aggregation of fragment particles which tended to occur in the heterogeneous precipitate slurry. This was overcome by diluting the precipitate slurry and by the gentle agitation of the sample before sizing. Sizing was undertaken on samples taken from precipitate slurry solutions with centrifuge feed flowrates corresponding to $Q/\Sigma = 1.78 \times 10^{-8}$m/s and with various agitation vessel shear histories. Three separate samples were taken from each run and results were averaged.

7.1.2.3Disc stack centrifugation

After 3000 seconds of impeller agitation at 60°C, the aged solution was added to twice its volume of chilled RO water (4-5°C) to prevent further aggregation and stored in a cold room at this temperature. This ratio of WPC to water (3.33% w/w) provided feed

from the pilot scale vessel of suitable solids content for centrifugal separation. The precipitate solution was removed from the cold room in a chilled jacketed vessel at 5°C and pumped as feed to a Westfalia CSA-1 disc stack semi-hermetic centrifuge (Westfalia Separator, Wolverton, Herts, England) with bowl volume 0.6L using a Watson Marlow 605 DI peristaltic pump (Watson-Marlow Limited, Falmouth, Cornwall, England). The centrifuge bowl operated at 9810 rpm providing a sigma value Σ of 1573m^2 according to equation 6.4. Four feed flowrates were chosen corresponding to Q/Σ of 9.11×10^{-9}, 1.34×10^{-8}, 1.78×10^{-8} and 2.21×10^{-8}m/s. Once steady state was achieved for a given feed flowrate after 5-6 bowl throughputs, samples were taken from the supernatant line at regular intervals and optical density (OD) readings at 360nm were taken on a Pharmacia Biotech Novapec II Spectrophotometer (Amersham Pharmacia, St. Albans, Herts, England). As well as taking supernatant OD readings ($OD_{supernat}$), the spectrophotometer was used to measure the OD of unaltered feed (OD_{feed}) and that of a feed sample spun at 10,000g for 1800 seconds (OD_{ref}) and equation 6.6 was used to estimate the clarification efficiency.

Particle size distribution of representative samples of diluted product sludge (from the solids product stream) were made for a number of runs in order to determine the effects of the centrifuge on particle size for particles with various precipitation and ageing shear histories.

7.1.3 Results

7.1.3.1Effect of agitation vessel scale-up at constant power input per unit volume on aggregate particle size distribution

Impeller speeds were chosen in the pilot scale agitation vessel to yield identical average spatial shear-rates to those at laboratory scale. Fig. 6.2 shows how aggregate size varies with the application of various agitation shear-rates for 170 seconds of acid addition followed by either relatively high (1124s^{-1}) or relatively low (486s^{-1}) shear-rates

during subsequent ageing periods between 120 and 3000 seconds. Comparing Fig 6.2 with Fig. 4.15, which shows aggregate sizes for identical shear and ageing conditions at laboratory scale, reveals similar trends though some differences in aggregate sizes depending on applied shear-rate are evident.

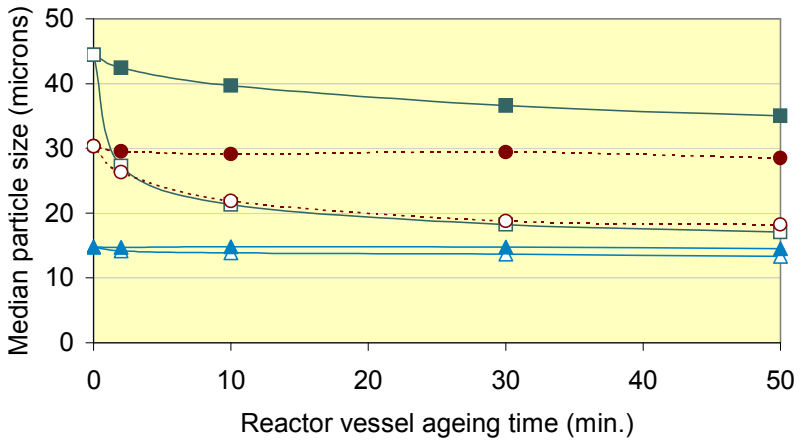

Figure 6.2 Effect of impeller shear-rate during acid addition and during ageing on median particle size in a 27 L agitation vessel (squares represent an acid addition impeller shear-rate of 398s^{-1} (low), circles are 580s^{-1} (med), triangles are 1247s^{-1} (high); filled symbols represent an ageing impeller shear-rate of 486s^{-1} (low), open symbols represent an ageing impeller shear-rate of 1124s^{-1} (high)).

Aggregates are typically larger after the acid addition period at pilot scale and this is most pronounced at lower acid addition shear-rates. A similar pattern of particle size reduction takes place when aggregates are subject to a relatively low ageing shear-rate (486 s^{-1}). However, at higher ageing shear-rates (1124 s^{-1}), the sizes of aggregates formed at a range of acid addition shear-rates tend to converge more quickly and to a greater extent with ageing time, principally as a result of substantial reductions in size of those aggregates which had been subject to lower acid addition shear-rates.

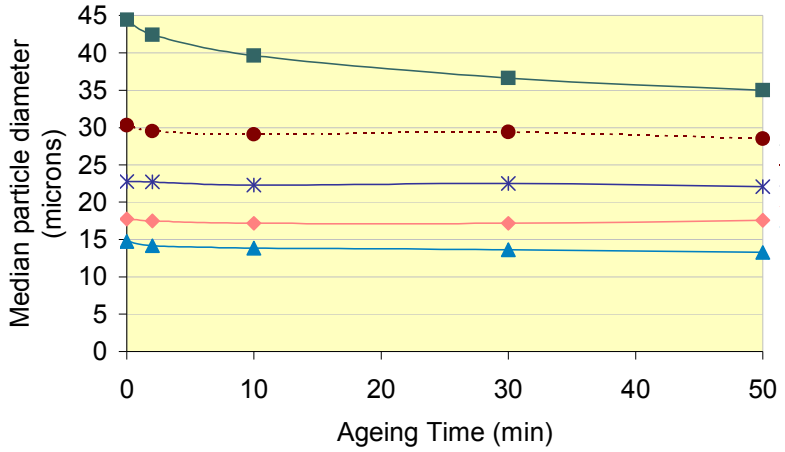

Figure 6.3 Effect of impeller shear-rate on median precipitate size in a 27 L agitation vessel for an ageing period of up to 3000 seconds at 486 s^{-1} (low) following various acid addition impeller shear-rates (squares 398 s^{-1} (low); circles 580 s^{-1} (med-low); crosses 783 s^{-1} (med); diamonds 1006 s^{-1} (med-high); triangles 1247 s^{-1} (high)).

This suggests aggregates formed at pilot scale are weaker as they are more susceptible to size reduction particularly when subject to higher ageing shear-rates. This is most evident if one compares Fig. 6.3 and Fig. 6.4 with the corresponding plots at laboratory scale (Fig. 4.16 and Fig. 4.17). All plots show aggregates which have been subject to a range of acid addition shear-rates from 398 s^{-1} to 1247 s^{-1}. Fig. 6.3 and Fig. 4.16 show aggregates which have then been aged at 486 s^{-1} for up to 3000 seconds. Each show very similar behaviour and exhibit a small but gradual particle size reduction over time when exposed to this relatively low level of ageing shear agitation.

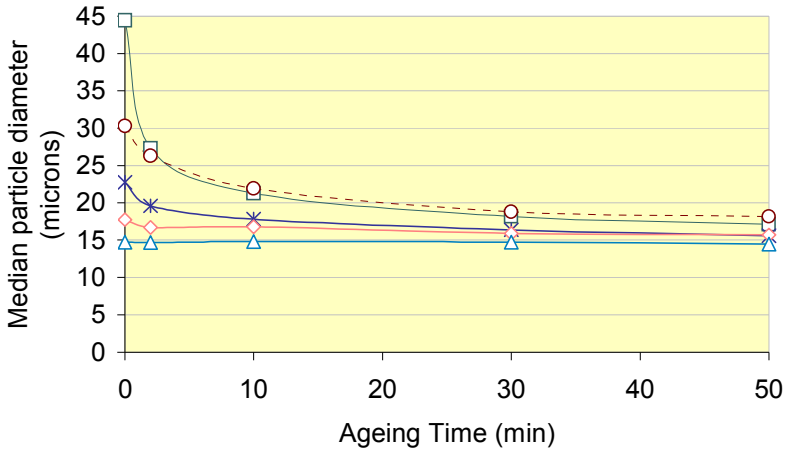

Figure 6.4 Effect of impeller shear-rate on median precipitate size in a 27 L agitation vessel for an ageing period of up to 3000 seconds at 1124 s^{-1} (high) following various acid addition impeller shear-rates (squares 398 s^{-1} (low); circles 580 s^{-1} (med-low); crosses 783 s^{-1} (med); diamonds 1006 s^{-1} (med-high); triangles 1247 s^{-1} (high)).

Fig. 6.4 and Fig. 4.17 show a less similar pattern when each are exposed to a far higher ageing shear-rate (1124 s^{-1}). The high ageing shear-rate causes substantial size reduction in aggregates which have been subject to lower shear-rates during acid addition in both cases but this reduction is far greater in the pilot vessel, and results in a greater level of convergence in median particle diameters after 3000 seconds of ageing. Clearly the high ageing shear-rate has greater impact on the larger but comparatively looser structured and weaker aggregates of the pilot scale vessel.

The differences in aggregate size upon scale-up from laboratory to pilot scale may be in part due to the use of different precipitation agents as well as their marginally different rates of addition which may have some effect on initial aggregate growth rates (Chan et al, 1986; Fisher et al, 1986). The different spatial sampling points in the two vessels may also have made a slight contribution to difference in apparent particle size though both laboratory and pilot scale vessels were well mixed. However the dynamic differences which arise upon scale-up also play an important role in aggregate formation. Agitation

vessel scale-up is on the basis of geometric similarity and constant power input but dynamic similarity is not preserved. Comparing impeller speeds in the smaller vessel (Table 4.3) with the larger one (Table 6.1) shows that if a constant average spatial shear-rate is maintained the impeller tip speed increases by 39% in the pilot vessel. This means that at similar average impeller shear-rates, the shear-rates experienced around the impeller zone are proportionally higher in the larger vessel. Correspondingly, to balance this the volume fraction in the agitation vessel occupied by fluid experiencing shear-rate less than the average is also greater in the larger vessel. In other words, the shear distribution becomes broader as vessel size increases. This has a number of implications on aggregate size.

The acid addition period is the formative period for aggregates; during this time precipitation and growth is opposed by the forces of breakage and restructuring due to impeller agitation. The physical properties which aggregates exhibit such as size, strength and compactness by the end the acid addition period are ultimately determined by the balance between particle growth and break up processes (Bell and Dunnill, 1982a). Aggregate formation occurs principally towards the end of the acid addition period as the bulk solution pH approaches the isoelectric point of α-lactalbumin. Before that, growth is principally perikinetic resulting in the formation of primary particles as samples taken at pH as low as about 5.0 during acid addition show exclusively sub micron particles present. For any given impeller shear-rate the typical particle circulation time (as estimated by equation 4.7 and displayed in Table 4.3 and Table 6.1) is 92% longer in the larger vessel. For example, circulation times are 4.10 and 7.87 seconds in the laboratory scale and pilot scale vessel at an average shear-rate of 398 s^{-1}. These are of great enough duration relative to the time it takes for aggregates to form to be significant. The longer circulation time in the pilot vessel, together with wider shear distribution and a short aggregate formation time combine to contrive that the PSD curve should be broader in larger vessels especially at low agitation intensity. This is indeed the case as is evident from Fig. 6.5. It should be noted that the PSD curves are

measured in terms of percent volume as opposed to actual numbers of aggregates present.

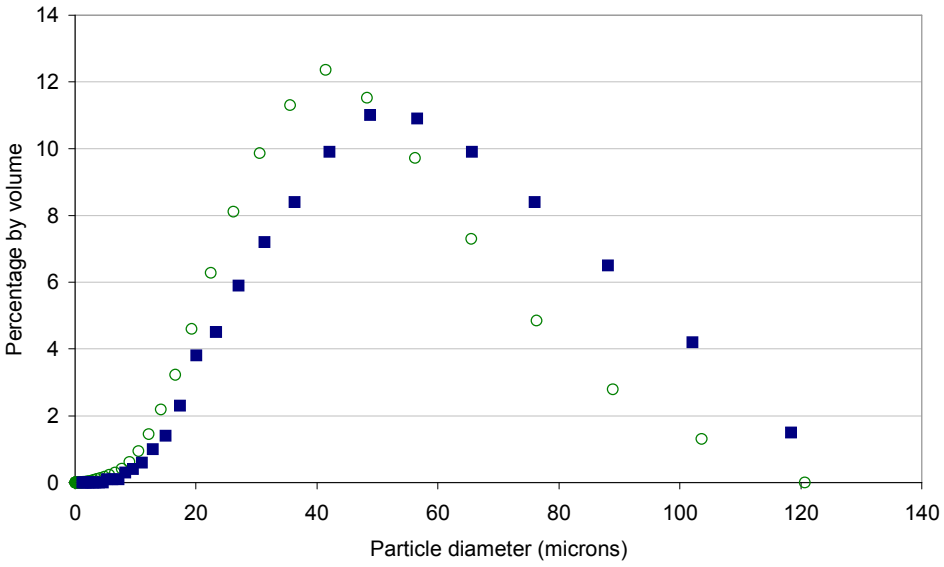

Figure 6.5 PSD curves for whey protein aggregates subject to average agitation vessel shear-rates of 398 s^{-1} (low) during acid addition in 1.4 L (open) and 27 L (fill) standard configuration vessels.

Erosion of primary particles, re-aggregation and restructuring of aggregates occur during the ageing period which follows acid addition as particle sizes are generally reduced. In this regime, it is the high intensity agitation zone around the impeller that is responsible for providing the necessary shear for particle erosion and restructuring (Reuss, 1988). Thus the impeller tip speed or maximum vessel shear plays an important role in size reduction during ageing. This is not surprising since the shear destructive forces which prevent aggregates attaining a given size during the formative acid addition period are not sufficient to cause larger particles to be broken down to this arbitrary size through erosion and breakage during subsequent ageing once larger aggregates have been formed. This is due to the strengthening effect of applied shear. Also during ageing the

circulation time loses its relative importance as aggregates have the opportunity to enter the high shear impeller zone many times.

This provides a basis to explain why changes in aggregate sizes during ageing upon scale-up differ. Exposure to higher maximum shear at pilot scale leads to greater aggregate erosion and restructuring and results in greater reduction in aggregate size. Secondly, the broader pilot scale PSD profile means that larger particles, which have been formed under exposure to comparatively lower shear-rates are more easily broken down during ageing.

Though the aggregates in Fig. 6.4, which have been subject to various shear-rates during the acid addition period prior to 3000 seconds ageing at similar shear-rates, exhibit similar median particle diameters there is no suggestion that they have similar structures. Fractal evidence from chapter 5 suggests that aggregates subject to acid addition at higher shear-rates continue to have more compact structures both before and after ageing. This is likely to be true at pilot scale as at laboratory scale.

7.1.3.2Effect of vessel agitation on centrifugal clarification efficiency of aggregates

During post agitation vessel processing and disc stack centrifugal separation, aggregates are exposed to elevated levels of shear. The most intense shear is experienced by aggregates as they enter the feed zone of a disk stack centrifuge and, at typically a couple of orders of magnitude greater than anything experienced heretofore in the agitation vessel, it causes extensive particle breakage (Bell, 1982; Bell and Dunnill, 1982b). Higher throughputs have been reported to cause increased centrifuge shear and hence increased particle breakage and reduced clarification efficiency (Clarkson et al, 1996).

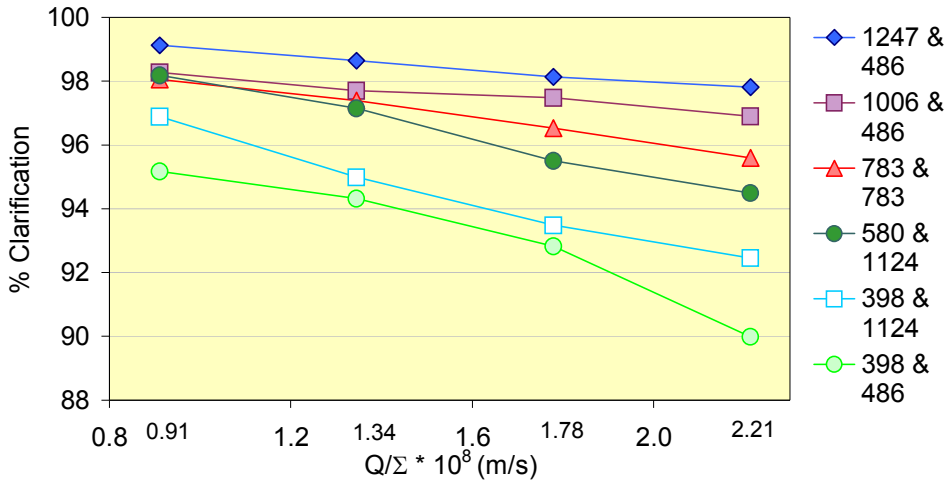

Figure 6.6 Disk stack centrifuge clarification curves for whey protein aggregates previously subject to various impeller shear-rates during acid addition and ageing in a 27 L batch agitation vessel (key displays shear-rates (s^{-1}) during acid addition (180 s) and ageing (3000 s) respectively).

Figure 6.6 shows centrifugal clarification curves for precipitates formed and aged at a number of agitation vessel shear-rates. This shows that shear-rate during acid addition has a significant effect on centrifugal clarification efficiency. At low Q/Σ values, 99% clarification efficiency is achieved at an average shear-rate of 1247 s^{-1} during acid addition versus 95% at 398 s^{-1}. Likewise at higher Q/Σ values, the clarification efficiency drops from 99% to 98% at the high acid addition shear-rate of 1247 s^{-1}, while it drops from 95% to 90% for the low shear-rate of 398 s^{-1}. In addition, the clarification efficiency of precipitates formed at very low shear-rates (398 s^{-1} during acid addition) improves if precipitates are subsequently subjected to high shear-rates during ageing.

Fig. 6.6. has important design implications. For example, for a given centrifuge throughput, a clarification efficiency of 98% can be obtained for aggregates formed at the high shear-rate of 1247 s^{-1}, while only 95% efficiency is obtained from a centrifuge with 2.4 times greater capacity when aggregates are formed at the low shear-rate of 398 s^{-1}.

These results compliment the laboratory scale separation projections based on the size and fractal geometry of aggregates subject to high shear processing. Clearly the intense agitation in the centrifuge feed zone causes substantial aggregate breakage particularly to larger weaker aggregates which lead to a substantial reduction in clarification efficiency.

7.1.3.3Size of precipitate aggregates leaving centrifuge

Precipitate samples were taken from the product solids sludge and sized. Fig. 6.7 shows the reduction in particle size as a result of centrifugal separation for particles with various agitation vessel shear histories. Regardless of shear history, there was substantial particle fragmentation during centrifugation though breakage seemed to be both brutal and random with no obvious link with shear history. There was considerable variation in measured particle size between consecutive samples taken at a given centrifuge flowrate as is evidenced by the large standard deviations. Moreover, there was no discernable trend evident among samples taken when centrifuge feed flowrates were altered. These effects were most likely due the clumping together of aggregates in the product precipitate sludge, a phenomenon also encountered by Bell and Dunnill (1982b), making it difficult to capture representative precipitate samples at pilot scale. Clarkson et al (1994, 1996) attempted to take account of particle breakage in the centrifuge feed zone and developed a centrifuge feed zone model in order to predict precipitate particle separation, meeting with some success.

In this study, ultimate post centrifuge approximate particle diameters fall somewhere between those exposed to capillary rig and ball-valve processing at laboratory scale lying somewhere between about 2 and 10 μm. This suggests similar shear-rates are prevalent at both scales. Thus the performance of aggregates formed at laboratory scale (which have been subject to similar vessel shear-rate and are of similar size) and subject to the more controlled turbulent high shear environments of the capillary rig and the ball-valve without the occurrence of precipitate clumping ought provide better

insights into how separation can be improved at pilot scale. For example, high shear agitation conditions during acid addition should be imposed in order to produce strong aggregates better able to withstand subsequent extreme levels of process shear. Such projections were confirmed by the pilot scale centrifuge clarification curves presented in Fig. 6.6.

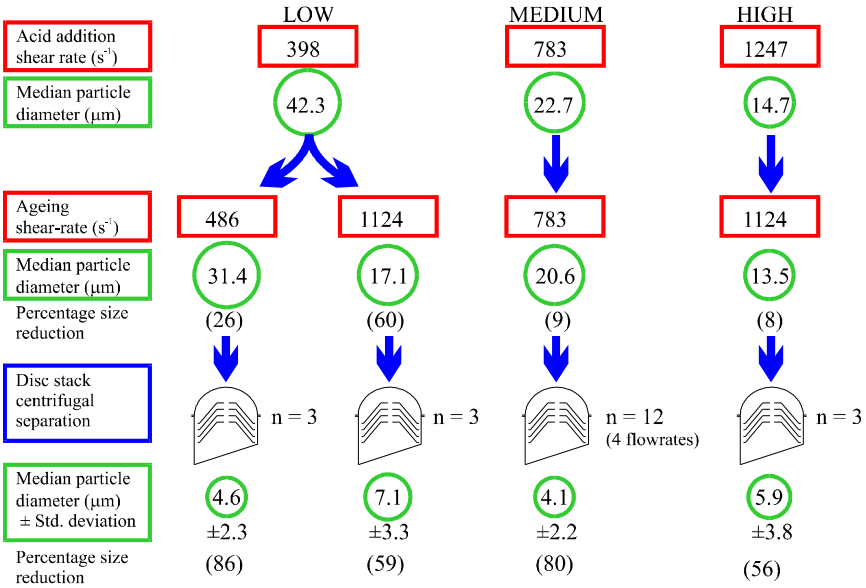

Figure 6.7 Effect of disc stack centrifuge processing on particle size on whey protein precipitates subject to various impeller shear-rates during acid addition and ageing in a 27 L batch agitation vessel.

7.1.4 Chapter conclusions

Geometric scale up of whey protein precipitation in a standard configuration agitation vessel on the basis of constant power input per unit volume can be satisfactorily applied to produce aggregates of broadly similar size though a greater distribution in fluid shear-rate around the average in the larger vessel leads to a broader PSD. Greater maximum shear at pilot scale results in greater size reduction during ageing at pilot scale

especially at higher shear-rates due to greater impeller tip speeds and impeller zone shear-rates.

Clarification efficiency curves confirm the laboratory based premise that the aggregates most suitable for efficient separation are those formed subject to high shear-rates during acid addition. It would appear that acid addition shear-rate has a significant positive effect on centrifugal clarification efficiency as these particles are better able to withstand the destructive high shear turbulent processing experienced around the entrance zone of a disc-stack centrifuge and hence separate more efficiently. As there seems to be no significant benefit to be gained from employing higher impeller speeds during ageing, lower shear-rates ought to be sufficient during an extended ageing period as this would reduce the overall agitator power requirement.

Chapter 8 General conclusions and process recommendations

8.1.1 Agitation vessel conditions for improved fractionation involving centrifugation

8.1.1.1Effect of shear-rate during acid addition

Impeller shear in an agitation vessel has a major effect on the size and structure of whey protein precipitates. Increased shear leads to smaller aggregates. This effect is far more pronounced during the aggregate formation stage when acid is added than during any subsequent ageing period. The application of higher agitation vessel shear leads to aggregates which are smaller, stronger and more compact (have higher fractal dimension).

Nevertheless aggregates formed and aged under a range of shear-rates are broken down to aggregates of broadly similar size when exposed to turbulent capillary pipe shear at Reynolds numbers in excess of about 5000. This is because the outer weaker layer consisting of loosely bound primary particles are eroded by this level of shear turbulence to largely leave particles which have a common inner core diameter (which is stronger and more compact and thus better able to survive turbulent shear). Higher turbulent shear exposure in a ball-valve rig or at the feed-zone of a centrifuge reveal differences in the strength of aggregates which have different acid addition shear histories as aggregates are broken down still further. Aggregates subject to high shear (e.g. 1247 s^{-1}) during acid addition are initially smaller but upon exposure to extreme shear suffer considerably less breakage and also remain more compact (D_f is higher) than those aggregates formed at low shear-rates (e.g. 398 s^{-1}).

8.1.1.2Effect of ageing time

A significant ageing time is required to allow mass transfer of precipitating α-lactalbumin from solution into the precipitate phase. There is an appreciable net increase in the α-lactalbumin fraction in the precipitate phase during ageing as a result of mass transfer.

The 20 - 30% of α-lactalbumin which precipitates out during acid addition increases to about 70 - 80% during 3000 seconds of ageing. Agitation shear-rate during ageing does not appear to affect the precipitation of α-lactalbumin from solution over time. However, the application of shear during an extended ageing period results in the aggregate restructuring of the loose outer layer creating a denser more compact and stronger structure.

8.1.1.3Vessel scale-up effects

Geometric agitation vessel scale-up on the basis of constant power input per unit volume results in the formation of broadly similar trends in terms of aggregate size during acid addition and ageing between laboratory scale and pilot scale operations. However, one needs to be careful when employing scale-up on this basis as dynamic similarity is not preserved and this results in some differences between aggregate size. Aggregate formation occurs over a short period at the end of the acid addition period. A longer particle circulation time and broader shear profile distribution at pilot scale is thus significant, resulting in a wider PSD at pilot scale and larger median aggregate size. However during extended ageing times of up to 3000 seconds, the higher impeller tip speeds in the scaled-up vessel signify greater maximum vessel shear around the impeller zone and this causes greater particle size reduction at pilot scale, particularly for larger weaker aggregates which have been subject to lower acid addition shear-rates.

8.1.1.4Centrifugal clarification efficiency

Centrifugal clarification efficiency provides the ultimate measure of the suitability of an agitation vessel shear regime for efficient separation. A high agitation shear regime during acid addition followed by ageing for 3000 s result in strong compact aggregates which suffer considerably less breakage in the highly turbulent shear centrifuge feed zone and hence provide substantially better clarification efficiency than aggregates formed and aged at low shear-rates. For example, at similar flowrates the clarification

efficiency of aggregates subject to an agitation vessel shear-rate of 1247 s^{-1} followed by 3000 seconds ageing at 486 s^{-1} is better than aggregates formed at an agitation vessel shear-rate of 398 s^{-1} followed by similar ageing conditions even if the latter aggregates are separated in a centrifuge with over 2.4 times greater capacity.

8.1.2 Process recommendations

Ideal agitation vessel conditions are those which provide the greatest amount of protein precipitation while producing the strongest possible aggregates in order to withstand higher levels of shear during subsequent processing and centrifugation and hence separate aggregates most easily.

A high agitation shear-rate during the period of acid addition is recommended for improved whey protein fractionation by isoelectric protein precipitation. An ageing time of at least 3000 seconds is required after acid addition to ensure a high yield of proteins precipitated. Ageing also aids aggregate restructuring and strengthening. A low ageing shear-rate is recommended as ageing shear-rate has little effect on the ultimate aggregate properties of small compact aggregates and a low ageing shear-rate requires less power input.

Improved protein fractionation may also be achieved by minimising the level of process shear experienced by aggregates through careful process design. This involves identifying the critical areas where extreme levels of shear are evident such as around sharp geometrical transitions. This work has shown that exposure to highly turbulent flow around such sharp geometrical transitions, for even very short exposure times (i.e. in the ball-valve rig) can lead to very large reductions in particle size. Once critical areas are identified, the next step is to reduce shear exposure by replacing or redesigning these critical points. The most obvious area is around the centrifuge feed zone of a disc stack centrifuge where fluid experiences rapid acceleration both radially and tangentially as it is redirected outwards from the central rotating shaft. Improved design or

amelioration here can lead to reduced particle breakage which can ultimately lead to significant improvement in clarification efficiency. Judicious selection of process pumps (e.g. choose diaphragm pumps ahead of centrifugal pumps to reduce shear exposure) and valves can also help.

8.2 References

A

Alizadehfard, M.R., Wiley, D.E., (1996), Non-Newtonian behaviour of whey protein solutions, *Journal of Dairy Research,* **63,** 315-320.

Al-Mashikhi, S.A., Nakai, S., (1987), Reduction of beta-lactoglobulin content of cheese whey by polyphosphate precipitation, *Journal of Food Science,* **52,** 1237.

Amundson, C.H., Watanawanichakorn, S., Hill, C.G., (1982), Production of enriched protein fractions of β-lactoglobulin and α-lactalbumin from cheese whey, *Journal of Food Processing and Preservation,* **6,** 55-71.

Aschaffenburg, R., Drewry, J., (1957), Improved method for the preparation of crystalline β-lactoglobulin and α-lactalbumin from cow's milk, *Biochemistry,* **65,** 273-277.

Ayazi Shamlou, P., Gierczycki, A.T., Titchener-Hooker, N.J., (1996a), Breakage of flocs in liquid suspensions agitated by vibrating and rotating mixers, *The Chemical Engineering Journal,* **62,** 23-34.

Ayazi Shamlou, P., Makagiansar, H.Y., Ison, A.P., Lilly, M.D., Thomas, C.R., (1994a), Turbulent breakage of filamentous microorganisms in submerged culture in mechanically stirred bioreactors, *Chemical Engineering Science,* **49,** 2621-2631.

Ayazi Shamlou, P., Stavrinides, S., Titchener-Hooker, N., Hoare, M., (1994b), Growth-independent breakage frequency of protein precipitates in turbulently agitated bioreactors, *Chemical Engineering Science,* **49,** 2647-2656.

Ayazi Shamlou, P., Stavrinides, S., Titchener-Hooker, N., Hoare, M., (1996b), Turbulent breakage of protein precipitates in mechanically stirred bioreactors, *Bioprocess Engineering,* **14,** 237-243.

Ayazi Shamlou, P., Titchener-Hooker, N., (1993), Turbulent aggregation and breakup of particles in stirred vessels, In: *Processing of solid-liquid suspensions,* Ayazi Shamlou, P. (Ed), Butterworth Heinmann, London, England, 1-26.

B

Barnes, H.A., Hutton J.F., Walters, K., (1989), *An introduction to rheology,* Elsevier, Amsterdam, Netherlands.

Bates, R.L., Fondy, P.L., Corpstein, R.R., (1963), *Industrial and Engineering Chemistry Process Design and Developments,* **2,** 310.

Bell, D.J., (1982), *The physical characteristics of protein precipitates and their centrifugal recovery,* PhD Thesis, University College London, England.

Bell, D.J., Dunnill, P., (1982a), Shear disruption of soya protein precipitate particles and the effect of aging in a stirred tank, *Biotechnology and Bioengineering,* **24,** 1271-1285.

Bell, D.J., Dunnill, P., (1982b), The influence of precipitation reactor configuration on the centrifugal recovery of isoelectric soya protein precipitate, *Biotechnology and Bioengineering,* **24,** 2319-2336.

Bell, D.J., Hoare, M., Dunnill, P., (1983), The formation of protein precipitates and their centrifugal recovery, *Advances in Biochemical Engineering,* **26,** 1-72.

Bernal, V., Jelen, P., (1984), Effect of calcium binding on thermal denaturation of bovine α-lacalbumin, *Journal of Dairy Science,* **67,** 2452-2454.

Bernal, V., Jelen, P., (1985) Thermal stability of whey proteins - a calorimetric study, *Journal of Dairy Science,* **68,** 2847-2852.

Bramaud, C., Aimar, P., Daufin, G., (1995), Thermal isoelectric precipitation of α-lactalbumin from a whey protein concentrate: Influence of protein-calcium complexation, *Biotechnology and Bioengineering,* **47,** 121-130.

Bramaud, C., Aimar, P., Daufin, G., (1997a), Optimisation of a whey protein fractionation process based on their selective precipitation of α-lactalbumin, *Lait,* **77,** 411-423.

Bramaud, C., Aimar, P., Daufin, G., (1997b), Whey protein fractionation: Isoelectric precipitation of α-lactalbumin under gentle heat treatment, *Biotechnology and Bioengineering,* **56,** 391-397.

Brew, K., Grobler, J.A., (1992), α-lactalbumin, In: *Advanced dairy chemistry, Vol.1:Proteins,* Fox, P.F. (Ed), Elsevier Applied Science, London, England, 191-229.

Brown, D.L., Glatz, C.E., (1987), Aggregate breakage in protein precipitation, *Chemical Engineering Science,* **7,** 1831-1839.

Bushell, G., Amal, R., (2000), Measurement of fractal aggregates of polydisperse particles using small-angle light scattering, *Journal of Colloid and Interface Science,* **221,** 186-194.

C

Camp, T.R., Stein, P.G., (1943), Velocity gradients and internal work in fluid motion, *Journal of the Boston Society of Civil Engineers,* **30,** 219-237.

Carrère, S., Sochard, S., Bascoul, A., Wilhelm, A.M., Delmas, H., (1994), Whey proteins extraction by fluidized ion exchange chromatography Isotherrms determination and process modelling, *Trans IChemE Part C,* **72,** 216-226.

Chan, M.Y.Y., Hoare, M., Dunnill, P., (1986), The kinetic of protein precipitation by different reagents, *Biotechnology and Bioengineering,* **28,** 387-393.

Chatterton D.E.W., Nielsen K.E., Holst H.H., Bartelsen H., Albertsen K., (1999), α-lactalbumin - A protein ingredient for use in infant nutrition, In: *Proceedings of the 25th International Dairy Congress, Part II Dairy Science and Technology,* Werner H. (Ed), The Danish National Committee of IDF, Aarhus, Denmark, 402-409.

Cheryan, M., (1998), *Ultrafiltration and microfiltration handbook,* Technomic Publishing Co., Lancaster, PA, USA.

Chmiel, J.F., (1997), Anti-tumor effects of dietary whey protein and its value for head and neck cancer patients, *Proceedings of the second international whey conference,* Chicago, USA, 27-29 October 1997, International Dairy Federation, Brussels, Belgium.

Clarkson, A.I., Bulmer, M., Siddiqi, S.F., Titchener-Hooker, N.J., (1994), Pilot scale verification of bioprocess models, *European Symposium on Computer Aided Process Engineering,* **18,** S651-S655.

Clarkson, A.I., Bulmer, M., Titchener-Hooker, N.J., (1996), Pilot-scale verification of a computer-based simulation for the centrifugal recovery of biological particles, *Bioprocess Engineering,* **14,** 81-89.

Coulson, J.M., Richardson J.F., (1991), *Chemical Engineering (Particle technology and separation processes), Volume 2, 4th Ed.* (with Backhurst, J.R., Harker, J.H.), Pergamon Press, Oxford, England.

Coultate, T.P., (1996), *Food the chemistry of its components, 3rd Ed.*, Royal Society of Chemistry, Cambridge, England.

D

Decker, E.A., Tak, H., Verdecchia, C., Horgan, M., (1997), Antioxidant activities of whey components, *Proceedings of the second international whey conference,* Chicago, USA, 27-29 October 1997, International Dairy Federation, Brussels, Belgium.

De Wit, J.N., (1989a), Functional properties of whey proteins, In: *Developments in dairy chemistry -4,* Fox, P.F. (Ed), Elsevier, London, England.

De Wit, J.N., (1989b), The use of whey protein products, In: *Developments in dairy chemistry -4,* Fox, P.F. (Ed), Elsevier, London, England.

De Wit, J.N., (1998), Nutritional and functional characteristics of whey proteins in food products, *Journal of Dairy Science,* **81,** 597-608.

Dimenna, G.P., Segall, H.J., (1981), High-performance gel-permeation chromatography of bovine skim milk products, **4,** 639-649.

Donnelly, W.J., Mehra, R.K., (1990), Fractionation of milk proteins, *Biochemical Society Transactions,* **18,** 238-240.

E

Eigel, W.N., Butler, J.E., Ernstrom, C.A., Farrell, H.M.Jr., Harwalker, V.R., Jenness, R., Whitney, R.McL., (1984), Nomenclature of proteins of cow's milk: Fifth revision, *Journal of Dairy Science,* **67,** *1599-1631.*

Etzel, M., (1995), Whey protein isolation and fractionation using ion exchangers, In: *Bioseparation Processes in Foods,* Singh, R.K., Rizvi, S.S.H. (Eds), Marcel Dekker, New York, USA.

F

Fauquant, J., Vieco, E., Brulé, G., Maubois, J.L., (1985), Clarification des lactosérums doux par aggrégation thermocalcique de la matière grasse résiduelle, *Lait,* **65,** 1-20.

Feder, J., (1988), *Fractals,* Plenum Press, New York, USA.

Fisher, R.R., Glatz, C.E., (1988), Polyelectrolyte precipitation of proteins II. Models of particle size distributions, *Biotechnology and Bioengineering,* **32,** 786-796.

Fisher, R. R., Glatz, C. E., Murphy, P.A., (1986), Effects of mixing during acid addition on fractionally precipitated protein, *Biotechnology and Bioengineering,* **28,** 1056-1063.

Food and Agriculture Organisation of the United Nations, FAOSTAT Agriculture Data, posted 5 February 2000, < *http://apps.fao.org/*>

Fox, P.F., Holsinger, V.H., Posati, L.P., Pallanch, M.J., (1967), Separation of β-lactoglobulin from other milke serum proteins by trichloroacetic acid, *Journal of Dairy Science,* **50,** 1363-1367.

Fox, P.F., McSweeney, P.L.H., (1998), *Dairy chemistry and biochemistry*, Blackie academic and professional, London, England.

G

Geankoplis, C.J., (1993), *Transport processes and unit operations, 3rd edition*, Prentice Hall Inc., New Jersey, USA.

Gésan-Guiziou, G., Daufin, G., Timmer, M., Allersma, D., Van der Horst, C., (1999), Process steps for the preparation of purified fractions of α-lactalbumin and β-lactoglobulin from whey protein concentrates, *Journal of Dairy Research,* **66,** 225-236.

Formatted

Glanbia, (2000), Richfield whey plant, <http://www.glanbiausa.com/GFoods/Richfield.htm> accessed 6 October 2000.

Glasgow, L.A., Leucke, R.H., (1980), Mechanisms of deaggregation for clay-polymer flocs in turbulent systems, *Industrial and Engineering Chemistry Fundamentals,* **19,** 148-156.

Glatz, C.E., Hoare, M., Landa-Veritz, J., (1986), The formation and growth of protein precipitates in a continuous stirred-tank reactor, *AIChE Journal,* **32,** 1196-1204.

Gray, R.M., Mackenzie, D.D.S., (1987), Effect of plane of nutrition on the concentration and yield of whey proteins in bovine milk, *New Zealand Journal of Dairy Science and Technology,* **22,** *157-165.*

H

Hambraeus, L., (1992), Nutritional aspects of milk proteins, *Madvanced Dairy Chemistry, Vol. 1: Proteins,* Fox, P.F. (Ed), Elsevier, London, England, 457.

Harper, W.J., Man Lee, K., (1997), Functional properties of 34% whey protein concentrates, *Proceedings of the second international whey conference*, IDF, Chicago, USA, October 1997, 140-153.

Heine, W.E., Klein, P.D., Reeds, P.J., (1991), The importance of α-lactalbumin in infant nutrition, *Journal of Nutrition,* **121,** 277-283.

Heine, W.E., Radke, M., Wutzke, K.D., Peters, E., Kundt, G. (1996), α-lactalbumin-enriched low-protein infant formulas: a comparison to breast milk feeding, *Acta Paediatrica,* **85,** 1024-1028.

Hoare, M., (1982), Protein precipitation and precipitate ageing; Part II: Growth of protein precipitates during hindered settling or exposure to shear, *Trans IChemE,* **60,** 157-163.

Hoare, M., Narendranathan, T.J., Flint, J.R., Heywood-Waddington, D., Bell, D.J., Dunnill, P., (1982), Disruption of protein precipitates during shear in couette flow and in pumps, *Industrial and Engineering Chemistry Fundamentals,* **21,** 402-406.

Hoare, M., Titchener, N.J., Foster, P.R., (1987), Improvement in separation characteristics of protein precipitates by acoustic conditioning, *Biotechnology and Bioengineering,* **29,** 24-32.

Hobman, P.G., (1992), Ultrafiltration and manufacture of whey protein concentrates, In: *Whey and Lactose Processing,* Zadow, J.G. (Ed), Elsevier Science Publishers Ltd, London, England, 195-229.

Huffman, L.M., (1997), The importance of whey protein fractions for WPC and WPI functionality, *Proceedings of the second international whey conference,* IDF, Chicago, USA, October 1997, 197-205.

J

Jost, R., Maire, J-C., Maynard, F., Secretin, M-C., (1999), Aspects of whey protein usage in infant nutrition, a brief review, *International Journal of Food Science and Technology,* **34,** 533-542.

K

Kaneko, T., Wu, B.T., Nakai, S., (1985), Selective concentration of bovine immunoglobulins and α-lactalbumin from acid whey using $FeCl_3$, *Journal of Food Science,* **50,** 1531.

Kinghorn, N.M., Norris, C.S., Paterson, G.R., Otter, D.E., (1995), Comparison of capillary electrophoresis with traditional methods to analyse bovine whey proteins, *Journal of Chromatography A,* **700,** 111-123.

Kuwata, T., Pham, A.M., Ma, C.Y., Nakai, S. (1985), Elimination of β-lactoglobulin from whey to simulate human milk protein, *Journal of Food Science,* **50**, 605.

L

Larson, B.L., Kendall, K.A., (1957), Protein production in the bovine. Daily production of the specific milk proteins during lactation period, *Journal of Dairy Science,* **40,** 377-386.

Lin, M.Y., Klein, R., Lindsay, H.M., Weitz, D.A., Ball, R.C., Meakin, P., (1990), The structure of fractal colloidal aggregates of finite extent, *Journal of Colloid and Interface Science,* **137,** 263-280.

Logan, B.E., Kilps, J.R., (1995), Fractal dimensions of aggregates formed in different fluid mechanical environments, *Water Research,* **29,** 443-453.

M

Mailliart, P., Ribadeau-Dumas, B., (1988), Preparation of β-lactoglobulin and β-lactoglobulin-free proteins from whey retentate by NaCl salting out at low pH., *Journal of Food Science,* **53,** 743.

Mandelbrot, B.B., (1975), *Les objets fractals: Forme, hasard et dimension,* Flammarion, Paris, France.

Mandelbrot, B.B., (1977), *Fractals; form, chance and dimension*, Freeman, San Francisco, USA.

Mandelbrot, B.B. (1982), *The fractal geometry of nature*, Freeman, San Francisco, USA.

Manji, B., Hill, A., Kakuda, Y., Irvine, D.M., (1985), Rapid separation of milk whey proteins by anion exchange chromatography, *Journal of Dairy Science,* **68,** 3176-3179.

Marincic, P.Z., McCune, R.W., Hendricks, D.G., (1999), Cow's Milk based infant formula: heterogeneity of bovine serum albumin content, *Journal of the American Dietetic Association,* **99,** *1575-1580.*

Maté, J.I., Krochta, J.M., (1994), β-lactoglobulin separation from whey protein isolate on a large scale, *Journal of Food Science,* **59,** 1111-1114.

Mather, I. H., (2000), A review and proposed nomenclature for major proteins of the milk-fat globule membrane, *Journal of Dairy Science,* **83,** 203-247.

Maubois, J.L., Pierre, A., Fauquant, J., Piot, M., (1987), Industrial Fractionation of Main Whey Proteins, In: *Bulletin of the Industrial Dairy Federation,* **no. 212,** 154-159.

Maubois, J.L., Olliver, G., (1992), Milk Protein Fractionation, In: *IDF Special Issue 9201,* 15-22.

Maubois, J.L., Ollivier, G., (1997), Extraction of milk proteins, In: *Food Proteins and their Applications,* Damodaran, S., Paraf, A. (Eds), Marcel Dekker, New York, USA, 579-595.

McIntosh, G.H., Regester, G.O., Le Leu, R.K., Royle, P.J., Smithers, G.W., (1995), Dairy proteins protect against dimethylhydrazine-induced intestinal cancers in rats, Journal of Nutrition, **125,** 809.

Meakin, P., (1988), Fractal aggregates, *Advances in Colloid and Interface Science,* **28,** 249-331.

Mie, G., (1908), Beiträge zur optik trüber medien, speziell kolloidaler metallösungen, *Annalen der physik*, **25,** 377-445.

Mleko, S., Achremowicz, B., Foegeding, E.A., (1994), Effect of protein concentration on the rheological properties of whey protein concentrate gels, *Milchwissenschaft,* **49,** 266-269.

Moir, D.N., (1988), Sedimentation centrifuges; know what you need, *Chemical Engineering,* **95,** 42-51.

Morr, C.V., (1987), Fractionation and modification of whey protein in the U.S., In: *Bulletin of the Industrial Dairy Federation,* **no. 212,** 145-149.

Morr, C.V., (1989), Whey proteins: manufacture, In: *Developments in dairy chemistry -4,* Fox, P.F. (Ed), Elsevier, London, England.

Morr, C.V., (1992), *Whey Utilisation,* In: *Whey and Lactose Processing,* Zadow, J.G. (Ed), Elsevier Science Publishers Ltd., England, 133-154.

Mulvihill, D.M., (1989), Casein and caseinates: manufacture, In: *Developments in dairy chemistry -4,* Fox, P.F. (Ed), Elsevier, London, England.

Mulvihill, D.M., (1994), Functional milk protein products, In: *Biochemistry of Milk Products*, Andrews, A.T., Varley J. (Eds), Royal Society of Chemistry, London, England, 94-113.

N

Negishi, H., Otomo, H., Gotou, T., Ueda, T., Kuwata, T. (1997), Cosmetic properties of whey minerals and their application to skin care products for babies, *Proceedings of the second international whey conference,* Chicago, 27-29 October 1997, 337-350, IDF, Brussels, Belgium.

Nelson, C.D., Glatz, C.E., (1985), Primary particle formation in protein precipitation, *Biotechnology and Bioengineering,* **27,** 1434-1444.

Nielsen, A.E., (1964), *Kinetics of precipitation,* Macmillan, New York, USA.

O

Ohtomo, H., Kuwata, T., (1993), Fractionation of β-lactoglobulin in bovine whey by intermittent up flow system with multi-stage ion exchange column, In: *Proceedings of the Sixth International Congress on Engineering and Food,* 23-27 May 1993, Makuhari Messe, Chiba, Japan.

Oldshue, J.Y., (1985), Mixing Processes, In: *Scaleup of Chemical Processes,* Bisio, A., Kabel, R.L. (Eds), Wiley, New York, USA.

P

Papiz, M.Z., Sawyer, L., Eliopoulos, E.E., North, A.C.T., Findlay, J.C.B., Sivaprasadarao, R., Jones, T.A., Newcomer, M.E. Kraulis P.J., (1986), The structure of β-lactoglobulin and its similarity to plasma retinal-binding protein, *Nature,* **324,** 383-385.

Parodi, P.W., (1998), A role for milk proteins in cancer prevention, *The Australian Journal of Dairy Technology,* **53,** 37-47.

Pearce, R.J., (1983a), Analysis of whey proteins by high performance liquid chromatography, *The Australian Journal of Dairy Technology,* **38,** 114-117.

Pearce, R.J., (1983b), Thermal Separation of β-lactoglobulin and α-lactalbumin in bovine cheddar cheese whey*, The Australian Journal of Dairy Technology,* **38,** 144-149.

Pearce, R.J., (1987), Fractionation of whey proteins, In: *Bulletin of the International Dairy Federation,* **212,** 150-153.

Pearce, R.J., (1989), Thermal denaturation of whey protein, In: *Bulletin of the International Dairy Federation,* **238,** 17-22.

Pearce, R. J., (1992), Whey processing, In: *Whey and Lactose Processing, Z*adow, J.G. (Ed), Elsevier Science Publishers Ltd, London, England, 73-89.

Pearce, R. J., (1992a), Whey protein recovery and whey protein fractionation, In: *Whey and Lactose Processing,* Zadow, J.G. (Ed), Elsevier Science Publishers Ltd., England, 271-316.

Pearce, R.J., Dunkerley, J.A., Wheaton, T.W., Marshall, S.C. Tobin, A. (1997), A solid fat replacer for manufactured meat products based on a β-lactoglobulin-rich whey protein ingredient, *Proceedings of the second international whey conference, IDF, Chicago, USA, October 1997,* 181-188.

Perry, R.H., (1997), *Perry's chemical engineers' handbook,* 7th Ed., McGraw-Hill, New York, USA.

Petenate, A.M., Glatz, C.E., (1983), Isoelectric precipitation of soy protein. II. Kinetics of protein aggregate growth and breakage, *Biotechnology and Bioengineering,* **25,** 3059-3078.

Pierre, A., Fauquant, J., (1986), Principes pour un procédé industriel de fractionnement des protéines du lactosérum, *Lait,* **66,** 405-419.

Q

Qingnong, T., Munro, P.A., McCarthy, O.J., (1990), Steady shear and oscillatory rheological measurements on solutions of commercially available whey protein concentrates, *Proceedings of the 18th Australasian chemical engineering conference,* 666-673.

R

Rantamaki, P., Koskinen, P.,Tupasela, T. Vasara, E., (1997), Use of β-lactoglobulin as ingredient of desert foam and its effect on the structure, *Proceedings of the second international whey conference, IDF, Chicago, USA, October 1997,* 233-238.

Records, F.A., (1977), Sedimenting centrifuges, In: *Solid/liquid separation equipment scale up,* Purchas, D.B. (Ed), Uplands Press Ltd., UK.

Regester, G.O., Smithers, G.W., (1991), Seasonal changes in the β-lactalbumin, glycomacropeptide, and casein content of whey protein concentrate, *Journal of Dairy Science,* **74,** 796-802.

Reuss, M., (1988), Influence of mechanical stress on the growth of *Rhizopus nigricans, Chemical Engineering Technology,* **11,** 178-187.

Richardson, J.F., Zaki, W.N., (1954), Sedimentation and Fluidisation: Part I, *Transactions of the Institution of Chemical Engineers,* **32,** 35.

Richert, S.H., Morr, C.V., Cooney, C.M., (1974), Effect of heat and other factors upon foaming properties of whey protein concentrates, *Journal of Food Science,* **39,** 42-48.

Rinn, J.C., Morr, C.V., Seo, A., Surak, J.G., (1990), Evaluation of nine semi-pilot scale whey pre-treatment modifications for producing whey protein concentrate, *Journal of Food Science,* **55,** 510-515.

Rogers,G.F.C., Mayhew,Y.R., (1988), *Thermodynamic and transport properties of fluids (4th Ed)*, Basil Blackwell Ltd., Oxford, England.

Ross, J.C., (1994), Modeling fractal profiles and structures, In: *Fractal surfaces*, Ross, J.C. (Ed), Plenum press, New York, USA.

S

Slack, A.W., Amundson, C.H., Hill, C.G., (1986), Production of enriched β-lactoglobulin and α-lactalbumin whey protein fractions, *Journal of Food Processing and Preservation,* **10,** 19-30.

Smithers, G.W., Ballard, F. J., Copeland, A. D., De Silva, K. J., Dionysius, D. A., Francis, G.L., Goddard, C., Grieve, P.A., McIntosh, G.H., Mitchell, I.R., Pearce, R.J., Regester,G.O., (1996), Symposium: Advances in dairy foods processing and engineering, New opportunities from the isolation and utilisation of whey proteins, *Journal of Dairy Science,* **79,** 1454-1459.

Smithers, G.W., McIntosh, G.H., Regester, G.O., Johnson, M.A., Royle, P.J., Le Leu, R.K., Jelen, P., (1987), Anti-cancer effects of dietary whey proteins, *Proceedings of the second international whey conference,* Chicago, 27-29 October 1997, 337-350, IDF, Brussels, Belgium.

Smoluchowski, M., (1917), Mathematical theory of the kineticsof the coagulation of colloidal solutions, *Zeitschrift für physikalische chemie,* **92, 129-168**.

Sonntag, R.C., Russel, W.B., (1987), Structure and breakup of flocs subjected to fluid stresses, II. Theory, *Journal of Colloid and Interface Science,* **115,** 378-389.

Spicer, P.T., Keller, W., Pratsinis, S.E., (1996), The effect of impeller type on floc size and structure during shear-induced flocculation, *Journal of Colloid and Interface Science,* **184,** 112-122.

Steventon, A.J., (1992), *Thermal aggregation of whey proteins,* PhD Thesis*,* Cambridge University, England.

Steventon, A.J., Gladden L,F., Fryer, P.J., (1991), A percolation analysis of the concentration dependence of the gelation of whey protein concentrates, *Journal of Texture Studies,* **22,** 201-218.

Stokes, G.G., (1851), On the effect of the internal friction of fluids on the motion of pendulums, *Transactions of the Cambridge Philosophy Society, **9,** 8.*

Svarovsky, L., (1981), *Solid liquid separation,* Svarovsky, L. (Ed), Butterworth Heinmann, London, England.

Swaisgood, H.E, (1982), Chemistry of milk proteins, In: *Developments in dairy chemistry, Vol. 1: Proteins,* Fox, P.F. (Ed), Elsevier Applied Science, London, England, 1-59.

T

Tambo, N., Hozumi, H., (1979), Physical characteristics of flocs -II. Strength of floc, *Water Research,* **13,** 421-427.

Tambo, N., Watanabe, Y., (1979a), Physical aspect of flocculation process - I. Fundamental treatise, *Water Research,* **13,** 429-439.

Tambo, N., Watanabe, Y., (1979b), Physical characteristics of flocs -I. The floc density function and aluminium floc, *Water Research*, **13,** 409-419.

Tomi, D.T., Bagster, D.F., (1978), The behaviour of aggregates in stirred vessels, Transactions of the Institution of Chemical Engineers, **56,** 1-18.

Tossavainen, O., Rantamaki, P., Outinen, M., Tupasela, T., Koskela, P., (1998), Functional properties of the whey protein fractions produced in pilot scale processes, *Milchwissenschaft,* **53,** 453-458.

Twineham, M., Hoare, M., Bell, D.J., (1984), The effects of protein concentration on the break-up of protein precipitate by exposure to shear, *Chemical Engineering Science,* **39,** 509-513.

V

Virkar, P.D., Hoare, M., Chan, M.Y.Y., Dunnill, P., (1982), Kinetics of the acid precipitation of soya protein in a continuous-flow tubular reactor, *Biotechnology and Bioengineering,* **24,** 871-887.

Virkar, P.D., Narendranathan, T.J., Hoare, M., Dunnill, P., (1981), Studies of the effects of shear on globular proteins: Extension to high shear fields and to pumps, *Biotechnology and Bioengineering,* **23,** 425-429.

Vogel, H., (2000), α-lactalbumin,
<http://groningen.bio.ucalgary.ca/~hans/alpha-lactalbumin.html>,
accessed 26 August 2000.

W

Walstra, P., Geurts, T.J., Noomen, A., Jellema, A., van Boekel, M.A.J.S., (1999), *Dairy Technology: principles of milk properties and processes*, Marcel Dekker, New York, USA.

Waniska, R.D., Shetty, J.K., Kinsella, J.E., (1981), Protein stabilized emulsions: Effects of modification on the emulsifying activity of bovine serum albumin in model system, *Journal of Agriculture and Food Chemistry,* **29,** 826-831.

Weinbrenner, W.F., Etzel, M.R., (1994), Competitive adsorption of α-lactalbumin and bovine serum albumin to a sulfopropyl ion-exchange membrane, *Journal of Chromatography,* **662,** 414-419.

X

Xiong, Y.L., Dawson, K.A., Wan, L., (1993), Thermal aggregation of b-lactalbumin: Effect of pH, ionic environment and thiol reagent, *Journal of Dairy Science,* **76,** 70-77.

Y

Yoshida, S., (1990), Isolation of β-lactaglobulin and α-lactalbumin by gel filtration using sepharacyl S-200 and purification by diethylaminoehtyl ion exchange chromatography, *Journal of Dairy Science,* **73,** 2292-2298.

Z

Zydney, A.L., (1998), Protein separations using membrane filtration: new opportunities for whey fractionation, *International Dairy Journal,* **8,** 243-250.

Postscript

It's been said a picture can paint a thousand words. On that basis I'll invoke some artists of narration to articulate some concluding thoughts.

On turbulent flow:

"I am an old man now, and when I die and go to heaven there are two matters on which I hope for enlightenment. One is quantum electrodynamics and the other is the turbulent motion of fluids. And about the former I am rather more optimistic."

Sir Horace Lamb (in 1932)
(Quoted in *Computational Fluid Mechanics and Heat Transfer*, Anderson, Tannehill & Pletcher (Eds), 1984.)

On fractals:

"I once read that if the folds in the cerebral cortex were smoothed out it would cover a card table. That seemed quite unbelievable but it did make me wonder just how big the cortex would be if you ironed it out. I thought it might just about cover a family-sized pizza: not bad, but no card-table. I was astonished to realize that nobody seems to know the answer. A quick search yielded the following estimates for the smoothed out dimensions of the cerebral cortex of the human brain.

An article in Bioscience in November 1987 by Julie Ann Miller claimed the cortex was a 'quarter-metre square.' That is napkin-sized, about ten inches by ten inches. Scientific American magazine in September 1992 upped the ante considerably with an estimated of 1 1/2 square metres; that's a square of brain forty inches on each side, getting close to the card-table estimate. A psychologist at the University of Toronto figured it would cover the floor of his living room (I haven't seen his living room), but the prize winning estimate so far is from the British magazine New Scientist's poster of the brain published in 1993 which claimed that the cerebral cortex, if flattened out, would cover a tennis court. How can there be such disagreement? How can so many experts not know how

big the cortex is? I don't know, but I'm on the hunt for an expert who will say the cortex, when fully spread out, will cover a football field. A Canadian football field."

Jay W. Ingram
Unlocking the Mysteries of the Brain, Penguin Books, 1995.

"Pick up a pinecone and count the spiral rows of scales. You may find eight spirals winding up to the left and 13 spirals winding up to the right, or 13 left and 21 right spirals, or other pairs of numbers. The striking fact is that these pairs of numbers are adjacent numbers in the famous Fibonacci series: 1, 1, 2, 3, 5, 8, 13, 21... Here, each term is the sum of the previous two terms. The phenomenon is well known and called phyllotaxis. Many are the efforts of biologists to understand why pinecones, sunflowers, and many other plants exhibit this remarkable pattern. Organisms do the strangest things, but all these odd things need not reflect selection or historical accident. Some of the best efforts to understand phyllotaxis appeal to a form of self-organization. Paul Green, at Stanford, has argued persuasively that the Fibonacci series is just what one would expects as the simplest self-repeating pattern that can be generated by the particular growth processes in the growing tips of the tissues that form sunflowers, pinecones, and so forth."

Stuart Kauffman
At Home in the Universe, Oxford University Press, 1995.

On aggregate settling (!):

"Swallows certainly sleep all winter. A number of them conglobulate together, by flying round and round, and then all in a heap throw themselves under water, and lye in the bed of a river."

Samuel Johnson (1709-1784)
(Quoted in *The Life of Samuel Johnson*, James Boswell (Ed), 1799.)

On drawing conclusions:

"Therefore, O students, study mathematics and do not build without foundations."

Leonardo Da Vinci
The Notebooks of Leonardo Da Vinci, Quaderni 17r.

"The difficulty lies, not in the new ideas, but in escaping the old ones, which ramify, for those brought up as most of us have been, into every corner of our minds."

John Maynard Keynes
(Quoted in *Engines of Creation: the Coming Era of Nanotechnology*, K. E. Drexler (Ed), Bantam, 1987.)

"Truth in science can be defined as the working hypothesis best suited to open the way to the next better one."

Konrad Lorenz

"The important thing in science is not so much to obtain new facts as to discover new ways of thinking about them."

Sir William Bragg

On pursuing this work:

"With reference to a correspondent:
The young specialist in English Lit, ...lectured me severely on the fact that in every century people have thought they understood the Universe at last, and in every century they were proved to be wrong. It follows that the one thing we can say about our modern 'knowledge' is that it is wrong. My answer to him was, ' ..when people thought the Earth was flat, they were wrong. When people thought the Earth was spherical they were wrong. But if you think that thinking the Earth is spherical is just as wrong as thinking the Earth is flat, then your view is wronger than both of them put together.' "

Issac Asimov (1920-1992)

“Basic research may seem very expensive. I am a well-paid scientist. My hourly wage is equal to that of a plumber, but sometimes my research remains barren of results for weeks, months or years and my conscience begins to bother me for wasting the taxpayer's money. But in reviewing my life's work, I have to think that the expense was not wasted. Basic research, to which we owe everything, is relatively very cheap when compared with other outlays of modern society. The other day I made a rough calculation which led me to the conclusion that if one were to add up all the money ever spent by man on basic research, one would find it to be just about equal to the money spent by the Pentagon this past year.”

Albert Szent-Györgyi, (1893-1984)
The Crazy Ape, Grosset and Dunlap, 1971.

..and seeking some perspective:

“I recognize that many physicists are smarter than I am -most of them theoretical physicists. A lot of smart people have gone into theoretical physics, therefore the field is extremely competitive. I console myself with the thought that although they may be smarter and may be deeper thinkers than I am, I have broader interests than they have.”

Linus Pauling, (1901-1994)
(Quoted in *The Meaning of Life*, David Friend (Ed), Little Brown, 1990.)

“We have a habit in writing articles published in scientific journals to make the work as finished as possible, to cover up all the tracks, to not worry about the blind alleys or describe how you had the wrong idea at first, and so on. So there isn't any place to publish, in a dignified manner, what you actually did in order to get to do the work.”

Richard Feynman
1966 Nobel Lecture.

“Engineering is the art of modelling materials we do not wholly understand, into shapes we cannot precisely analyse so as to withstand forces we cannot properly assess, in such a way that the public has no reason to suspect the extent of our ignorance.”

Dr. A.R. Dykes
British Institution of Structural Engineers, 1976.

“ ‘The scientific method,’ Thomas Henry Huxley once wrote, ‘is nothing but the normal working of the human mind.’ That is to say, when the mind is working; that is to say further, when it is engaged in correcting its mistakes.

Taking this point of view, we may conclude that science is not physics, biology, or chemistry -is not even a ‘subject’ - but a moral imperative drawn from a larger narrative whose purpose is to give perspective, balance, and humility to learning.”

Neil Postman
(Quoted in *The End of Education*, A.A. Knopf (Ed), 1995.)